

## Chemical Analysis of Microplastics and Nanoplastics: Challenges, Advanced Methods, and Perspectives

Natalia P. Ivleva\*



Cite This: *Chem. Rev.* 2021, 121, 11886–11936



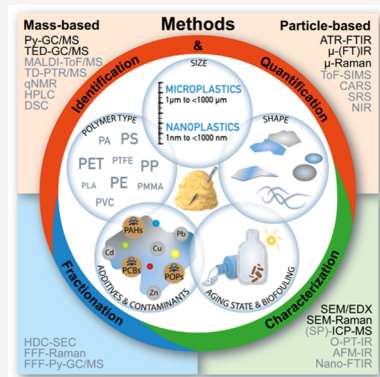
Read Online

ACCESS |

Metrics & More

Article Recommendations

**ABSTRACT:** Microplastics and nanoplastics have become emerging particulate anthropogenic pollutants and rapidly turned into a field of growing scientific and public interest. These tiny plastic particles are found in the environment all around the globe as well as in drinking water and food, raising concerns about their impacts on the environment and human health. To adequately address these issues, reliable information on the ambient concentrations of microplastics and nanoplastics is needed. However, micro- and nanoplastic particles are extremely complex and diverse in terms of their size, shape, density, polymer type, surface properties, etc. While the particle concentrations in different media can vary by up to 10 orders of magnitude, analysis of such complex samples may resemble searching for a needle in a haystack. This highlights the critical importance of appropriate methods for the chemical identification, quantification, and characterization of microplastics and nanoplastics. The present article reviews advanced methods for the representative mass-based and particle-based analysis of microplastics, with a focus on the sensitivity and lower-size limit for detection. The advantages and limitations of the methods, and their complementarity for the comprehensive characterization of microplastics are discussed. A special attention is paid to the approaches for reliable analysis of nanoplastics. Finally, an outlook for establishing harmonized and standardized methods to analyze these challenging contaminants is presented, and perspectives within and beyond this research field are discussed.



### CONTENTS

1. Introduction	11887	2.4.4. Methods for Chemical Characterization of Weathered NMPs	11912
2. Chemical Analysis of Microplastics	11888	3. Chemical Analysis of Nanoplastics	11913
2.1. Challenges and Objectives	11888	3.1. Challenges and Objectives	11913
2.2. Mass-based Methods for Analysis of Microplastics	11889	3.2. Preconcentration, Enrichment and Fractionation of Nanoplastic Samples	11913
2.2.1. Thermal Degradation Combined with GC/MS	11889	3.3. Mass-based Methods for Analysis of Nanoplastics	11914
2.2.2. Further Thermoanalytical Methods	11894	3.4. Nondestructive Spectroscopic Methods for Analysis of Nanoplastics	11916
2.2.3. Additional Techniques for the Mass-based Analysis of Microplastics	11895	3.4.1. Scanning Probe Microscopy Coupled to Spectroscopy	11918
2.3. Particle-based Methods for Nondestructive Analysis of Microplastics	11898	3.4.2. Raman-based Analysis of Nanoplastics Enabled by Optical Tweezers	11918
2.3.1. Vibrational Spectroscopy	11898	4. Validation of Methods, Quality Assurance, and Quality Control	11919
2.3.2. Additional Techniques for Particle-based Chemical Analysis of MPs	11910	4.1. Reference Materials for Microplastics and Nanoplastics	11919
2.4. Combination of Different Methods for Comprehensive MP Analysis	11911		
2.4.1. Identification of Individual MP Particles	11911		
2.4.2. Simultaneous Identification and Quantification of Polymers from Complex Samples	11911		
2.4.3. Electron Microscopy for Detailed Characterization of MP Particles	11911		

Special Issue: Frontiers of Analytical Science

Received: March 3, 2021

Published: August 26, 2021



4.2. Interlaboratory Comparison Studies	11920
5. Summary and Perspectives	11921
Author Information	11924
Corresponding Author	11924
Notes	11924
Biography	11924
Acknowledgments	11924
Abbreviations	11924
References	11925

## 1. INTRODUCTION

Microplastics and nanoplastics are tiny pieces of synthetic polymers (plastics), found in the environment (including fresh and seawater, sediments, biota, soils, and ambient air) as well as in drinking water and food, and therefore are recognized as emerging particulate anthropogenic pollutants.<sup>1–15</sup> The term microplastics was introduced by Thompson et al.<sup>16</sup> in 2004 to report on small plastic fragments in marine environment. An upper size limit of 5 mm for microplastics was proposed by Arthur et al.<sup>17</sup> in 2009. Currently, plastic particles and fibers smaller as 1  $\mu\text{m}$  and in the size range 1  $\mu\text{m}$  to 1 mm are defined as nanoplastics and microplastics, respectively.<sup>18–21</sup> Fragments in the size range 1–5 mm can be referred as large microplastics.<sup>19,20</sup> In what follows, we will use abbreviations MPs for microplastics, NPLs for nanoplastics (instead of NPs, to avoid the confusion with nanoparticles), and NMPs for both nanoplastics and microplastics, in the case of tiny plastic particles and fibers, are discussed in general.

On the one hand, plastic materials, being lightweight, versatile, durable, formable, corrosion- and flame-resistant, etc., improve the quality of life for millions of people across the globe by making it easier, safer, and more enjoyable.<sup>22</sup> On the other hand, we are facing now the global challenges when plastics end up in the environment or food. While the plastic production in Europe slightly decreases (61.8 Mt and 59.7 Mt in 2018 and 2019, respectively), globally it grows from year to year, reaching 368 Mt in 2019.<sup>22</sup> The production level of thermoplastics such as polyethylene (PE) of high density (HDPE) and low density (LDPE), polypropylene (PP), polystyrene (PS), polyvinyl chloride (PVC), and polyethylene terephthalate (PET) is reflected in the degree of MP contamination, e.g., on the order of globally detected MPs in freshwaters and drinking water: PE  $\approx$  PP > PS > PVC > PET.<sup>23</sup> In addition to conventional polymers, including those mentioned above plus poly(methyl methacrylate) (PMMA), polyamide (PA), and polyurethane (PUR), also bioplastics (plastics which are biodegradable and/or have biobased content) are produced. The latter are more and more frequently utilized for food packaging (e.g., polylactide, PLA) and agriculture (e.g., polybutylene adipate-*co*-terephthalate, PBAT). According to the recent definition,<sup>18</sup> to MPs are also assigned tire wear particles (TWP), which contain 40–60% of synthetic polymers (e.g., styrene–butadiene rubber, SBR) and paint particles/surface coatings. The latter are multicomponent systems consisting of binders, pigments, fillers, and additives, where synthetic polymers are used as film formers, like curing coating systems (e.g., polyester (PES), alkyds, epoxy resin, urethane resins), and physically drying systems (e.g., acryl and vinyl (co)polymers).<sup>18,24</sup>

Generally, NMPs can be categorized as being of “primary” or “secondary” origin. “Primary” NMPs are intentionally manufactured in their size and shape for a broad variety of applications

(e.g., pellets for industrial production, nano- and microbeads for personal care products, and industrial cleaners). The “secondary” NMP particles and fibers (e.g., nylon or PA and PES) are formed via fragmentation and degradation of plastic debris in the environment (due to mechanical abrasion, UV radiation, and (micro)biological degradation) or through wear and tear of plastic-containing items.<sup>2,18,25,26</sup>

From the global perspectives, MPs are widespread from the equator<sup>12,27,28</sup> to the poles<sup>29,30</sup> and from the deep-sea sediments<sup>31,32</sup> to mount Everest (PES fibers were found at height of 8440 m).<sup>33</sup> The numerous reports on the MP occurrence around the globe raised many questions on impacts of MPs on biota. Potentially negative impacts may be associated with the leaching of monomers and additives, some of which have been proven to be toxic, carcinogenic, or endocrine-disrupting.<sup>15,34,35</sup> Additionally, harmful volatile organic compounds (VOCs, e.g., acrolein and benzene) can be formed and released due to oxidative photodegradation of plastic debris.<sup>36</sup> Furthermore, MPs can sorb persistent organic pollutants<sup>37</sup> and/or toxic metals<sup>38</sup> from the environment and act as a vector for pathogenic and/or antibiotic resistant microorganisms.<sup>39,40</sup> However, effects of MPs on the biota reported so far are highly contradictory, ranging from negative (including lethal) through no impacts up to detoxification (when the initial concentration of pollutants in organisms was higher than in the ingested MPs). Furthermore, many such studies were conducted with MP particle concentrations exceeding those measured in, or (for particles <10  $\mu\text{m}$ ) extrapolated for the environment by a factor of  $10^2$ – $10^7$ . This fact underlines the importance of MP exposure studies at environmentally realistic concentrations.<sup>41–43</sup> While negative effects of NPLs on biota are under discussion<sup>44</sup> and NPL penetration through the blood-to-brain barrier in fish has been demonstrated,<sup>45</sup> realistic experiments are hampered by missing quantitative information on the occurrence of these particles in the environment. Degree of human exposure with MPs via air, water, and food and associated effects are currently under intensive investigation.<sup>46–48</sup> While MPs have been found in several products of human diet,<sup>47,49–56</sup> the highest exposure via inhaled air is assumed.<sup>57,58</sup> Generally, more hazardous effects are expected from smaller MPs. The information about NPL effects on humans is limited yet,<sup>59</sup> but it has been already shown that NPLs can cross the gut barrier.<sup>60</sup>

To assess actual risks associated with NMPs, the reliable data on the occurrence of these particles in environmental and food samples are needed. Although visual identification of MPs represents the easiest and cheapest way of analysis, the fraction of false-positive and false-negative results increases with decreasing particle size (e.g., only 1.4% of the particles visually resembling MPs were found to have synthetic polymer origin<sup>61</sup>), which underlines the importance of proper chemical analysis of NMPs.

The diversity and complexity of plastic sources, usage patterns, emission pathways, and material properties is reflected in the diversity of NMP particles, exhibiting a high variety of physical, chemical, and biological characteristics (e.g., size, shape, density, polymer type, surface properties, etc.).<sup>1,2,9,62</sup> Therefore, advanced methods are required for the reliable identification, quantification, and characterization of this analyte, probably one of the most challenging analytes in the environment and food.

In the past decade, there have been several reviews partially or fully focused on the methods for detection, identification, and quantification of MPs.<sup>10–13,15,62–67</sup> Already in 2012, Hidalgo

Ruz et al. highlighted the importance of chemical analysis for reliable MP identification, but only FTIR spectroscopy was applied at that time.<sup>63</sup> Advances in the development and application of both spectroscopic and thermoanalytical approaches were then reflected in the later reviews. In particular, Primpke et al. recently presented a critical assessment of analytical methods with the focus on harmonized and cost-efficient analysis of MPs.<sup>67</sup> In the last three years, more and more attention has been paid to the chemical analysis of small microplastic and also nanoplastic particles.<sup>5,7,14,68,69</sup> However, the analytical challenges for reliable and representative chemical analysis of NMPs and possible solutions were only partially addressed until now. Also, the applicability and complementarity of different mass-based and particle-based methods as well as their automation, validation, and harmonization were insufficiently discussed.

The principal aims of the present review are (i) to point out the challenges in microplastic and nanoplastic studies, (ii) to critically assess the methods applicable for reliable and representative chemical analysis of these particles, and (iii) to discuss perspectives within and beyond the NMP research field. Therefore, first the advantages and limitations of both mass-based and particle-based approaches for the identification and quantification of MPs are discussed, with the focus on sensitivity and lower size limit for detection as well as on automation and high throughput analysis. Besides well-established methods and their applications for the analysis of model and real samples, new and promising techniques are presented. Then the complementarity of different analytical methods for the comprehensive characterization of MPs is highlighted. Special part of the review is devoted to the rapidly progressing field of nanoplastic studies, with a particular focus on small masses and sizes of NPLs. Finally, efforts for the validation, harmonization, and standardization of NMP studies are analyzed, and an outlook for applications of the advanced methods for the analysis of plastic and nonplastic micro- and nanoparticles is presented.

## 2. CHEMICAL ANALYSIS OF MICROPLASTICS

### 2.1. Challenges and Objectives

The complex nature of MPs is characterized by at least five dimensions that have to be considered in the analysis of these tiny particles:

- Broad size range, i.e., 1  $\mu\text{m}$  to 1 mm (and up to 5 mm for large MPs).
- Different polymer types with various chemical composition (including conventional and biopolymers of different structure and density).
- Different shapes (spheres, irregular particles, fibers, films, foams).
- Various additives (antioxidants, light stabilizer, plasticizer, flame retardants, pigments, etc.), weathering products and sorbed contaminants (persistent organic pollutants, antibiotics, heavy metals, etc.).
- Different aging state (primary and secondary MPs, biofouling), surface charge, and hydrophobicity.

Therefore, taking into account the diversity of MPs and also the broad concentration range, expressed in terms of MP mass and particle numbers in real samples (which can vary by 10 orders of magnitude, e.g.,  $10^{-2}$ – $10^8$  MPs/ $\text{m}^3$  for freshwater and drinking water samples<sup>73</sup>), we are facing the following challenges for the analysis of MPs:

- Depending on the pollution level of different media (water, soil, air, etc.) with MPs and the desired information (MP mass- or number of particle and size range), which defines the choice of detection method, the sample size (volume or mass) can vary significantly and has to be representative. Because substantially more particles are expected in smaller size ranges, small sample sizes can be sufficient for the determination of particle numbers down to the lower  $\mu$ -range. However, if also larger particles and/or mass are of interest, larger sample size will be required.
- The identification and quantification of MPs in complex samples may resemble searching for a needle in a haystack, thus requiring the preconcentration of the sample (e.g., via filtration) and efficient removal of (in)organic matrix.
- Sensitive methods are necessary for chemical identification and quantification of MPs. While many methods provide reliable identification of polymers (and additives), the quantification is either mass-based or particle-based (delivering information on MP particle number, size/size distribution and shape). Furthermore, the characterization of specific properties/compounds (degradation state, surface properties, additives, products of weathering, sorbed chemicals, etc.) needs additional method(s). Hence, depending on desired information, one method or a combination of several methods are required.
- The validation of methods, their comparison, harmonization, and standardization is inevitable in order to ensure the reliable results on the contamination of different media with MP particles. For this purpose, suitable reference materials are needed. However, the reference materials which resemble MP particles found in real samples (including variety of polymer types, broad size range, different shapes, and aging state) are still lacking.
- The ubiquity of plastics makes indispensable the measures to prevent the contamination during the entire analytical procedure (sampling, sample storage, and preparation as well as detection).

It has been widely recognized that the choice of an appropriate method or method combination strictly depends on the research questions and objectives of the study.<sup>20,62,70</sup> For the monitoring and modeling, the information on MP mass can be sufficient. In this case, destructive mass-based methods which provide information on polymer content in the sample regardless of particle number, size, and shape can be suitable. Using mass-based methods, one should keep in mind that a few large particles overprint many small particles, i.e., small particles contribute only slightly to the mass.<sup>20</sup> If more detailed information is needed, e.g., for the understanding of the transport and fate of MPs as well as their impact on the environment and human health, the nondestructive particle-based methods can be applied. These methods allow for the chemical identification and quantification of MPs, providing information on the particle number, size/size distribution (the size range is determined by the detection limit of the method) and shape. The characterization of specific properties/compounds requires additional dedicated methods. Thus, a comprehensive analysis of MP particles with diverse characteristics cannot be performed with a single method and assumes a combination of analytical approaches. Last but not least,

depending on the detection method(s) of choice, complexity of samples to be analyzed and the level of MP contamination, suitable methods for the sampling, and sample preparation have to be considered in order to achieve representative and reliable results.

## 2.2. Mass-based Methods for Analysis of Microplastics

### 2.2.1. Thermal Degradation Combined with GC/MS.

Thermal degradation methods are shown to be very efficient for the identification and quantification of plastic contamination in environmental and food samples. These methods rely on degradation (most often pyrolysis, Py) products generated at defined temperatures under the exclusion of oxygen. After gas chromatographic (GC) separation, the so-called pyrogram represents fingerprint of the respective polymer. Using mass spectrometry (MS), the volatile degradation products can be subsequently identified on molecular level. On the basis of specific pyrolysis products, the determination of polymer mass is possible, hence the simultaneous identification and quantification of different MP in complex environmental samples can be performed. This information for different polymers is indispensable for mass balances and modeling as well as for the future legislation. Furthermore, these methods allow for the detection of plastic-associated additives as well as of degradation byproducts and, hence, they deliver the data necessary for reliable risk assessment of MP for the environment and human health. However, these mass-related data have to be considered as bulk values of a given plastic type, e.g., PS, disregarding if it is a pure polymer or a share of a copolymer, and are independent from any kind of particle characteristics such as size, shape, form, etc.<sup>67,71</sup>

Already in the year 1966 (almost 40 years before the term “microplastics” was introduced), Thompson et al. used a technique combining pyrolysis and chromatography for the detection of vehicle tire abrasion products in roadway.<sup>72</sup> The presence of PS as anthropogenic pollutant in sediment and soil analyzed by Py-GC/MS was first reported by Leeuw et al. in 1986.<sup>73</sup> In following studies, Fabbri and colloquies focused on the Py-GC/MS analysis of PS and PVC as well as poly(vinyl acetate) (PVA), polybutadiene (PB), poly(acrylonitrile-*co*-styrene-*co*-butadiene) (ABS), styrene-butadiene random (SBR), and block (SBS) copolymers in coastal sediments.<sup>74–76</sup> Meanwhile, these methods have been widely applied for the MP analysis in marine and freshwater environment (sediments,<sup>77–84</sup> water,<sup>80,85–89</sup> and biota<sup>71,80,90,91</sup>), sewage sludge,<sup>82,92</sup> airborne emissions from laundry dryers,<sup>93</sup> soil,<sup>94,95</sup> commercial sea salt,<sup>54,96</sup> and drinking water.<sup>53</sup> Recently, the potential of Py-GC/MS for the analysis of nanoplastics in model and real samples has been demonstrated,<sup>97–100</sup> as will be discussed in more details in section 3.3 “Mass-based Methods for Analysis of Nanoplastics”.

With respect to the applied instrumentation, there are two different types of pyrolysis unit and its coupling with gas chromatograph, namely (i) Py-GC/MS and (ii) TED (thermo-extraction and desorption) GC/MS.

**2.2.1.1. Pyrolysis-based Methods.** Generally, different working modes can be applied by Py-GC/MS, i.e., (i) “single-shot” analysis, (ii) “double-shot” (or “multi-shot”) analysis, (iii) evolved gas analysis (EGA-MS), and (iv) reactive or thermochemolysis Py-GC/MS.<sup>101</sup>

By “single-shot” mode, the pyrolysis is performed at a distinct temperature, usually above 500 °C. The sample temperature is rapidly (<20 ms for modern systems) elevated from ambient to

the pyrolysis temperature. The macromolecules are almost instantly fragmented in the pyrolyzer, and pyrolysis products are then separated in the GC column and used for the MS-based detection of polymer(s) and some additives.<sup>67,81,101</sup>

The “double-shot” (or “multi-shot”) mode or so-called thermodesorption (TD) Py-GC/MS involves several (at least two) steps and allows for the sequential analysis of different compounds, e.g., volatile (low molecular weight compounds released at low temperature during a thermal desorption step) and nonvolatile (decomposition fragments of the macromolecules formed at high temperature(s) during pyrolysis step). This mode has shown to be efficient for the characterization of different volatile and nonvolatile polymer additives<sup>102,103</sup> and even sorbed organic compounds<sup>104</sup> combined with the identification of polymer(s) based on the analysis of pyrolysis products.<sup>77,78</sup> Furthermore, the “double-shot” mode can be used for the effective thermal desorption of potentially interfering organic compounds from the complex organic rich samples before the pyrolysis step, enabling the improved identification and quantification of MP decomposition products.<sup>105</sup>

EGA-MS involves the separation of degradation products during slow temperature ramp (which leads to a sequential macromolecules degradation in the pyrolyzer) and the replacement of the chromatographic column by a short and narrow (2.5 m, 0.15 mm i.d.) deactivated silica capillary tube without a stationary phase, to connect directly GC injector and MS detector.<sup>101</sup>

Thermochemolysis Py-GC/MS implies the addition of a derivatization agent, e.g., tetramethylammonium hydroxide (TMAH) solution, which induces a reaction of ester- and ether-cleavage followed by methylation<sup>67,101</sup> and help to significantly improve the detection sensitivity for some polymers (e.g., PET and PC).<sup>71</sup>

For the polymer identification by means of Py-GC/MS, an individual (plastic) particle or a representative sample fraction ( $\mu\text{g}$ -range) is transferred into a pyrolyzer target. Several types of pyrolyzers and respective targets are available, having different dimensions and, hence, sample capacity, namely (i) filament pyrolyzers, (ii) Curie point (CP) pyrolyzers, and (iii) micro furnace (MF) pyrolyzers.<sup>67</sup> Filament pyrolyzers use open or semiclosed quartz tubes (system-dependent variable dimensions approximately  $\varnothing$  0.2–1.3 cm and different length,<sup>77–79,106</sup> placed in a platinum coil. CP pyrolyzers utilize semiclosed ferromagnetic targets (typical dimensions  $\varnothing$  2 mm, 8 mm height).<sup>71</sup> MF pyrolyzers use stainless steel cups (typical dimensions approximately  $\varnothing$  4 mm, 8 mm height,<sup>54,81,96</sup> and, hence, offer favorable larger sample capacity compared to CP pyrolyzers.<sup>96</sup> In each case, the sample is heated to a defined temperature in an inert atmosphere (usually He or N<sub>2</sub>), which is also utilized as carrier gas for GC separation.<sup>67</sup>

For the reliable identification and quantification of polymers based on decomposition products, Py-GC/MS systems are usually equipped with quadrupole mass analyzer. Significantly increased detection capacity can be achieved by GC time-of-flight mass spectrometry (Py-GC/ToF) as recently reported by Sullivan et al.<sup>100</sup>

Depending on the complexity of pyrolysis products as well as decomposition mechanisms and kinetics, the respective pyrograms differ significantly among various polymer types. The pyrogram of individual polymer can be highly complex (e.g., PE, PP, PET) over moderate (e.g., PS) to simple (e.g., PMMA).<sup>67,107,108</sup>

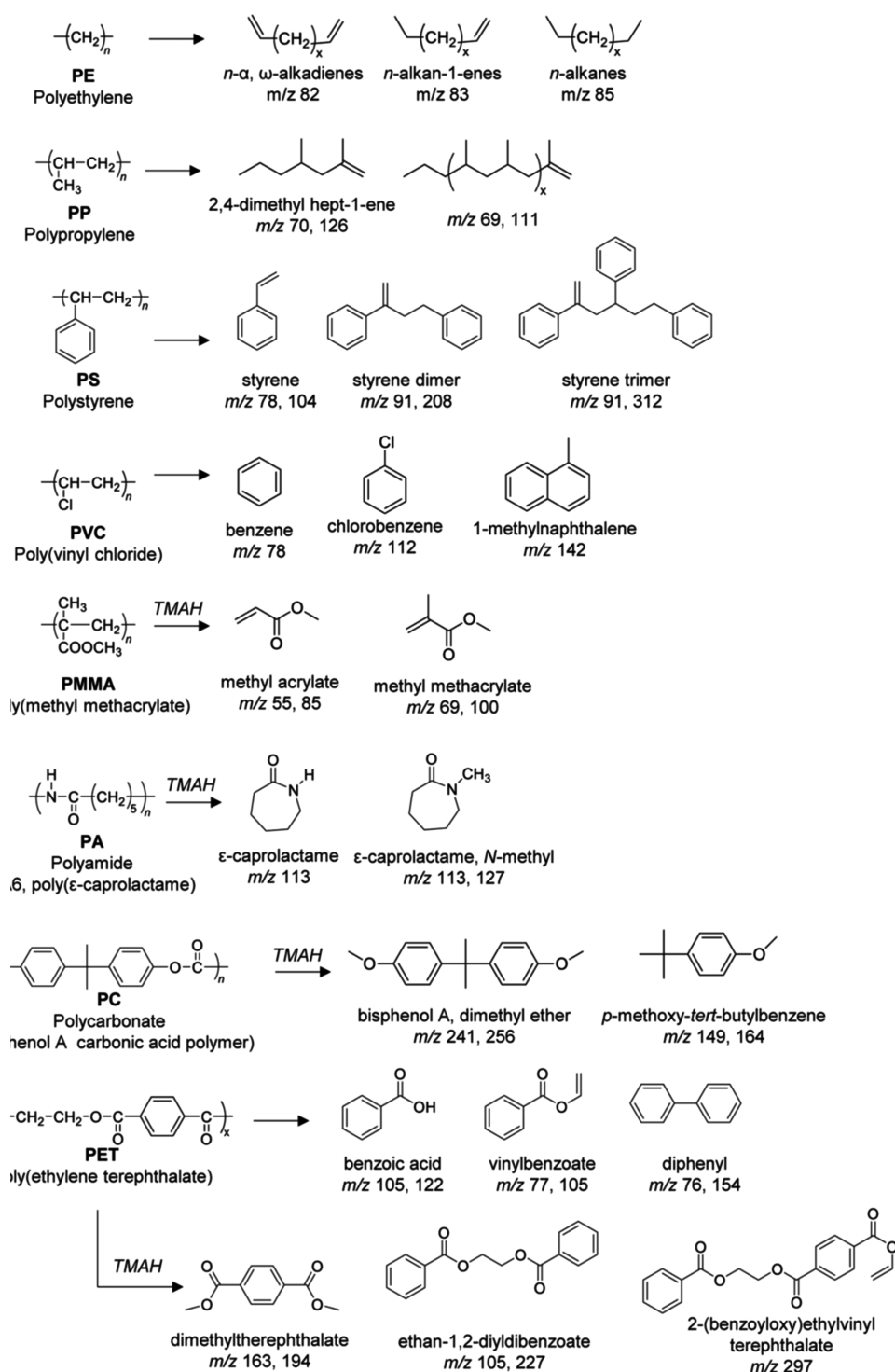


**Figure 1.** Molecular structures of polymers investigated for MPs and of their main pyrolysis products, with corresponding  $m/z$  (TMAH: pyrolysis products produced in the presence of tetramethylammonium hydroxide). Reproduced with permission from ref 108. Copyright 2020 Elsevier.

Besides monomers and oligomers of the respective polymers which are usually present, pyrolytic reaction products, determined by the chemical reactivity of the polymer, are built (Figure 1).<sup>108</sup> The pyrograms obtained reproducibly provide a unique signature pattern (fingerprint) characteristic for a given polymer which can be compared with commercial or customer made pyrogram databases. The identification of additives requires extensive compound knowledge (inclusively their

thermal behavior) and appropriate mass spectrometric chemical libraries.<sup>67</sup>

**2.2.1.1.1. Identification of Individual Particles and Associated Additives.** The Py-GC/MS has been applied by several groups for the identification of individual (plastic) particles isolated from marine and river sediments, surface water, and biota.<sup>77–80,89,90</sup> Fries and colleagues analyzed marine microplastic particles down to approximately 100  $\mu\text{m}$ , as well as associated additives, using “double-shot” mode (TD-Py-GC/

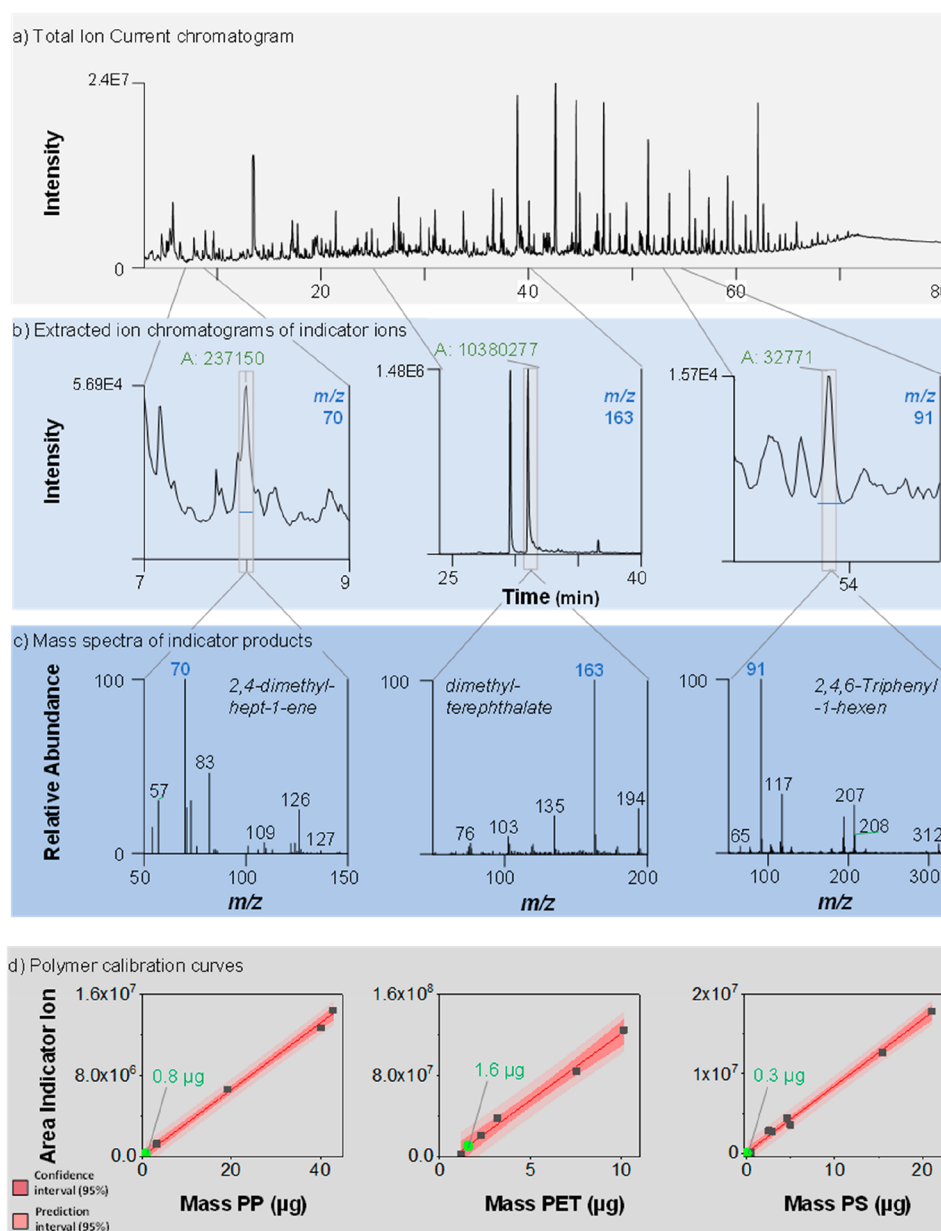


**Figure 2.** Example for the quantification procedure of three polymers (PP, PET, and PS) in seawater filter. (a) Total ion current of the sample. (b) Sections of the respective indicator ion chromatograms with integrated signals. (c) Respective full mass spectra of the individual pyrolysis products. (d) Calibration curves from pure polymers for the quantification of the respective polymer cluster. Reproduced with permission from ref 110 (supporting information). Copyright 2021 American Chemical Society.

MS). They were able to identify different plastic types (including PE, PP, PS, PET, PVC, PA) and detect many associated additives (e.g., benzophenone, 1,2-benzenedicarboxylic acid, dimethyl phthalate, diethylhexyl phthalate, dibutyl phthalate, diethyl phthalate, phenol, and 2,4-di-*tert*-butylphenol).<sup>77,78</sup> Although the analysis of individual particles by Py-GC/MS is rather time-consuming, namely it takes a half an hour or even more for each GC-MS run (compared to minutes or even less for the spectroscopic analysis with, e.g.,  $\mu$ -FTIR), it allows for the proper identification of particles and provide additional valuable information on additives and copolymers. It has been recently illustrated by Käppler et al.<sup>81</sup> and Hermabessiere et al.,<sup>80</sup> who compared Py-GC/MS results with FTIR and Raman microspectroscopy data, respectively (see section 2.4 “Combination of Different Methods for Comprehensive MP Analysis”). Hence,

the complementary analysis of individual particles can be performed by the combination of Py-GC/MS and spectroscopic methods. Furthermore, the application of EGA-MS has a potential for the time efficient identification of additives and polymers.<sup>67</sup> While Py-GC/MS is applicable for the analysis of individual particles, the real power of Py-GC/MS for the simultaneous identification and quantification of MP for complex samples has been recently recognized (refs 53, 54, 71, 82, 85, 94–96, 105, 106, 109, and 110).

**2.2.1.1.2. Simultaneous Identification and Quantification of Polymers from Complex Samples.** Depending on the amount of polymers and matrix composition, the samples can be analyzed directly<sup>94,106</sup> or after one or several sample preparation step(s) which can include chemical and enzymatic digestion of organic matrix and removal inorganic matrix by density

separation.<sup>53,71,85,96,97,109,110</sup> Alternatively, solvent extraction<sup>83</sup> and pressured liquid extraction (PLE)<sup>82,105</sup> can be applied for the preconcentration of polymers from complex matrices before Py-GC/MS analysis. Furthermore, the applicability of cloud point extraction (CPE) has been reported for the preconcentration of nanoplastics from water samples.<sup>99</sup>

The detection of MPs directly in bulk soil and soil fractions has been reported by Watteau et al.<sup>94</sup> The application of approximately 0.5–1 mg sample allows for detection of specific features of plastic (e.g., typical for PS) differing from soil organic matter. Funk et al. have performed the identification and quantification of MPs by Py-GC/MS in wastewater after cascade filtration without sample preparation besides the sample extraction and drying. They applied 300–400  $\mu\text{g}$  of sample and reported on LOQs of 0.03  $\mu\text{g}$  and 1  $\mu\text{g}$  absolute for PS and PE, respectively.<sup>106</sup>

To improve the sensitivity of Py-GC/MS for the quantification of different polymers in complex samples, the removal of organic and inorganic matrices has shown to be efficient. After the sample preparation and drying, MPs deposited on a filter are pyrolyzed; for this purpose, the pieces or even the entire glass fiber filter with a  $\varnothing$  15 mm can be directly inserted in pyrolyzer for the analysis.<sup>53,96,97,109</sup>

The preconcentration of polymers from complex matrices before Py-GC/MS analysis can be also performed by liquid extraction of soluble polymers.<sup>82,83,95,105</sup> Dierkes et al. developed a method combining PLE and Py-GC/MS for the MP quantification in environmental samples.<sup>82</sup> The extraction includes a pre-extraction step via methanol to reduce disturbing matrix effects followed by a subsequent PLE using tetrahydrofuran (THF). For the most frequently used synthetic polymers (PE, PP, PS) LOQs down to 0.007 mg/g have been achieved. Okoffo et al. have combined PLE (using dichloromethane, DCM) and “double-shot” Py-GC/MS for the identification and quantification of PE, PP, PS, PET, PVC, PC, and PMMA in biosolids (treated sewage sludge). The thermal desorption of potentially interfering coextracted compounds before pyrolysis has found to be very efficient for the MP analysis in complex organic rich samples. The validation of the method has revealed a linear range between 0.01  $\mu\text{g}$  and 2  $\mu\text{g}$  of polymer absolute, the found MP contamination of biosolids ranged between 0.1 mg/g and 4.1 mg/g dry weight across the samples.<sup>105</sup> Furthermore, the applicability of 1,2,4-trichlorobenzene (TCB) for the dissolving of PE, PP, and PS in soil for subsequent Py-GC/MS analysis, providing instrumental detection limits of 1–86 ng absolute and method detection limits of 1–86  $\mu\text{g}/\text{g}$  has been shown.<sup>95</sup> Moreover, in combination with solvent extraction (using DCM) followed by gel permeation chromatography (GPC), in order to separate higher and lower molecular weight fractions, Py-GC/MS can be efficiently applied for the characterization not only of MPs but also of their degradation byproducts in costal sediments, as was reported by Ceccarini et al.<sup>83</sup> The authors found up to 30 mg MPs (essentially PS and polyolefin byproducts) in 1 kg sand.

Recently the efficiency of cloud point extraction in combination with Py-GC/MS for the analysis of nanoplastics in environmental waters has been demonstrated. Using Triton X-45-based CPE, an enrichment factor up to 500 was obtained for PS (approximately 65 nm) and PMMA (approximately 85 nm) nanoplastics, without disturbing their original morphology and sizes.<sup>99</sup>

While the proper sample preparation can significantly improve the performance of Py-GC/MS analysis, the reliable

identification and quantification of polymers in complex mixtures remains a most challenging and essential part.

The identification can be realized based on the specific pyrograms of characteristic and selective degradation products, representing different polymers. The relative intensity of indicator compounds varies from polymer to polymer, strongly influencing the detection sensitivity for the respective polymer. Because ion chromatograms can enhance the detection sensitivity, they are often applied for the detection of polymers in complex samples (Figure 2).<sup>110</sup> The ion chromatograms represent the ion current over time, extracted for a selected fragment ion of an indicator compound from mass spectrometric data.

In this context, the selection of characteristic indicator products and their respective ions for each polymer based on their intensity and specificity becomes essential, whereof the latter is decisive for the proper identification and quantification of distinct polymer.<sup>67</sup> For example, PS has two favored indicator compounds, styrene and its trimer (5-hexene-1,3,5-triyltribenzene), which differ in specificity and abundance. While the former is very abundant but nonspecific, the opposite is true for the latter. Therefore, styrene is a perfect indicator compound for PS quantification in matrix-free samples. However, in natural matrices, it may be generated from several anthropogenic polymers and natural compounds, e.g., chitin. Therefore, the use of less intensive styrene trimer is more reliable in this case because its generation can be unequivocally linked to the presence of PS in the sample.<sup>67,71</sup> For the identification and quantification of PE, matrix interfered *n*-alkanes and *n*-alkenes can be chosen. Although biogenic material rich in long alkyl chains (e.g., natural fats and waxes) tends to release *n*-alkanes and *n*-alkenes during pyrolysis, their generation can be minimized by the digestive treatment of samples. Furthermore, the interferences decrease strongly with increasing carbon numbers, *n*-alkenes. Therefore, *n*-alkenes and *n*-alkanes from C<sub>16</sub> to C<sub>26</sub> found to be most appropriate for the calibration and PE analysis.<sup>71</sup> Generally, the presence of further polymer specific degradation products ensures polymer identification.<sup>67</sup> For the extended list of indicator compounds and respective indicator ions, allowing for the simultaneous identification and quantification of different types of plastics using thermal decomposition methods, the reader is referred to recent publication by Primpke et al. (see table 1 in ref 67).

For the reliable quantification of MPs in complex samples, the preconcentration of polymers via the removal of accompanying (in)organic matrix or extraction of polymers by liquid solvents is highly recommended in order to avoid or at least minimize interferences of nonplastic pyrolysis products with the indicator ions and to prevent surface interactions and contaminations inside the pyrolysis system. The pyrolysis performed at reproducible conditions results in the ion chromatogram, where the area under the signals of the indicator ions correlates with the mass of the polymer present in the sample vessel. This correlation is linear in a system-dependent concentration range and can be used for the external calibration of the respective polymers. The addition of an internal standard(s) will further improve the data quality. Different substances can be used for this purpose, e.g., deuterated compounds (styrene,<sup>106</sup> polystyrene,<sup>111</sup> and chlorobenzene<sup>100</sup>) or a mixture of 9-dodecyl-1,2,3,4,5,6,7,8-octahydro anthracene, anthracene-d10, androstane, and cholanic acid.<sup>96,110,112</sup>

An excellent example for the simultaneous identification and quantification of PP, PET, and PS in a complex seawater sample

Peak Assignment	Structure	Substance	Characteristic fragment ions	Retention time in min	Parental Elastomer
		Styrene	104, 78, 51	7.2	SBR
		Methylstyrene	118, 103, 78	9.6	
		Cyclopentylbenzene	117, 104, 146, 91	16.6	
		Cyclopentenylbenzene	144, 129, 115	17.8	
SB		Cyclohexenylbenzene	104, 158, 129, 115	19.6	
SBB		Phenyl-[4.4.0]bicyclodecene	104, 91, 156, 212	26.8	
But2		Vinylcyclohexene	79, 54, 93, 108	5.6-6.4	SBR, BR
But3		Trimers of Butadiene & Homologues	91, 148, 162, 176	13.1-21.7	BR
Iso2		Dipentene	68, 93, 121, 136	11.0	NR
Iso3		Trimers of Isoprene	119, 162, 189, 204	21.5-23.3	
Iso4		Tetramers of Isoprene	121, 93, 134, 272	31.0-36.0	

**Figure 3.** Summary of identified decomposition products for elastomer and tire materials using TED-GC/MS. Reproduced with permission from ref 111. Copyright 2018 American Chemical Society.

after matrix removal has been presented by Dibke, Fischer, and Scholz-Böttcher (Figure 2).<sup>110</sup> Figure 2a shows the section of interest from the resulting total ion chromatogram (pyrogram) and represents the complexity of an environmental sample with high diversity of organic pyrolysis products. Characteristic pyrolysis product for PP, namely 2,4-dimethyl-hept-1-ene can be identified via its mass spectrum, and the selectively extracted as ion chromatogram of its indicator ion  $m/z$  70. Integration of the respective signal results in an area of 237 150 units (Figure 2b,c). This corresponds to 0.8 mg of PP, determined via the external calibration (Figure 2d). For PET and PS, the quantification was performed using dimethylterephthalate (indicator ion  $m/z$  163) and styrene trimer (5-hexene-1,3,5-triyltribenzene, indicator ion  $m/z$  91), respectively.<sup>110</sup>

It is worth mentioning that despite the destructive character of thermal degradation methods hampering any remeasurements, the resulting pyrograms can be reanalyzed retrospectively for further indicator ions of new polymers. By applying internal standards, even semiquantitative data of these new polymers can be obtained.<sup>67</sup> For example, recently Goßmann et al. retrospectively analyzed the Py-GC/MS data for complex environmental samples such as road dust, fresh water and marine sediments, blue mussels, and marine salts, in order to get information on the contamination with tire wear particles which are assumed to be the predominant source of environmental MPs.<sup>113</sup> The authors developed an approach to differentiate between car and truck tire wear and found the dominance of car compared to truck tire wear mass loads in all analyzed samples (ratios of car to truck tire wear were up to 16 to 1). While detected TWP concentrations in road dust significantly exceeded those of thermoplastic (e.g., PE, PP, PS) MP (around 5 g of TWP vs 0.3 g of MP per kg road dust, dry weight), the

samples collected far away from TWP sources show lower or even no TWP contamination. At the same time, thermoplastic polymers were still ubiquitously distributed.<sup>112</sup>

Generally, the detection sensitivity for distinct polymer in complex mixtures depends on the relative intensities of indicator products. Additionally, the quality of the organic matrix removal determines the polymer quantification in terms of general background and possible interferences. Furthermore, the solubility or nonsolubility (and hence the readability and repeatability of balance used) of the polymers has a direct impact on the calibration range of given polymer. For example, for the soluble PS the calibration down to 0.01  $\mu\text{m}$  can be performed. From this calibration LOD (S/N-ratio >3) of 3 and 59 ng for the prominent but unspecific pyrolysis product styrene monomer and for very specific but significantly weaker styrene-trimer, respectively, was calculated. The corresponding LOQ values (S/N-ratio >10) are 16 and 282 ng, respectively. The reported lower calibration points for PP and PA 6 are 0.3  $\mu\text{g}$  and 0.5  $\mu\text{g}$ , respectively.<sup>96</sup> Working with solid standards, the LOQ for Py-GC/MS can be set by available balance and ranges, dependent on the polymer type, between 0.7 and 1  $\mu\text{g}$  absolut.<sup>85</sup> Thus, practically the Py-GC/MS analysis can be performed with LOQ of 0.01–1  $\mu\text{g}$ , depending on polymer type and pyrolysis unit.<sup>20</sup>

It has to be mentioned that the direct pyrolytic products of some polymers (e.g., PET and PC) show high diversity and different polarity, leading to limited sensitivity and poor chromatography. To improve the method sensitivity for these polymers, thermochemolysis, e.g., by addition of TMAH can be applied. The latter induces a reaction of ester and ether-cleavage followed by methylation. The thermochemolysis products of PET and PC are more specific, resulting in improved sensitivity for these polymers. At the same time, the pyrolytic behavior for

most other polymers stayed unaffected. Thus, simultaneous quantification of PE, PP, PS, PET, PVC, PMMA, PC, PA 6, and methylene-diphenyldiisocyanate-PUR using online pyrolytic derivatization can be successfully performed.<sup>67,71,96</sup>

Taking into account the maximum sample capacity of the pyrolyzer ( $\mu\text{g}$ -range) as well as the expected content of MPs and the respective calibration range, the initial sample volume has to be adapted for the MP quantification with Py-GC-MS using preconcentration step(s).

The analysis of a significantly larger sample amount (mg-range) can be realized by applying thermo-extraction and desorption (TED) GC/MS.

**2.2.1.2. TED-GC/MS.** In the TED-GC/MS approach, a thermogravimetric analyzer (TGA) is utilized for the sample pyrolyzation under inert gas (usually  $\text{N}_2$ ) and controlled temperature-ramped conditions up to approximately 600 °C. Decomposition products are purged from the TGA and transferred through a heated coupling device to a solid-phase adsorber bar (containing e.g., polydimethylsiloxane, PDMS), which is coupled to the decomposition product gas flow only in certain temperature range(s). The temperature range of the trapped gases can be selected in advance, e.g., 25–650 °C or 350–600 °C. The first range is representative for all volatile pyrolysis products. The second is characteristic for most common polymers which have degradation temperatures above 350 °C but excludes a large share of pyrolysis products generated by thermo-labile organic matrix compounds.<sup>67,111</sup> After the solid phase is loaded with an excerpt of the decomposition products, the adsorber is transferred (manually<sup>91</sup> or utilizing autosampling robot<sup>111,114</sup>) to a thermal desorption unit (TDU) of the GC/MS instrument. In the TDU unit, the decomposition products are thermally desorbed and mobilized, cryo-focused in a cooled injection system, separated through a GC column, and measured quantitatively by MS.<sup>111</sup>

The TED-GC/MS has been first applied for the analysis of environmental samples (mussel and suspended particulate matter from river) spiked with PE and detection of this polymer down to 1 wt % by Dümchen et al. in 2015.<sup>91</sup> Meanwhile, TED-GC/MS has been established for the reliable quantification of different polymers in complex environmental matrices (samples from aquatic and terrestrial systems). The corresponding LOQ for PE, PP, and PS were about 10, 1, and 0.2  $\mu\text{g}$ , respectively.<sup>114</sup> Furthermore, applicability of TED-GC/MS for the analysis of tire wear content in environmental samples has been recently shown.<sup>111,115,116</sup> In highway street runoff samples, styrene butadiene rubber (SBR, major compound of passenger car tires, see Figure 3 for decomposition products of elastomer and tire materials) was found in the range 3.9–9.3 mg/g.<sup>111</sup> Thus, fast and simultaneous analysis of microplastics in environmental samples, including thermoplastic polymers and tire wear became possible. The analysis of natural rubbers (main elastomeric compound of truck tires) in environmental samples was found to be impossible using this approach because plant matter with similar decomposition products cannot be excluded from the sample. Recently the applicability of TED-GC/MS for the determination of the MP mass content in beverages filled in plastic bottles was demonstrated by Braun et al.<sup>117</sup> The authors developed a smart filter crucible as sampling and detection tool which allows for a filtration of MPs down to 5  $\mu\text{m}$ . Depending on beverages bottle type, MP contents below 0.01  $\mu\text{g}/\text{L}$  and up to 2  $\mu\text{g}/\text{L}$  were measured.

Compared to Py-GC/MS, TED-GC/MS is characterized by a significantly larger sample capacity, namely up to 100 mg (which

is about 200 times higher than used in Py-GC/MS). This is useful both for sensitivity (although LOD and LOQ for TED-GC/MS are lower compared with Pyr-GC/MS) and representativeness of the analysis of environmental samples (in which the matrix accounts for most of the overall mass). Thus, the MP analysis in highly polluted samples (containing more than 0.5–1 wt % for each type of polymer analyzed) can be performed without sample preparation which can be either not exhaustive or not simple to perform (e.g., for PET and PA).<sup>118</sup> However, sample-dependent organic matrix still can interfere the polymer quantification by the use of the entire temperature range 25–650 °C, and an adsorption cut out below 350 °C leads to losses of more thermolabile polymers like PVC.<sup>67</sup>

Because the expected MP content in the most real environmental and food samples is below 1 wt %, MP preconcentration per (cascade) filtration and removal of accompanying (in)organic matrices will improve the detection and quantification sensitivity of both Py-GC/MS and TED-GC/MS (as well as spectroscopic methods, as discussed later) for the analysis of environmental and food samples.<sup>20,91</sup> The removal of nonplastic organic matter will help to avoid their interference with the indicator ions as well as the contamination of the instrument. While the inorganic matrix has rather neglectable impact on the pyrogram, the lower amount of inorganic matrix will increase plastic/matrix ratio and, hence, improve the sensitivity of the method. Furthermore, it is strongly recommended to include an appropriate number of calibration standards as well as procedural blanks and occasional blank cups in the measurement series. The blank values will help to assess secondary contamination and possible memory effects and, if necessary, to make appropriate corrections to the measured values.<sup>67,119</sup>

Thus, thermoanalytical methods provide quantitative mass-based polymer-specific (and additive-specific) information on the MP contamination, independent of particle related information, i.e., number, size, shape, etc. These methods can be considered not as competitive but as complementary to spectroscopic methods (delivering quantitative particle-based information). Being destructive, thermoanalytical methods have to be applied after nondestructive spectroscopic analysis. The combination of mass-based and particle-based methods will enable performing of detailed comprehensive characterization of MPs, which is necessary for the reliable assessment of the MP impact on the environment and human health.

**2.2.2. Further Thermoanalytical Methods.** Recently, a new method for the chemical characterization of NMPs, which based on thermal desorption–proton transfer reaction-mass spectrometry (TD-PTR/MS, where hydronium ions generated from water vapor are used for the ionization of analytes) has been proposed by Materić et al.<sup>120</sup> The method, which is characterized by high sensitivity and high mass resolution, has been already widely used in the analysis of various complex organic mixtures in the environment, including real-time monitoring of volatile organic compounds, semivolatiles, and organic aerosols in air and dissolved organic matter (DOM) in environmental waters and ice.<sup>120,121</sup> The authors have reported on LOD of <1 ng for PS compound present in a sample and applied this method for (semi)quantification of NMPs in Alpine snow. The high sensitivity of the method allowed use of small volumes of samples (1 mL) and to carry out experiments without any preconcentration steps. Unique features in the high-resolution mass spectrum of different synthetic polymers were found to be suitable for fingerprinting, even when the samples

contain mixtures of other organic compounds, e.g., a positive fingerprint was detected when only 10 ng of PS was present within the DOM of snow. The analysis of melted cores showed the presence of PET, PVC, and polypropylene carbonate (PPC), but after the 0.2  $\mu\text{m}$  filtration, only PET was found, indicating that PET fibers represent the dominant form of airborne pollution. Although the recovery rates of mere 15% were estimated for PS<sup>120</sup> and interference by even minor impurities originating from different sources has to be considered,<sup>122</sup> the TD-PTR/MS method seems to have a potential for the sensitive analysis of NMPs.

The quantitative analysis of MP in complex matrices can be also performed by TGA-MS. David et al. developed a method for the quantification of PET in soil samples without pretreatment. Sample mixtures (ca. 50 mg) were pyrolyzed with a 5  $^{\circ}\text{C}/\text{min}$  ramp (40–1000  $^{\circ}\text{C}$ ), while sample mass loss and MS signal intensity of typical PET pyrolysis products were recorded. The reported LOD and LOQ were 0.07 and 1.72 wt % PET, respectively.<sup>123</sup> Furthermore, the analysis of gas evolved during TGA can be performed spectroscopically by applying TGA-FTIR.<sup>124,125</sup>

Another thermoanalytical approach useful for the determination of MP content in complex samples combines TGA and differential scanning calorimetry (DSC),<sup>20,126–131</sup> where endothermic phase transition temperatures can be utilized for the identification and quantification of polymers. Generally, this technique is applicable for polymer with crystalline components (PE, PP, PA, and PET), while the polymers without crystalline portion (e.g., PS) cannot be analyzed. Majewsky et al. have evaluated endothermic phase transition heat flows and peak temperatures of LDPE, PP, PET, PES, and PA by heating from 20 to 800  $^{\circ}\text{C}$  with 5  $^{\circ}\text{C}/\text{min}$  under  $\text{N}_2$  atmosphere.<sup>127</sup> In accordance with the literature, it was found that LDPE, PP, and PA exhibit low melting points with peak temperatures at around  $101 \pm 2$   $^{\circ}\text{C}$ ,  $164 \pm 1$  and  $216$   $^{\circ}\text{C}$ , and show no overlap with the other tested plastic types. The other polymers have peak temperatures between 250 and 261  $^{\circ}\text{C}$  and are largely overlaying each other. Because unambiguous polymer identification in the presence of multiple polymers with phase transition temperatures  $>200$   $^{\circ}\text{C}$  is challenging, the authors focused on the determination of PE and PP. They found LOD of 2.5 and 5 wt % for PE and PP, respectively, using defined mixtures of polymers and a total sample weight of 10 mg. The application of this approach for the analysis of MP in two wastewater effluent samples (after density separation and  $\text{H}_2\text{O}_2$  treatment for the removal of (in)organic matrices, size range 12–1000  $\mu\text{m}$ ) revealed 34% and 17% of PE in the remaining solid mass corresponding to 81 and 257  $\text{mg}/\text{m}^3$  of the MP contamination, respectively, while PP was not detected.<sup>127</sup>

Rodríguez Chialanza et al. investigated the performance of DSC for the analysis of LDPE, HDPE, PP, and PET and analyzed in details the influence of particle size on the DSC signal for polymer mixtures.<sup>128</sup> They used size fractions of 23–256, 256–645, and 645–1000  $\mu\text{m}$  (obtained by sieving) and found that the signals of four polymers were well distinguishable using 10  $^{\circ}\text{C}/\text{min}$  heating rate, as illustrated in Figure 4. However, both the identification and mass quantification of polymers (based on onset temperature and on heat flow, respectively) were strongly affected by particle size. Therefore, the authors recommended proper sample treatment, which includes sieving of suspended particles for the MP determination using DSC, and tested this approach for the analysis of seawater samples spiked with polymers.<sup>128</sup>

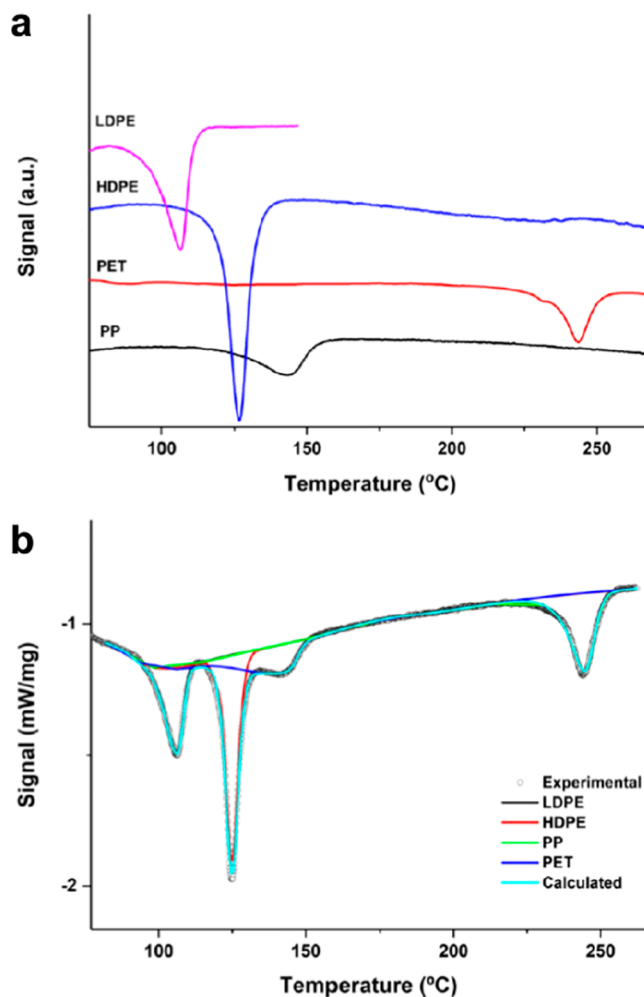


**Figure 4.** (a) DSC signals for different MPs of 300  $\mu\text{m}$  (2.0 mg). Conditions: heating rate, 10  $^{\circ}\text{C}/\text{min}$  under  $\text{N}_2$  atmosphere. (b) Multiplex fitting example of a polymer mixture with particle size in the range 23–256  $\mu\text{m}$ . Adapted with permission from ref 128. Copyright 2018 Springer.

Recently, Bitter and Lackner have presented extended study for the quantification of semicrystalline MP in industrial wastewaters.<sup>130</sup> By applying of modified DSC protocol proposed by Majewsky et al.<sup>127</sup> (including three steps in a  $\text{N}_2$  atmosphere: first heat-up step from 30 to 290  $^{\circ}\text{C}$  at 20  $^{\circ}\text{C}/\text{min}$  heating rate, subsequent cooling step from 290 to 0  $^{\circ}\text{C}$  at 10  $^{\circ}\text{C}/\text{min}$ , and second heat-up step from 0 to 290  $^{\circ}\text{C}$  at 5  $^{\circ}\text{C}/\text{min}$ ), they were able to analyze the samples treated with  $\text{H}_2\text{O}_2$  in the size ranges for small (10–1000  $\mu\text{m}$ ) and large (1000–5000  $\mu\text{m}$ ) MPs. PE and PP were found to be the most abundant polymers, but PA and PET were also present. As all three industrial sites had wastewater treatment plants (WWTPs), low mass concentrations for MPs ranging from 0.5 to 35.5  $\mu\text{g}/\text{L}$  were detected, that is comparable to the level for organic micropollutants in municipal WWTP effluents. The analysis of both influent and effluent for one exemplary industrial WWTP revealed the removal capacity of  $>99.99\%$ .<sup>130</sup>

**2.2.3. Additional Techniques for the Mass-based Analysis of Microplastics.** **2.2.3.1. MALDI-ToF/MS for Identification and Quantification of NMPs.** The matrix-assisted laser desorption/ionization time-of-flight mass spectrometry (MALDI-ToF/MS) allows for the soft ionization and wide mass detection and has been already recognized as a

powerful technique for the characterization of (bio)polymers.<sup>132</sup> Recently, the feasibility of MALDI-ToF/MS for the analysis of NMPs has been explored by Lin et al.<sup>133</sup> They combined this technique with thermal fragmentation and used PS particles of different molecular weight ( $M_w$ , ranging from 2200 to 280 000) and broad size range (from approximately 120 nm to 3 mm) as a model for NMPs. For the analysis, the thermally treated sample was dissolved with THF and mixed with dithranol and Ag trifluoroacetate solutions at a ratio of 1:10:1 (v/v), and 1  $\mu$ L of the mixture was measured. The PS NMPs were identified by fingerprint peaks in both low-mass ( $m/z$  90, 104, 128, 130, and 312–318) and high-mass regions (repeated peaks with  $\Delta m/z$  104 in the  $m/z$  range of 350–5000) and quantified using the styrene trimer peak at  $m/z$  315.3, which was more specifically linked to the presence of PS. The different ionization behaviors enabled the differentiation of NMPs with different molecular weights. Furthermore, the authors found that a simple thermal pretreatment at 380 °C can facilitate the fragmentation of PS and significantly enhanced the intensities of fingerprint peaks in low-mass regions, yielding LOD of 25 mg/L (25 ng absolute for the applied sample volume of 1  $\mu$ L; linear relationship between the peak intensity and the concentration from 25 to 400 mg/L) for PS NMPs. The developed method was applied for the quantification of PS in different sample matrices (e.g., fish samples spiked with PS particles, after the treatment with KOH and density separation for the matrix removal). Additionally, the method was adopted for the quantification of PET, where the thermal treatment led to the increase in the intensity of peak at  $m/z$  385 used for the quantification. The calibration for PET revealed linear relationship between the peak intensity at  $m/z$  385 and the PET concentration from 0.2 to 800 mg/L.<sup>133</sup> Thus, thermal fragmentation followed by MALDI-ToF/MS seems to be a promising approach for detailed studies which require the sensitive identification and quantification of NMPs. But because of the complexity of the method and the small sample size, the practical applicability of MALDI-ToF/MS for systematic and representative analysis of environmental and food samples is limited. Moreover, further research is needed to prove its feasibility for the analysis other polymer types.

#### 2.2.3.2. Analysis of Microplastics by ICP-based Methods.

An alternative analytical approach for the MPs analysis is focused on the detection and quantification of their individual chemical components, e.g., trace elements (after microwave-assisted acid digestion of the samples). For this purpose, the methods which are widely used for the trace analysis in water, environmental, and food chemistry, namely inductively coupled plasma mass spectrometry (ICP-MS) and ICP optical emission spectrometry (ICP-OES) are more and more frequently applied in the field of MP studies.<sup>115,131,134–137</sup> The trace elements are mostly associated with the use of additives which are essential for the tailoring of plastic product properties to variety of needs and applications. Additives are used for the production of the polymer (e.g., catalysts, agents for vulcanization, curing, or blowing), for achievement of certain physical properties of the product (e.g., pigments, dyes, plasticizers), for safety and stability purposes (e.g., flame retardants, heat stabilizers, photo stabilizers, antioxidants, biocides), for better processability of raw materials (e.g., slip agents, lubricants), or for cost reduction (e.g., calcium carbonate or silica are used as fillers).<sup>136,138</sup> The amount of used additives is strongly related to the application field. For example, only a limited number of additives are permitted for materials in contact with food, whereas a high variety of both organic and inorganic additives are utilized for

production of construction materials and tires. Elements such as Fe, Ti, and Cu are frequently included in pigments, whereas Br and Zn in flame retardants. The latter element is also a component of tires. Furthermore, metals can also be present in plastics as a relic of previous products due to recycling processes.<sup>20,136,139</sup> In this light, Wang et al. applied ICP-MS for the analysis of MPs (identified by  $\mu$ -FTIR) in surface sediments and found Ni, Cd, Pb, Cu, Zn, and Ti (40–55 mg of separated MPs were analyzed).<sup>135</sup> On the basis of data from the long-term sorption of metals by MPs and a comparison of metal burden for MPs from the environment and fresh plastic products, the authors assumed that the majority of heavy metals carried by MPs were derived from inherent load.<sup>135</sup> Wijesekara et al. reported on the quantitative analysis of biosolids-derived microbeads by ICP-MS.<sup>140</sup> They revealed the presence of trace metals including Cd (2.34 ng/g), Cu (180.64 ng/g), Ni (12.69 ng/g), Pb (1.17 ng/g), Sb (14.43 ng/g), and Zn (178.03 ng/g). Moreover, the authors found that surface modified microbeads were capable of adsorbing Cu compared to the pure microbeads, which was attributed to the complexation of Cu with dissolved organic matter associated with the microbeads in the matrix.<sup>140</sup> The application of ICP-OES and ICP-MS for the analysis of marine MPs (identified by  $\mu$ -FTIR) has been presented by Kühn et al.<sup>131</sup> In total, 13 elements (Al, Ba, Cd, Co, Cr, Cu, Fe, Mn, Mo, Ni, Pb, V, and Zn) were detected by both methods (subsamples of 3 g were digested for the analysis), however, the determined concentrations were always higher with ICP-MS than with ICP-OES. Furthermore, the elements identified at very low concentrations by ICP-MS (e.g., Co and V with 3.0 and 3.2  $\mu$ g/g, respectively) were below the detection limits of ICP-OES.<sup>131</sup> Klöckner et al. have presented recently an extended study on metals and metalloids (As, Ba, Bi, Cd, Co, Cr, Cu, Fe, Mn, Ni, Pb, Sb, Sn, and Zn) for plastic samples from different origins, including household items and electric supplies as well as marine, urban, and lake litter and tire tread rubber samples.<sup>136</sup> Total metal contents found ranged from 3  $\mu$ g/kg up to 7 g/kg. The median content of most metals was below 1 mg/kg and did not exceed legal limits. Fe and Zn were the metals with the highest contents, with medians of approximately 50 mg/kg. Investigations on the potential origin of the metals in plastics revealed that pigments were the most likely source. Multivariate statistics ( $k$ -means clustering and principal component analysis, PCA) did not reveal a polymer-specific metal composition, except for samples of tire tread rubber that was obtained from passenger car tires.<sup>136</sup> On the basis of the latter finding, this group developed a method for the analysis of tire and road wear particles (TRWPs) from road environment, which allows for the quantification and assessment of particle dynamics by Zn determination after density separation.<sup>115</sup> Zn was identified as the most suitable elemental marker for TRWPs, due to its high concentration (approximately 1 wt %) in tire tread and the possibility of separation from other Zn sources. The mean concentration of 21 tire samples was  $8.7 \pm 2.0$  mg Zn/g. The measured Zn concentration in the light fraction of the solids (which floated during density separation, the density of the separation solution prepared using Na polytungstate was adjusted to 1.9 g/cm<sup>3</sup>) was used to calculate the content of tire abrasion in the total environmental sample. The estimated TRWP concentrations in particulate matter collected in two road runoff treatment systems ranged from 0.38 to 150 mg TRWP/g. These values were in agreement with the data obtained by TED-GC/MS, where the markers for SBR were used for the quantification of TRWP mass in the samples.<sup>115</sup> The

further study presented by Klöckner et al. revealed that the quantification of TRWPs via density separation and Zn analysis may overestimate TRWPs, if particulate Zn from other sources is present in the density range  $<1.9 \text{ g/cm}^3$ . Such sources could, for example, be Zn bound to or contained within organic particles of low density. On the other hand, it was found that aging of TRWPs can lead to the increase of their particle density and hence to the incomplete enrichment of TRWPs in the light fraction. Together with possible leaching of Zn from TRWPs, it can result in an underestimation of TRWP.<sup>116</sup>

The applicability of ICP-MS operated in single-particle (SP) mode for the detection of MPs has been recently tested by Bolea-Fernandez.<sup>141</sup> The technique being frequently used for the characterization of metallic nanoparticles, has been adopted for the analysis of PS microspheres of 1 and 2.5  $\mu\text{m}$  in diameter. The developed approach relies on the ultrafast monitoring of transient signals (with a dwell time of 100  $\mu\text{s}$ ) in SP mode and registering the signal spikes produced by individual micro-particles by monitoring the signal intensity at a mass-to-charge ratio ( $m/z$ ) of 13 ( $^{13}\text{C}^+$ ). This stable isotope ion was selected in order to minimize the background signal obtained by monitoring of  $^{12}\text{C}^+$ . Additionally, a low flow rate of only 10 mL/min was applied to increase the signal-to-background ratio (MP signal spikes versus background signal coming from dissolved C in each “time window”). The accuracy of the number-based concentration results (particle number densities) has been assessed by comparing the number of events detected by the monitoring of  $^{13}\text{C}^+$  and of  $^{165}\text{Ho}^+$  for 2.5  $\mu\text{m}$  lanthanide-doped PS beads. Although the instrument optimization and reduction of the background (caused by dissolved atmospheric  $\text{CO}_2$  and other C species present in the samples of interest) are mandatory for the future establishment of this technique and the identification of different polymer types based on  $^{13}\text{C}^+$  ions is excluded, the authors have concluded that SP-ICP-MS could provide information on both the size distribution and mass concentration of MPs.<sup>141</sup> The feasibility of this technique for the determination of MPs in real samples has been recently reported by Laborda et al.<sup>142</sup> The analysis of  $^{13}\text{C}^+$  ions for reference PS particles in the size range of 1.2–5  $\mu\text{m}$  was achieved using microsecond dwell times. The developed approach allowed for the detection of MPs, their quantification using aqueous dissolved carbon standards, and the measurement of the size distribution of the detected particles. LOD of 100 particles/mL was achieved for an acquisition time of 5 min. The method was applied for the screening of MPs in personal care products and those released from food packaging materials. The chemical identity of the detected MPs was confirmed by ATR-FTIR spectroscopy. The authors found high MPs number for personal care products (e.g.,  $3.6 \times 10^7 \pm 0.2 \times 10^7$  particles/g and  $4.4 \times 10^{10} \pm 0.5 \times 10^{10}$  particles/g for exfoliating hair conditioner and facial exfoliating cleanser, respectively). However, the authors pointed out that the reported particle content corresponds to the particles detected by SP-ICP-MS under the conditions selected, which were limited to particles over ca. 1  $\mu\text{m}$  and below 10  $\mu\text{m}$ . Moreover, particles bigger 2–3  $\mu\text{m}$  were underestimated because they were nebulized with lower efficiency. Thus, the information presented confirms the presence of MPs in the low  $\mu\text{m}$ -range but the results must be considered as semiquantitative.<sup>142</sup>

**2.2.3.3. Identification and Quantification of Extracted Polymers.** As already discussed in section 2.2.1.1 “Py-GC/MS”, polymers extracted using suitable solvents can be analyzed by thermoanalytical methods. Alternatively, quantitative proto-

nuclear magnetic resonance ( $^1\text{H}$  NMR or qNMR)<sup>83,143–146</sup> or high performance liquid chromatography (HPLC) methods can be utilized for the characterization of polymer containing extracts. Furthermore, polymers insoluble in common solvents (PET, PA, and PC) can be analyzed after depolymerization step.<sup>118,147,148</sup>

The qNMR, being one of the standard analytical methods applied for the analysis of organic substances, has been recently adopted for the qualitative and quantitative analysis of dissolved MPs. Peez et al. have illustrated the suitability of this method for the analysis MPs consisting of LDPE (granules  $<300 \mu\text{m}$ ), PET fibers (length of approximately 500  $\mu\text{m}$  and diameter of approximately 10–20  $\mu\text{m}$ ), and PS (beads with a size distribution of 0.5–1 mm) in model samples using a calibration curve method.<sup>143</sup> For qNMR, MP particles were dissolved in suitable deuterated solvent, i.e., deuterated toluene (for PE) and deuterated chloroform (for PET and PS). The calculated LOD (19–21  $\mu\text{g/mL}$ ) and the LOQ (74–85  $\mu\text{g/mL}$ ) demonstrated that the method is applicable for the quantification of MP particles at environmentally relevant concentrations.<sup>143</sup> Furthermore, the effects of different environmental matrices on the identification and quantification of PET fibers using qNMR were evaluated, and high recovery rates were obtained from spiked environmental model samples (without matrix  $\sim 90\%$ , sediment  $\sim 97\%$ , freshwater  $\sim 94\%$ , aquatic biofilm  $\sim 95\%$ , and invertebrate matrix  $\sim 72\%$ ), demonstrating the high analytical potential of the method.<sup>144</sup> Recently, the method has been extended for the identification and quantification of MPs made of PVC (powder with a particle size  $<50 \mu\text{m}$ ), acrylonitrile butadiene styrene (ABS, granules with a size distribution of 100–300  $\mu\text{m}$ ), and PA (fibers with a length of approximately 500  $\mu\text{m}$  and a diameter of approximately 20–30  $\mu\text{m}$ ). For the quantification, the integration method or the peak-fitting method, combined with the calibration curve method, was used and LODs and LOQs in the ranges of 40–84 and 132–281  $\mu\text{g/mL}$ , respectively, were obtained.<sup>145</sup> The applicability of the qNMR for the quantification of synthetic polyesters from biodegradable mulch films in soils has been recently reported by Nelson et al.<sup>146</sup> They used Soxhlet extraction or accelerated solvent extraction (ASE) with subsequent qNMR spectroscopy for the analysis of polyester PBAT. Because  $^1\text{H}$  NMR peak areas of aromatic PBAT protons increased linearly with PBAT concentrations dissolved in deuterated chloroform ( $\text{CDCl}_3$ ), the accurate quantitation of PBAT was possible. Determined LOD and LOQ for PBAT in  $\text{CDCl}_3$  were 1.3 and 4.4  $\mu\text{g/mL}$ , respectively, and assumed to be sufficiently low for using qNMR to follow PBAT biodegradation in field soils.<sup>146</sup> Thus, despite the necessity for MP solving in suitable deuterated solvents, qNMR was shown to be efficient method for the mass-based quantification of high variety of polymers including LDPE, PET, PS, PVC, ABS, PA, and PBTA in different complex matrices.

The HPLC-based analysis of polymers insoluble in common solvents (e.g., PA and PET) can be performed after depolymerization procedure, as proposed by Castelvetro et al.<sup>118,147</sup> The depolymerization of PA (nylon-6 and nylon-6,6) was performed by acid hydrolysis followed by derivatization of the monomers 6-aminohexanoic acid (AHA) and hexamethylene diamine (HMDA) with a fluorophore. Reversed-phase HPLC analysis with fluorescence detection resulted in high sensitivities for both AHA (LOD and LOQ of  $8.85 \times 10^{-4}$  mg/L and  $3.73 \times 10^{-3}$  mg/L, respectively) and HMDA (LOD and LOQ of  $2.12 \times 10^{-4}$  mg/L and  $7.04 \times 10^{-4}$  mg/L, respectively).<sup>118</sup> PET quantification involved depolymerization

alkaline hydrolysis, followed by HPLC analysis of its comonomer terephthalic acid and allowed to achieve the LOD and LOQ of  $15.3 \times 10^{-3}$  mg/L and  $5.11 \times 10^{-2}$  mg/L, respectively. The analysis of sludge samples from WWTPs in Italy showed contamination in the 29.3–215.3 ppm and 10.6–134.6 ppm range for nylon-6 and nylon-6,6, respectively, and in the 520–1470 ppm range for PET.<sup>118</sup> Although the polymer depolymerization step is required for the analysis, the achieved sensitivity makes this approach very promising for the mass-based quantitative analysis of PA and PET NMPs as well as fibers in different complex matrices. Furthermore, alkali-assisted thermal hydrolysis can be used not only for the depolymerization of PET, but also of PC, as was demonstrated by Wang et al.<sup>148</sup> The authors used LC–tandem MS to determine the concentrations of the depolymerized building block compounds (i.e., *p*-phthalic acid and bisphenol A) and to quantify the amounts of PET and PC MPs in environmental samples.

### 2.3. Particle-based Methods for Nondestructive Analysis of Microplastics

**2.3.1. Vibrational Spectroscopy.** Vibrational spectroscopic methods, (Fourier transform, FT) infrared (IR) and Raman spectroscopy, which are both based on the interaction of radiation with molecular vibrations, are efficient methods for the representative analysis of microplastic and also nanoplastic particles.

Currently, the application of FTIR spectroscopy and Raman microspectroscopy is widely spread, because these methods enable the determination of polymer type (identification) together with the number, size/size distribution (quantification), and shape of (plastic) particles (characterization).

Because plastic particles and fibers are ubiquitous, generally the plastic-free (or limited) working conditions are essential during all steps of NMP analysis, i.e., sampling, sample preparation, and detection.<sup>20,23,66</sup> The measures include the avoidance of plastic items during the entire process and sample preparation in (MP)-particle/fiber-free or -poor atmosphere (as summarized in section 44, “Validation of Methods, Quality Assurance, and Quality Control”). In addition, the determination of procedural and laboratory blank values (negative control) is necessary. Procedural blanks values account for contaminations during sampling, sample preparation, and detection. Laboratory blank values become necessary in case preparation and detection take place in separate laboratories. These determine internal MP contaminations and help to find and eliminate their sources. On the basis of laboratory blank values, LOD and LOQ values for the laboratory can be calculated.<sup>149–151</sup> For the LOD and LOQ determination at least three (optimal 10) laboratory blank values are recommended.<sup>20,66</sup> Furthermore, a determination of recovery rates (positive control) with reference materials which mimic MP particles in real samples is of high importance<sup>20,23,66</sup> (as discussed in details in section 4.1, “Reference Materials for Microplastics and Nanoplastics”).

**2.3.1.1. IR Spectroscopy.** Already in the paper by Thompson et al. published in 2004, where the term “microplastics” was introduced for the first time, the identification of MPs from marine samples was performed by FTIR spectroscopy. Since then, this method remains most applicable in MP studies worldwide<sup>152</sup> and has already shown to be efficient for the identification, quantification, and characterization of MP contaminations in aquatic<sup>29,30,32,150,151,153–168</sup> and terrestrial<sup>33,169</sup> environments, in influents, effluents, and sludge of

WWTPs,<sup>150,170,171</sup> in ambient air<sup>47,172,173</sup> as well as in drinking water<sup>51–53,149,174</sup> and food.<sup>47,151,175</sup>

IR spectroscopy is a nondestructive technique based on the analysis of molecular vibrations excited by the absorption of radiation in the mid-infrared (MIR) region ( $4000\text{--}400\text{ cm}^{-1}$ ) of the electromagnetic spectrum. The resulting characteristic vibrational fingerprint spectra allow for the accurate identification of the polymer type for MP as well as for the assignment of nonplastic particles using spectral databases<sup>176–178</sup> or other chemometric methods.<sup>179,180</sup> However, the samples have to be dried before analysis because water exhibits very strong and broad IR bands which can partially or even completely overlap the spectral signature of plastic and nonplastic particles of interest. This susceptibility of IR spectroscopy to water is considered as a biggest limitation of the method.

The variety of measurement possibilities available makes IR spectroscopy advantageous to many other methods. Generally, IR analysis can be performed in reflectance or transmission mode.<sup>61,67</sup> In the case of transmission mode, IR radiation penetrated through the sample is detected. For this mode IR transparent substrates or filters (e.g., aluminum oxide (Anodisc) membranes,<sup>176,181</sup> silicon filters,<sup>182,183</sup> or zinc selenide windows<sup>46,157</sup>) are required. Although high-quality data are usually obtained and the resulting spectrum is representative for the entire sample thickness (or entire particle) and, therefore, is beneficial for the MP identification, this mode can be affected the total absorption.<sup>67</sup> Especially for colored, dark, or opaque particles, IR beam can be partially or completely blocked leading to spectra of low quality. This drawback can be avoided by the application of the reflectance mode, where the IR beam, reflected by the sample, is measured.<sup>158,184</sup> For this type of analysis, reflective surface, e.g., metal-coated (Au, Ag, Al)<sup>150,158,182,185</sup> are required. Although this mode is useful for the analysis of (aged) surface of the sample or particle, the signal can be disturbed by light scattering.

For the efficient analysis of MPs, attenuated total reflection (ATR) can be applied. According to Pimpke et al., this technique has been used in 58% of the IR studies, especially for larger particles because it most cost efficient.<sup>67</sup> Furthermore, it requires no sample preparation or difficult mathematic corrections (which are necessary for transmission or (pure and diffuse) reflection mode, respectively). For the measurement, an ATR crystal with high refractive index (e.g., made of diamond, zinc selenide, or germanium) is pressed onto the sample surface. Upon the reflection at the crystal/sample interface, the IR light penetrates into the sample to a depth of up to few micrometers (evanescent wave), and the IR data from the sample are obtained. ATR-FTIR is often used for the identification of visually presorted particles (sizes larger than 200–500  $\mu\text{m}$ )<sup>67,158,183</sup> and for the characterization of weathered MP because the information on modified particle surfaces, due to aging (additional OH, C=O, and COOH), can be easily achieved.<sup>186,187</sup> Furthermore, ATR-FTIR can be efficiently applied for the differentiation of natural and synthetic (micro)fibers.<sup>188,189</sup> The proper identification of man-made cellulosic fibers, namely viscose or rayon (produced by the derivatization of cellulose with carbon disulfide, followed by a ripening period and subsequent regeneration of the viscose fiber) has been also reported.<sup>162</sup>

The analysis of smaller particles and fibers can be performed directly on the filters or windows using  $\mu$ -ATR objective which is brought into contact with the sample.<sup>190</sup> However, because of applied pressure, which is necessary to generate required

interaction between the crystal and particle surface, the sample can be damaged or destroyed. Additionally, the tight contact between crystal and stiff inorganic particles (resembling MPs) may lead to the damage of expensive  $\mu$ -ATR instrumentation. Furthermore, the ATR-FTIR analysis is generally very time-consuming because particles have to be measured one-by-one.<sup>15,20</sup>

The most applicable FTIR-based method for the analysis of (MP) particles <500  $\mu\text{m}$  is micro-FTIR spectroscopy ( $\mu$ -FTIR), where FTIR spectrometer is coupled with optical microscope. The spatial resolution of the analysis is diffraction limited (theoretically ca. 1.7  $\mu\text{m}$  at 4000  $\text{cm}^{-1}$  to 13  $\mu\text{m}$  at 500  $\text{cm}^{-1}$ )<sup>191</sup> and practically particles larger than 10  $\mu\text{m}$ <sup>157,158,192</sup> or 20  $\mu\text{m}$ <sup>52,159,181</sup> can be efficiently identified and quantified by  $\mu$ -FTIR. Especially for the IR analysis, which includes small particles, the removal of inorganic and organic matrices is essential. For this purpose, density separation<sup>5,193,194</sup> and chemical<sup>5,171,195,196</sup> or enzymatic<sup>197</sup> digestion are usually applied. For more information regarding sample preparation, the reader is referred to the recent review by Lusher et al.<sup>198</sup> The matrix removal will increase the plastic/nonplastic particle ratio and, hence, favorably improve the representativeness and statistical certainty of the analysis for the given sample. Additionally, it will help to reduce the entire number of particles and, therefore, to avoid or minimize the agglomeration and overlapping of MPs with natural particles that can lead to under- or overestimation of particle number and size during the manual or automated analysis. To further minimize the number of particles, often only a small fraction of the extracted sample is deposited on the filter or slide.<sup>67,158,199</sup>

Generally,  $\mu$ -FTIR analysis can be performed (i) for preselected particles or (ii) for the (entire) filter area (chemical imaging). The preselection of particles prior IR measurements can be performed manually<sup>32,170,175,200</sup> or automatically<sup>201</sup> using optical images. The preselection strategy is usually applied for Raman microspectroscopic analysis of MP particles and addressed in more detail in section 2.3.1.3. "From Manual to Automated Analysis by  $\mu$ -Raman Spectroscopy". Furthermore, the application of staining techniques (e.g., staining of MP particles with Nile Red, a fluorescent dye that binds to neutral lipids and synthetic polymers) for the preselection and subsequent chemical identification by IR is shown to increase the identification rate and reduce researcher bias.<sup>47,64,202–204</sup> To avoid or minimize "false positive" recognition, due to costaining of some of the natural organic material, the removal of organic matrix before staining has been recommended.<sup>62,64</sup>

By applying chemical imaging (FTIR imaging), all particles located in analyzed area are measured and, hence, the chemical composition of overlapped and agglomerated particles can be addressed in more detail compared with the particle preselection option. However, the number of spectra which have to be measured and processed is significantly higher.<sup>67</sup> The chemical imaging using mercury cadmium telluride (MCT) detectors is possible, but the measurements of large areas are extremely time-consuming. Therefore, the spectra are usually collected only from subarea(s) of filter, e.g., 0.17% (3  $\text{mm}^2$  areas on 47 mm diameter PC membranes)<sup>205</sup> or 5.6% of total filtered surface (12 sampling unit areas of 4.5  $\text{mm}^2$  each on 47 mm diameter fiberglass filters).<sup>190</sup> However, by the optimization of a measurement protocol (i.e., application of silver filters, use of pixel resolution of 25  $\mu\text{m}$ ), 92% of the filtration area of 11.6 mm  $\times$  11.6 mm can be analyzed, as was recently demonstrated by Johnson et al.<sup>149</sup> and Horton et al.<sup>150</sup> The authors successfully

applied this method for the identification and quantification of MPs in potable water, and their sources within water treatment works or in complex wastewater samples.

The application of focal plane array (FPA)-based detection, where several detectors are placed in a grid pattern allows for more time efficient  $\mu$ -FTIR analysis of large filter areas. Thus, hyperspectral imaging (HSI, record of a three-dimensional hypercube), which combines spatial and spectral information in one huge data set (where  $x$  and  $y$  represent spatial and  $\lambda$  spectral dimensions, respectively) becomes possible. Löder et al. described FPA detector with 64  $\times$  64 detector elements cooled by liquid  $\text{N}_2$ . Combined with the 15 $\times$  IR objective lens, the FPA facilitates the simultaneous measurement of 4096 spectra in the wavelength range 3800–900  $\text{cm}^{-1}$  (the FPA detector is limited to this wavenumber range) within a single measurement on an area of 170  $\times$  170  $\mu\text{m}$ , i.e., with a pixel resolution of 2.7  $\mu\text{m}$ . Because of diffraction limited lateral resolution (around 10  $\mu\text{m}$ ) and in order to reduce the data amount, a binning (pooling measured FPA detector-pixel quadrates together to one single pixel) can be useful, e.g., 4  $\times$  4 binning allows for the analysis with spatial resolution down to 20  $\mu\text{m}$ .<sup>181</sup> During the analysis, the whole system is usually flushed inside with compressed dry air to prevent signals caused by air humidity and  $\text{CO}_2$ .<sup>29,181</sup> Meanwhile,  $\mu$ -FTIR instruments with FPA detectors of different sizes are available and can be utilized for the analysis of the entire filter. Depending on the detector size and applied magnification objectives, FPA detectors can analyze areas of approximately 0.7  $\times$  0.7  $\text{mm}^2$  in one measurement (about 1 min, up to 16384 spectra).<sup>20</sup> The time required to scan an area of 14  $\times$  14  $\text{mm}^2$  area is currently 4 h, with pixel resolution of around 5  $\mu\text{m}$ <sup>199</sup> or 11  $\mu\text{m}$ <sup>206</sup> using 128  $\times$  128 or 64  $\times$  64 FPA, respectively.<sup>67</sup> These recent technical advances in  $\mu$ -FTIR analysis resulted in several high detailed studies on MP contamination of different ecosystems,<sup>29,153</sup> waste management systems,<sup>159,184,199</sup> as well as drinking water.<sup>52,149</sup> For the high throughput analysis by means of FPA  $\mu$ -FTIR, the aluminum oxide (Anodisc) filters are commonly used for the measurement in transmission mode. Although the measuring range of Anodisc filters is limited (3600–1250  $\text{cm}^{-1}$  compared to the range accessible with FPA detector 3800–900  $\text{cm}^{-1}$ ), and they have relatively small pore size (max. 0.2  $\mu\text{m}$ ) that results in low filtration velocity and retention of particles smaller than the IR detection limit, these filters are comparatively inexpensive that makes them well suited for detailed studies with high number of samples.<sup>67</sup> In case a broader spectral range has to be measured, silicon filter substrates (e.g., with the pore size of 10  $\mu\text{m}$ ), which guarantee sufficient transparency for the broad mid-infrared region of 4000–600  $\text{cm}^{-1}$  can be used.<sup>182</sup> For measurements in reflection mode, Au-coated PC filters found to be suitable.<sup>158,187</sup> Both filter types (Si and Au-coated PC) also allow for complementary Raman analysis<sup>158,182,183,187</sup> (see section 2.3.1.5 "Combination of (FT)IR and Raman Analysis").

Imaging-based analysis results in large data set, especially if (automated) FPA  $\mu$ -FTIR option is applied. These data sets have to be processed in order to get information on the particle identity as well as further characteristics (number, size, and shapes of particles), required for the detailed quantitative analysis. Therefore, automated data analysis methods, including spectral preprocessing (baseline correction, smoothing, etc.) and evaluation becomes indispensable.<sup>67,177</sup> For the assignment of spectra, library search (which belongs to instance-based supervised machine learning methods) is commonly applied, where search algorithms (Euclidean distance, Pearson correla-

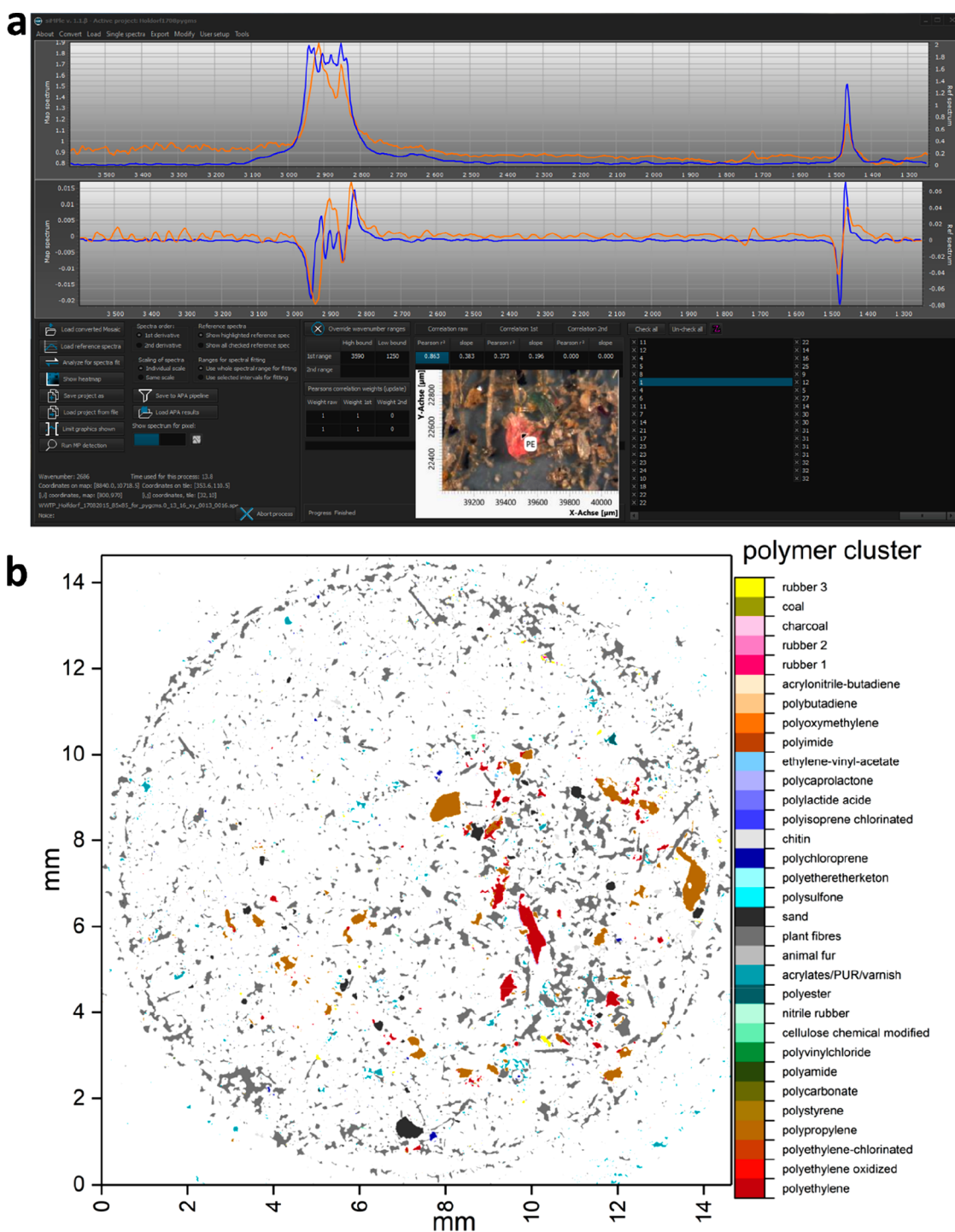


**Figure 5.** (a) FT-IR spectra of an identified PE particle (inset: optical image) from FTIR imaging data obtained using the free software siMple<sup>210</sup> (courtesy of Sebastian Primpke). (b) False color image of the filter area of filter RefEnv278 after automated analysis and image analysis. Adapted with permission from ref 176. Copyright 2018 CC BY 4.0.

tion, or  $k$ -nearest neighbors classification)<sup>177,207,208</sup> are used to create a hit quality index (HQI). HQI represents a measure of similarity between the query spectrum and each reference spectrum. Although distinct HQI levels (e.g., 0.7)<sup>167,175</sup> are suggested as threshold in different studies, the HQI values generated using different algorithms and software might be not comparable. These values also strongly depend on the quality of spectra in the database and sample type. It is also important to stress that the reference spectra collected with different types of instrumentation (ATR and  $\mu$ -ATR, (FPA)  $\mu$ -FTIR in trans-

mittance or reflectance, detector type) and using different parameter settings (number of scans, spectral resolution) and spectral range can differ significantly.<sup>162,209</sup> Therefore, the applied database(s) have to be adapted for distinct applications and the used HQI index level has to be validated.<sup>66</sup> Furthermore, databases have to include not only the reference spectra of pristine synthetic polymers (typical for commercial libraries) but also the spectra of different plastic products (which includes additives) and weathered plastic particles (realized in custom-made libraries).<sup>178</sup> For the automated identification of heavily

weathered and contaminated plastic without any cleaning, Renner et al. have introduced a new chemometric approach based on an automated curve fitting of most relevant vibrational bands to calculate a highly characteristic fingerprint that contains all vibrational band area ratios. By applying this approach for the ATR-FTIR spectra of weathered plastic particles, the accuracy of identification can be significantly increased (from 76% by means of conventional library searching algorithms to 96% by identifying MPs).<sup>179</sup> Besides polymers, it is highly recommended to include the spectra of typical matrix components like quartz sand, cellulose, wood, seaweeds, fish parts, wool, animal fur, proteins, human hair, and skin particles in the library in order to avoid misidentifications.<sup>176,177</sup> Primpke et al. have provided an adaptive reference database which can be applied for single-particle identification as well for chemical imaging based on FTIR microscopy. The novel database design is based on the hierarchical cluster analysis of reference spectra in the spectral range from 3600 to 1250  $\text{cm}^{-1}$  (measuring range of Anodisc filters commonly applied for automated analysis). Moreover, the proposed adaptive database design can be expanded with new spectra in the future, allowing the harmonization of the FTIR analysis.<sup>176</sup>

Recently, a novel free-of-charge software tool, allowing the systematic identification of MPs in the environment (siMPle) has been developed by Primpke et al.<sup>210</sup> The siMPle is a combination of the software MPHunter, presented in Liu et al.,<sup>211</sup> and the automated approach for MP analysis using FPA  $\mu$ -FT-IR imaging, introduced previously by Primpke et al.<sup>212</sup> The siMPle algorithm compares the IR spectra of the sample with each reference spectra in the database then assigns a material to them along with a probability score. Figure 5 shows an overview for the software siMPle applied for FTIR imaging and an example for identified MPs on the filter. The spectral fit can be calculated by Pearson correlation for the untreated data, the first derivative and the second derivative. It has been demonstrated that this software allows for the rapid and harmonized analysis of MP across FT-IR systems from different manufacturers, with different detector systems as well as optical resolutions. The software can be applied for the analysis of single spectra (IR and Raman) as well as for large data sets generated by imaging techniques (FPA  $\mu$ -FTIR). In particular, data analysis time by spectral correlation using this software tool can be reduced significantly, e.g., for 1.8 million spectra from several days to 4–5 h.<sup>67,210</sup> Subsequently, the resulting data can be further analyzed for particle and fiber numbers using automated analysis tools.<sup>67,192,212</sup>

As an alternative to the common instance-based spectral library search, model-based classification (or supervised learning) for the automated evaluation of FTIR imaging data, where the labeled training data are applied to predict the class affiliations of unknown data seems to be very promising.<sup>180,208,213–215</sup> The key difference between common database searches and model-based classification is that instead of using reference data for deciding the class affiliation, a multivariate model of the actual data is applied in the latter case. Hufnagl et al. have presented a methodology which allows discrimination between different polymer types and measurement of their abundance and their size distributions with high accuracy using random decision forest (RDF) classifiers. The methodology has been applied for identification of five polymer types (i.e., PE, PP, PMMA, PS, and polyacrylonitrile, PAN).<sup>180</sup> Recently, the extended RDF approach has been successfully used for the identification of 11 polymer types in mussel samples analyzed by

FPA  $\mu$ -FTIR imaging.<sup>213</sup> The model-based approach utilizing partial least-squares discriminant analysis (PLS-DA) and soft independent modeling of class analysis (SIMCA) models has been developed by da Silva et al. for the evaluation of FPA  $\mu$ -FTIR hyperspectral imaging data. The approach was efficient for the classification and quantification of MPs < 100  $\mu\text{m}$  of nine of the most common polymers produced worldwide (PA, PC, PE, PET, PMMA, PP, PS, PU, PVC). The authors reported that PLS-DA presented a better analytical performance in comparison with SIMCA models and was characterized by higher sensitivity, sensibility, and lower misclassification error. On the other hand, PLS-DA was less sensitive to edge effects on spectra and poorly focused regions of particles.<sup>215</sup> It has to be noted that the design of classifiers (training data sets) is time-consuming and requires experienced operator(s), also further efforts are required in order to increase the number of polymer types (and include nonplastic analytes). However, taking into account the rapid development of methods based on hyperspectral imaging, the model-based approaches become more and more attractive because they can enable reliable evaluation of huge data sets which often include spectra of low signal-to-noise ratio.

Recently, the exploratory analysis of FPA  $\mu$ -FTIR imaging data obtained from environmental microplastic samples has been introduced. This approach uses the multivariate similarity of spectra to identify species or particles without introducing prior knowledge. As a core concept the dimensionality reduction with PCA and uniform manifold approximation and projection (UMAP) was applied, which allows for improved visual accessibility of the data and created a chemical two-dimensional image of the sample. Spectra of particles were separated from blank spectra (reducing the amount of data significantly) and further studied applying PCA and UMAP. Groups of similar spectra were identified by cluster analysis using *k*-means, density-based, and interactive manual clustering and assigned to chemical species based on reference spectra. While the obtained results were in good agreement with a targeted analysis based on automated library search, exploratory analysis points the attention toward the group of unidentified spectra that remained and are otherwise easily overlooked.<sup>216</sup>

Besides FPA  $\mu$ -FTIR systems, an alternative approach, namely laser direct infrared (LDIR) analysis, seems to have a high potential for the fast and automated identification and quantification of MP particles, as has been first reported recently by Scircle et al.<sup>217</sup> LDIR has been applied for the analysis of MP particles >20  $\mu\text{m}$  in aquatic environment (marine and river water)<sup>217–219</sup> and soil.<sup>220,221</sup> The key novel aspect is the light source, a proprietary quantum cascade laser (QCL). The QCL is a semiconductor-based laser, where electrons cascade (tunnel) through a series of quantum wells formed by thin layers of semiconductor material. Photon wavelength is not determined by the semiconductor materials but rather by the thickness and distribution of the semiconductor layers. Thus, a QCL can be rapidly tuned through a wavelength range (e.g., mid-IR range from 1800 to 975  $\text{cm}^{-1}$  can be covered). QCL lasers have the advantage of significantly higher radiation power compared to commonly used IR sources, thus the cooling of the detector with liquid  $\text{N}_2$  (necessary for (FPA)  $\mu$ -FTIR systems) is not required. The LDIR system with single-point MCT detector (thermometrically cooled) and rapid scanning optics allows measurements in two modes. In the first, the LDIR parks the frequency at a single wavelength (e.g., 1800  $\text{cm}^{-1}$ , a frequency at which little or no absorption occurs, but the light is scattered when encountering a particle) and scans through the objective as it

moves over the sample. At each point (pixel), information is acquired in as little as 40  $\mu\text{s}$ , allowing fast scanning of large areas, significantly faster than traditional with FTIR spectroscopes. The resulting IR image is used for both the location of particles in the sample and the determination of their size and shape. In the second mode, the objective is parked at a single point, while the QCL sweeps through the frequency range. A full spectrum is obtained in <1 s and is used for the identification of (plastic) particles.<sup>217</sup> For measurements the sample can be suspended in ethanol and deposited on an infrared reflective glass slide. After drying, the analysis is performed in trans-flection. Fully automated analysis of 800 particles and comparison of the generated spectra to the database took about 1 h to complete.<sup>219</sup> Although LDIR systems have been applied to the analysis of particles >20  $\mu\text{m}$  yet, it is expected that the size limit for analyzed particles could be extended down to approximately 10  $\mu\text{m}$  in the automated mode.<sup>219</sup> However, it has been reported that for the small particles (<30  $\mu\text{m}$ ), the system may determine a need to automatically refocus in order to obtain an optimum spectrum. In this case, the per particle analysis time may be up to 8 s. The application of this method for the MP analysis of water samples indicated that LDIR tends to detect more particles than the fluorescence-based method (Nile Red staining)<sup>217</sup> even though detailed comparison has to prove his tendency in the future. Furthermore, the performance of LDIR in comparison to FTIR-based techniques has yet to be investigated.

In combination with microbolometers working as FPA detectors, the QCL-based hyperspectral IR chemical imaging can be realized, as recently reported by Primpke et al.<sup>222</sup> This method (which applies external cavity (EC) QCLs assembly of four different lasers covering the wavelength range of 1800–950  $\text{cm}^{-1}$ ) allows for the measurement of an area of 144  $\text{mm}^2$  in 36 min, with a pixel resolution of 4.2  $\mu\text{m}$ , which is an appropriate time frame and spatial resolution for routine measurements. Applying this method, the highest number of MP was found in the size class, which is close to the diffraction limit of approximately 10  $\mu\text{m}$ . While few smaller particles could be detected, the result clearly shows that even with a lower pixel resolution on the FPA, the diffraction limit affects the analysis. Compared to FPA  $\mu\text{-FTIR}$  analysis, similar, if not better, data quality for polymer type and particle number could be achieved due to the application of EC-QCL laser as a more powerful light source. Still, especially for samples with small particles, the currently used database may overlook weathered particles to a higher extent compared to FTIR, while having a higher sensitivity for others (e.g., PVC and poly(phenyl)-sulfone, PPSU). Furthermore, the identification of PTFE and silicone which cannot be detected with FPA  $\mu\text{-FTIR}$  system becomes possible.<sup>222</sup>

Thus, (FT)IR-based techniques are very efficient for the identification, quantification, and characterization of MP particles >10  $\mu\text{m}$ . On the other hand, the IR analysis at the nanoscale can be realized by application of scanning near-field optical microscopy (SNOM), namely nano-FTIR and atomic force microscopy (AFM)-IR (photothermal-induced resonance microscopy). The characterization of NPLs with these techniques is addressed in detail in section 3 “Chemical Analysis of Nanoplastics”. Fortunately, the gap between the conventional IR microspectroscopy (where the spatial resolution is diffraction limited) and nanoscale IR spectroscopy in the analysis of plastic particles has been recently bridged by novel technique: optical photothermal (O-PT) IR spectroscopy.<sup>10</sup> In this technique, an intense IR beam source, such as a QCL, modulated at a high

frequency, is utilized for the sample illumination. If the frequency of the IR beam matches with a molecular vibrational frequency of the sample, the light is absorbed and the energy is converted to heat. When the excited molecules return to their ground vibrational state, a temperature fluctuation occurs at the source modulation frequency, leading to the modulated changes in volume (photoacoustic effect) and refractive index (photo-thermal effect) of the sample. These modulated changes are probed using a highly focused visible laser beam (i.e., 532 nm) with a spatial diffraction limit much smaller than that of the IR source.<sup>223</sup> It has to be noted that, phenomenologically, photothermal AFM-IR and O-PTIR are the same. They only differ in the method used to detect the photothermal expansion upon absorbance of the incident IR radiation (AFM tip vs a reflected visible probe laser). Furthermore, along with the O-PTIR signal, the probing laser simultaneously generates a Raman scattering signal which can be detected by a dedicated Raman spectrometer. Thus, simultaneous complementary measurements of IR absorption and Raman scattering at the same location and with the same spatial resolution can be realized with this novel technique.<sup>223,224,225</sup> Because O-PTIR spectra are compatible with commercial FTIR database searching,<sup>223</sup> dual IR and Raman database search is possible. Moreover, even if the Raman signal is (strongly) interfered by fluorescence, the O-PTIR signal remains unaffected. The feasibility of O-PTIR spectroscopy (in combination with simultaneous Raman measurements) for the characterization of MPs has been reported recently by Marcott et al.<sup>226</sup> and discussed in the review by Hale et al.<sup>9</sup>

**2.3.1.2. Near IR Spectroscopy.** Besides MIR region of fundamental molecular vibrations (4000–400  $\text{cm}^{-1}$ ), which is most often used for the identification, quantification, and characterization of MPs, also near-infrared (NIR) region (12800–4000  $\text{cm}^{-1}$  or 780–2500 nm) can be utilized. Although NIR spectroscopy has been applied for decades as a standard method for online quality assurance in food production and for online sorting of plastic packaging in recycling,<sup>20,227,228</sup> only recently the potential of this method (along or in combination with hyperspectral imaging) for the MP analysis in different environmental samples including seawater<sup>229,230</sup> and surface water,<sup>231</sup> biota,<sup>232</sup> and soil<sup>233,234</sup> has been recognized.

NIR spectra are characterized by the broad overlapping bands of overtone and combination vibrations for a limited number of molecular vibrations, mostly of the type X–H, e.g., C–H, O–H, and N–H, that makes the spectral evaluation rather challenging. Therefore, automated statistical methods from the field of chemometrics and/or appropriate databases are required for NIR applications. On the other hand, the use of NIR region offers several advantages for the MP analysis compared to MIR. Because of the low absorption coefficients of the higher overtones compared to fundamental vibrations, NIR radiation can penetrate deeper than MIR and thus handle larger sample volumes and provide fingerprints. Additionally, NIR region is characterized by much lower sensitivity to water and to contaminants such as biofilms. Furthermore, the possibility to utilize quartz materials for fibers and optical elements in NIR spectroscopy<sup>234</sup> results in a variety of instrumentation setups, ranging from hand-held spectrometers suitable for the in situ analysis in the field<sup>235</sup> to laboratory equipment often used for hyperspectral imaging, as discussed below. The spectral range used and the lower size limit of MP particles strongly depend on the applied instrument and analyzed samples. Currently, the NIR images can be collected with the pixel sizes in the range of

50  $\mu\text{m}$  or larger.<sup>20</sup> A lower spatial resolution by NIR analysis compared to MIR could be explained by a larger sample volume which is required in order to obtain enough signal for (very) weak overtone and combination vibrations. Karlsson et al. have tested three different imaging systems with wavelength ranges of 375–970, 960–1662, and 1000–2500 nm for hyperspectral analysis of MP contamination in seawater filtrates. They have found that the wavelength span 1000–2500 nm in combination with the PCA model approach is the most applicable for this specific type of sample and allows studying of preselected MP particles down to 300  $\mu\text{m}$ .<sup>229</sup> Schmidt et al. have reported on semiautomated method for the analysis of MP particles larger than 450  $\mu\text{m}$  in surface water samples filtered onto glass fiber filters. In about 20 min, 10 whole filters of 47 mm diameter could be scanned (measurement speed: 52048  $\text{mm}^2$  per hour). Hyperspectral images with a pixel size  $280 \times 280 \mu\text{m}^2$  and spectral signature consisting of 256 spectral bands within the wavelength range of 968–2498 nm enables counting of MP particles, classifying the plastic types, and determining particle sizes.<sup>231</sup> High-throughput detection of MP in soil has been reported by Paul et al., who applied the NIR analysis in combination with chemometrics models, namely support vector machine regression (SVR) and PLS-DA. For calibration, artificial MP/soil mixtures containing defined ratios of PE, PET, PP, and PS < 125  $\mu\text{m}$  were used. It has been shown that reliable detection and classification of MP at levels above 0.5 to 1.0 wt %, depending on the polymer, can be achieved without any chemical pretreatment.<sup>234</sup> The possibility for the rapid and efficient analysis of MP particles in intestinal tracts of fish, omitting any digestion protocol (reagent free), has been presented by Zhang et al. The authors applied HSI in combination with a support vector machine classification model for the detection, identification, and characterization of five types of MPs > 200  $\mu\text{m}$ .<sup>232</sup> Thus, NIR-based methods, especially in combination with HSI and chemometric approaches, can be very efficient for the rapid monitoring of MP contamination without sample pretreatment. Although the lower size of analyzed particles is limited to around 200–500  $\mu\text{m}$ , NIR-based monitoring could be a first step for the MP prescreening (e.g., following traffic-light principle) before the detailed analysis of particles < 500  $\mu\text{m}$  for all or only suspicious samples is performed by, e.g.,  $\mu$ -(FT)IR or  $\mu$ -Raman spectroscopy.

**2.3.1.3. Raman Spectroscopy.** Raman spectroscopy is a nondestructive analytical method which is more and more frequently used, especially for the analysis of small microplastics in different environmental samples, including marine and fresh water,<sup>158,172,236–239</sup> sediments,<sup>134,168,183,240</sup> biota,<sup>241–245</sup> compost,<sup>92</sup> ambient particulate matter,<sup>172,246</sup> as well as in effluents of municipal wastewater treatment plants,<sup>247</sup> in drinking (tap and bottled) water,<sup>49–51,248,249</sup> beverages, and food.<sup>56,250,251</sup> Recently, the applicability of Raman spectroscopy has also been demonstrated for analysis of nanoplastics.<sup>252,253</sup> This method is based on the effect of inelastic or Raman light scattering<sup>254</sup> on molecules and (similar to IR spectroscopy) provides vibrational fingerprint spectra. Therefore, proper identification of plastic particles and some of additives (e.g., pigments, oxides) as well as other (in)organic and (micro)biological compounds can be performed<sup>31,134,183,236,240</sup> using homemade and commercial spectral databases. Besides the analysis of MP particles, Raman spectroscopy is applicable for the differentiation of synthetic and natural fibers.<sup>245,251,255</sup>

The combination of Raman spectroscopy with confocal optical microscopy (Raman microspectroscopy or  $\mu$ -Raman spectroscopy) and the application of excitation lasers in the visible range enables a significantly better spatial resolution, i.e., down to 1  $\mu\text{m}$  and even below (down to approximately 300 nm) compared to micro-(FT)IR spectroscopy (where spatial resolution of approximately 10  $\mu\text{m}$  can be achieved). Therefore,  $\mu$ -Raman spectroscopy has been recommended, especially for the analysis of plastic particles smaller than 10–20  $\mu\text{m}$ .<sup>15,256</sup>

Furthermore, in contrast to IR, the Raman-based methods offer the advantage of insensitivity toward water. This makes it possible to investigate microplastics in aqueous and (micro)-biological samples (2D and 3D chemical imaging). Figure 6 shows microscopic image of *Daphnia magna* fed with PVC MPs as well as corresponding Raman spectrum and 3D Raman image of the gut area with PVC particles.

A major disadvantage of Raman spectroscopy, especially by the analysis of MPs in environmental samples, is the interference by fluorescence which can be induced by inorganic (e.g., clay minerals, dust particles), organic (e.g., humic substances), and (micro)biological impurities in the matrix<sup>15,256,257</sup> as well as some additives (pigments).<sup>257,258</sup> Therefore, the removal of inorganic and organic nonplastic particles<sup>198,259–261</sup> (by density separation<sup>5,193,194</sup> and chemical<sup>5,195,196</sup> or enzymatic<sup>197</sup> digestion) is often required before the Raman analysis. The matrix removal will also significantly increase the plastic/nonplastic particle ratio and, hence, improve the representativity and statistical certainty of the MP analysis. Additionally, agglomeration and overlapping of MP with natural particles, leading to over- or underestimation of particle size and number, can be minimized.<sup>67</sup> Furthermore, the choice of suitable measurement parameters (laser wavelength and power, photobleaching, and acquisition time, as well as magnification of the objective and confocal mode) is important to minimize or avoid interferences caused by strong fluorescence. The choice of appropriate laser wavelength is essential.<sup>256</sup> Usually 532 nm,<sup>49,50,183,238,262–264</sup> and 785 nm<sup>158,237,239,265–267</sup> lasers are utilized, but also 442 nm<sup>268</sup> 455 nm,<sup>236</sup> 514.5 nm,<sup>242</sup> and 633 nm<sup>134,172</sup> lasers are applicable. Although the use of laser with longer wavelength (e.g., 785 nm) can help to reduce the fluorescence background, several constraints should be considered: (i) the relative intensity of CH str. vibrations (at around 3000  $\text{cm}^{-1}$ ) in comparison with bands in fingerprint region (below 1500  $\text{cm}^{-1}$ ) is significantly lower than at, e.g., 532 nm excitation. These vibrations are, however, very helpful for the proper (automatic) identification of many polymers (e.g., PE, PP, PVC);<sup>193</sup> (ii) the spectral range which can be obtained at the fixed position of grating with the same instrument is significantly narrower, resulting in longer acquisition times for the entire spectrum; (iii) higher laser power has to be applied because the intensity of the Raman scattering ( $I$ ) decreases with the fourth power of the excitation wavelength ( $\lambda$ ,  $I \sim \lambda^{-4}$ ).

Generally, the use of inappropriately high laser power has to be avoided (e.g., higher than 10 mW for 532 nm) because it can lead to the thermal decomposition of plastic particles and, most often, also organic impurities and appearance of typical soot bands in Raman spectra. Furthermore, the photobleaching before or during Raman measurements (by applying longer acquisition times) can be very useful for the reduction of the fluorescence and, hence, for the improvement of signal-to-noise ratio. In particular, longer acquisition times can help to perform correct identification of pigmented plastic and paint particles.<sup>134,256</sup> The later are formed from surface coatings (such

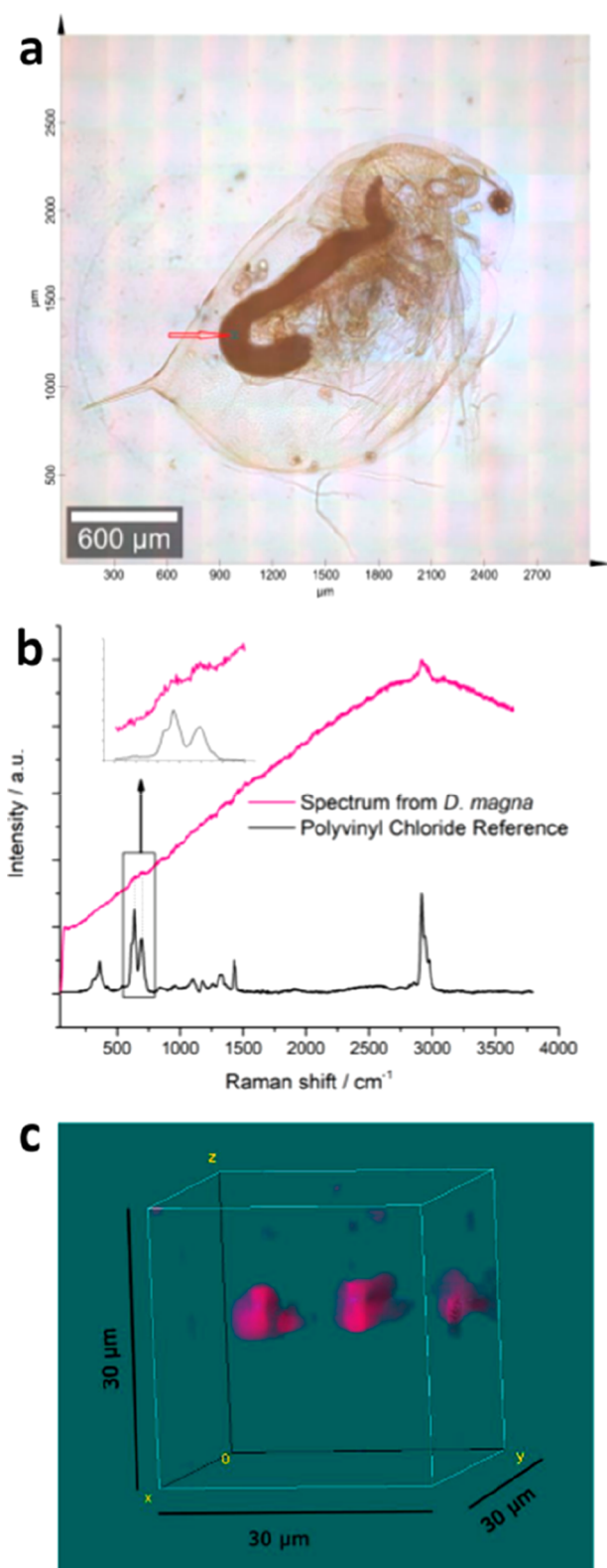


**Figure 6.** (a) Microscopic image, (b) Raman spectra of *Daphnia magna* fed with PVC, and (c) 3D Raman image of the gut area marked with arrow in (a) with PVC particles marked in magenta. Courtesy of Philipp Anger.

as paints) and includes pigments as well as film formers (e.g., (modified) natural resins), curing coating systems (e.g., polyester, alkyds, epoxy resin, urethane resins), and physically drying systems (acryl and vinyl(co)polymers).<sup>18,24</sup> Because of

relatively strong (pre)resonant Raman signals of pigments (e.g., Cu phthalocyanine), the spectra collected at short acquisition times (around 1 s) can be wrongly assigned to paint particles, whereas increasing acquisition time will help to obtain additionally Raman signals of polymers. Because pigments and polymers usually exhibit sharp signals, pigments (in case they do not exhibit strong fluorescence signal) normally do not hamper the identification of polymer type of MPs.

**2.3.1.3.1. From Manual to Automated Analysis by  $\mu$ -Raman Spectroscopy.** In the first examples for the MP analysis by  $\mu$ -Raman spectroscopy, only limited number of selected particles were examined.<sup>31,238–240,242,267</sup> The particles >300–500  $\mu\text{m}$  can be manually picked up and analyzed on substrates with low background signal, smaller particles are usually analyzed directly on a filter in order to avoid contamination and particle loss.<sup>15,67</sup> However, despite processing, many natural particles can still be expected in environmental and food samples deposited on filters. The visual presorting of MP is not only time-consuming but also associated with researcher bias toward large and brightly colored particles.<sup>67,257</sup> Lenz et al. reported on both false positives (e.g., quartz sand or aluminosilicate particles are counted as MPs) and false negatives (e.g., darkly colored MPs mistaken for naturally occurring particles) with increased error by decreasing of particle size (83% and 63% of particles >100  $\mu\text{m}$  and 10–50  $\mu\text{m}$ , respectively, were assigned correctly).<sup>258</sup> Therefore, large number of particles has to be investigated without presorting in order to avoid human bias and to ensure representative MP analysis.

But how many particles have to be analyzed to get a statistically meaningful result? This question has been addressed by Anger and von der Esch et al.<sup>256</sup> by applying a random sampling approach (*simple random sample of units selected without replacement*, srswor<sup>269</sup>). The number of particles which have to be identified ( $n$ ) depends on the total number of particles on the filter ( $N$ ), estimated MP content ( $P$ ), margin of error ( $e$ ), and confidential interval ( $\sigma$ ):

$$n \geq \frac{P(1-P)}{\frac{e^2}{\sigma^2} + \frac{P(1-P)}{N}}$$

As an example, for a filter with  $10^6$  particles,  $\sigma = 1.65$  (90%) and a tolerated margin of error  $e = 10\%$ , the analysis of around 5000 particles will be sufficient, if the MP content  $P = 5\%$ . However, if MP content is lower (e.g.,  $P = 0.5\%$ ), the analysis of around 50 000 particles will be necessary in order to achieve the results with the same margin of error. This example illustrates clearly both the importance of sample preparation, i.e., removal of inorganic and organic matrices (which will lead to decreasing of total number of particles on the filter by increasing of MP content) and the necessity of the automated procedure for the MP analysis of thousands of particles, including their detection, identification, quantification, and characterization.

The (semi)automated analysis can be performed in two inherently different modes as illustrated recently by Brandt et al.,<sup>201</sup> and shown in Figure 7, namely (i) imaging mode and (ii) particle measurement mode.

In the imaging mode (i), the sample surface is scanned by the laser step-by-step and spectroscopic measurement is performed for each pixel. As result, a chemical image is created, where each pixel is assigned to a certain chemical class and neighboring pixels of the same class are grouped in one particle.<sup>201</sup> Obviously, the spectra are acquired not only at positions where particles are located, but also from the entire scanned

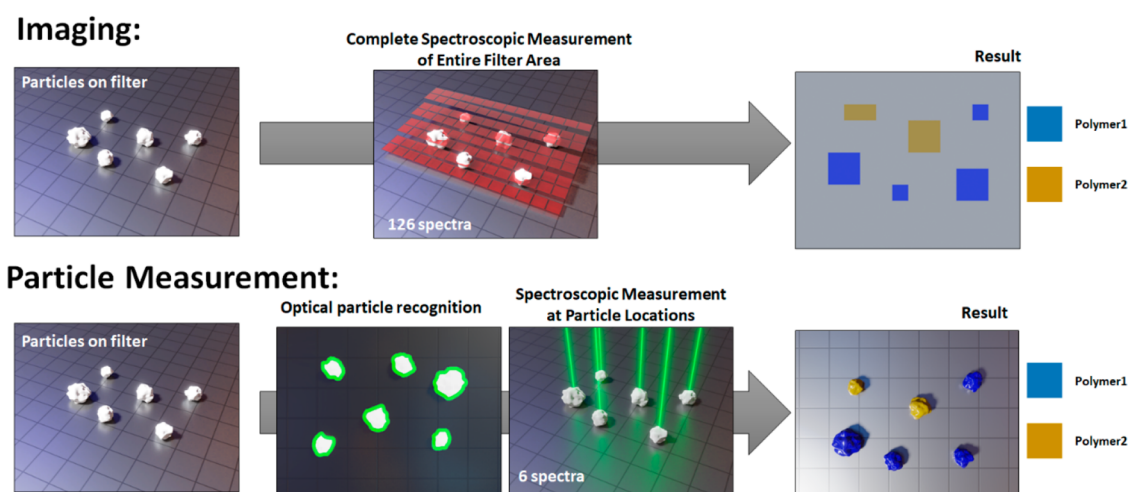
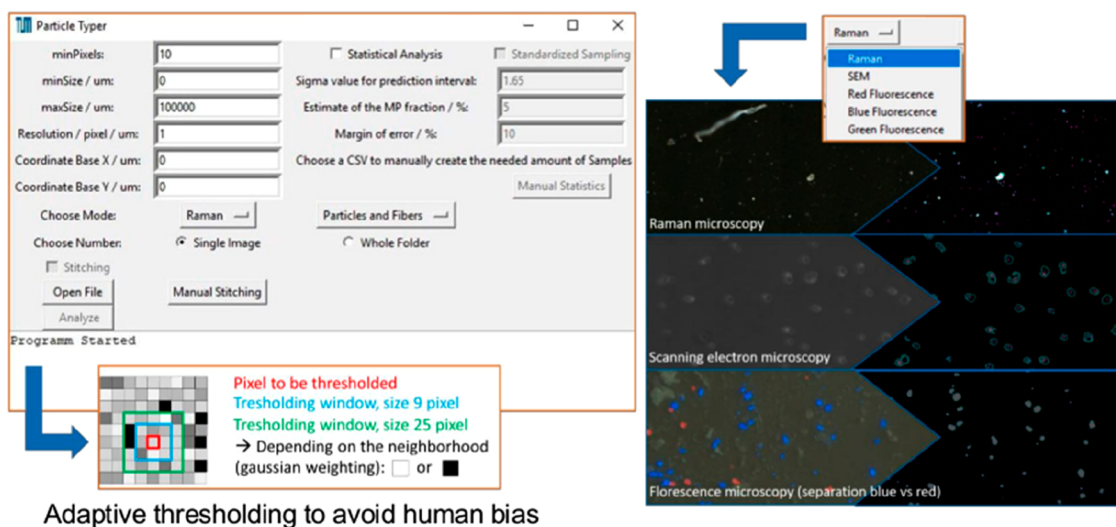


**Figure 7.** Imaging and particle measurement as two different (semi)automated approaches for analyzing particles on a filter substrate. Reproduced with permission from ref 201. Copyright 2020 SAGE.

## Automated Detection, Characterization, Quantification of Particles & Fibers



### Identification by $\mu$ -Raman

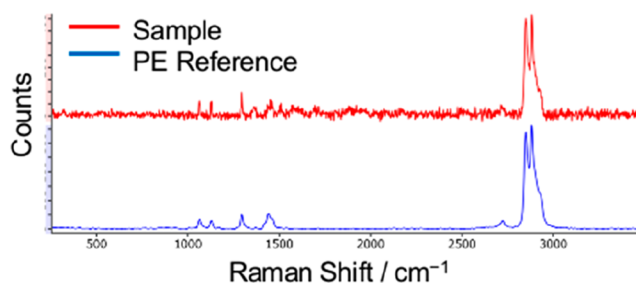


**Figure 8.** Overview for the automated detection, characterization, and quantification of particles and fibers using the free software *TUM-ParticleTyper* (Courtesy of Elisabeth von der Esch).

surface, resulting in plenty of spectra which are superfluous (similar to  $\mu$ -FTIR imaging). The elegant solution with FPA detector which allows obtaining of thousands of spectra simultaneously<sup>181,212</sup> by FTIR spectroscopy is not applicable for the Raman microspectroscopy, where the detectors have to be sensitive in the visible region. Thus, the chemical imaging with step-by-step measurements can be very time-consuming. Although the application of sensitive electron-multiplying charge coupled device (EM-CCD) detectors can help to reduce

an acquisition time per spectrum,<sup>67,183</sup> only restricted area can be analyzed in reasonable time even using EM-CCDs. Especially if the analysis has to be performed with high spatial resolution (i.e., step size  $\leq 1 \mu\text{m}$ ), only a small subarea of the filter is usually investigated, e.g., in Li et al., particles down to  $0.8 \mu\text{m}$  were measured at 0.667% of the filter surface ( $1.5136 \text{ mm}^2$  from  $227 \text{ mm}^2$ ).<sup>262</sup> However, if only a small part of the sample is measured, the question of the representativeness of the chosen area(s) for the entire sample remains open because the

distribution of the (plastic) particles of different size and composition on the filter is not accessible. Furthermore, the error of results obtained after the extrapolation cannot be estimated using classical approaches. Additionally, the data processing of many spectra requires very high computational power. All these restrictions make  $\mu$ -Raman spectroscopy not feasible for high-resolution imaging of MPs on larger surfaces.<sup>201</sup>

The alternative approach is particle measurement mode (ii), which implies an acquisition of optical image of the sample filter, followed by the automated recognition of particles in the image. Finally, the (semi)automated Raman measurements of all or a subset of particles are performed one-by-one. In 2016, Frère et al. first reported on the semiautomated method which involves a combination of static image analysis of particles with automated Raman measurements. The method has been successfully tested for the analysis of around 1000 particles ( $>300 \mu\text{m}$ ) from an environmental sample.<sup>270</sup> Meanwhile, besides several commercial solutions which were already applied in MP studies,<sup>49,50,158,271</sup> open source software (i.e., GEPARD<sup>201</sup> and *TUM-ParticleTyper*<sup>272</sup>) for the automated MP analysis are also available.

The GEPARD (Gepard Enabled PARTicle Detection) package, recently presented by Brandt et al.,<sup>201</sup> involves four main steps: (1) optical image acquisition, (2) particle recognition, (3) spectroscopic measurement, and (4) data evaluation and reporting, and can be applied not only for  $\mu$ -Raman but also for  $\mu$ -FTIR analysis. The recognition algorithm includes the segmentation by thresholding the image into foreground and background, and interactively controllable watershed segmentation. The latter can, however, lead to (strong) oversegmentation of particles and especially fibers,<sup>273</sup> therefore manual corrections to recombine oversegmented particles or to split agglomerates can be performed in the final particle evaluation step. Although this manual step can help to improve the reliability for particle size information, it may involve human bias because the entire recognition procedure will differ from sample to sample as well as from operator to operator. As valuable outputs of the GEPARD approach, the detailed information including particle sizes, particle size distributions, and the type of polymer for thousands of microparticles analyzed on the filter can be achieved.<sup>201</sup>

The *TUM-ParticleTyper* program, recently introduced by von der Esch and Kohles et al.,<sup>272</sup> enables the automated detection, quantification, and morphological characterization of fragments, including particles and fibers, in images from optical, fluorescence, and scanning electron microscopy (SEM). It can be used to automatically select targets for subsequent chemical analysis, e.g.,  $\mu$ -Raman spectroscopy (as shown in Figure 8) or any other single particle identification method. The *TUM-ParticleTyper* localizes particles using an adaptive threshold with results comparable to the “gold standard” method (manual localization by an expert) and surpasses the Otsu thresholding (commonly used particle recognition approach) by doubling the rate of true positive localizations. An additional useful option is the inclusion of a statistical process to calculate the minimum number of particles and/or fibers that must be chemically identified to be representative for all fragments recognized on the substrate or filter.<sup>272</sup>

Generally, the recognition of particles on the entire filter will provide more reliable results.<sup>201,272</sup> However, especially for the particles in the lower  $\mu$ -range, it is often not feasible due to technical limitations and/or time reasons. Therefore, the subset of filter is usually analyzed. The percentage of measured filter

area varies from study to study and strongly depend on the lower size limit for analyzed particles. Because the number of particles (exponentially) increase with decreasing the particle size, smaller areas are usually measured if particles below 5–10  $\mu\text{m}$  included in the analysis. For example, 30% (five sections with the area of 23.6  $\text{mm}^2$ ) and 5% (five sections with the area of 3.8  $\text{mm}^2$ ) of the filter area have been analyzed for the size ranges 10–500 and 1–10  $\mu\text{m}$ , respectively, by Cabernard et al.<sup>158</sup> In the other study by Oßmann et al., particles down to 1  $\mu\text{m}$  have been measured on the 4.4% of the filter (five sections with the area of 5.0  $\text{mm}^2$ ). Obviously, it is difficult to compare the percentages of measured filter areas from different studies because the filters with different total area are used. Even more relevant is the fact that the number of particles on the same area can vary significantly from filter to filter, strongly depending on the sample origin and sample preparation procedure. Therefore, the number of obtained spectra and hence the analysis time can vary significantly. The important question regarding the representative subsampling on the filter is currently under discussion. Here, the distribution of the particles has to be considered in order to avoid over- and/or under-estimations of extrapolated particle counts, as has been pointed out by Thausen et al.<sup>274</sup> Furthermore, the choice of the subsampling modus (systematic or random windows) as well as the number and size of windows can have significant influence on the representativity of the achieved results, as reported by Schwaferts et al.<sup>275</sup> A comprehensive assessment of different proposed subsampling methods on a selection of real-world samples from different environmental compartments has been recently presented by Brandt et al.<sup>276</sup> They compared the performance of different subsampling approaches, based on two different method categories: (i) particle-based methods and (ii) measure box placement methods on 27 environmental samples from different compartments, such as rainwater, river water, sediment, and wastewater sludge. The results indicated that the subsampling errors are mainly due to statistical counting errors (i.e., extrapolation from low numbers) and only in edge cases additionally impacted by inhomogeneous distribution of particles on the filters. Furthermore, increasing the fraction of MP particles in the samples leads to the lower subsampling errors, highlighting the importance of proper sample preparation,<sup>276</sup> as already discussed above.

Automated Raman measurements lead to high number (many thousands) of spectra, therefore time-efficient and reliable processing of spectra (baseline correction, smoothing, normalization)<sup>177,258</sup> and their assignment are inevitable.<sup>178</sup> Usually, library search tools are applied for the evaluation of spectra. These tools rely on instance-based supervised machine learning. Meanwhile, automated evaluation approach is available and used in several studies.<sup>187,201,271,272</sup> Although commercial libraries are often applied, they are usually include only pristine/virgin synthetic polymers.<sup>178</sup> However, it has been reported that MP spectra of the same polymer type can differ significantly due to the presence of additives (e.g., pigments) and especially weathering of MPs (e.g., UV induced degradation).<sup>257,258,263,277,278</sup> Therefore, it is essential to include the spectra of MPs, found in the environment into custom-made libraries. To address this issue, Munno et al. created two spectral libraries (available free of costs) that are representative of MPs found in environmental samples. They present a spectral library of plastic particles (SLoPP), consisting of 148 reference spectra, including a diversity of polymer types, colors, and morphologies. To account for the effects of MP aging, a spectral library of

plastic particles aged in the environment (SLoPP-E) consisting of 113 reference spectra was created. The latter includes a diversity of MP types, colors, and morphologies from environmental samples, obtained across a range of matrices, geographies, and time. SLoPP and SLoPP-E increase the likelihood of spectral matching for a broad range of MP particles because they include plastics containing a range of additives and pigments that are not generally included in commercial libraries.<sup>278</sup> Dong et al. also introduced a preliminary Raman database of weathered MPs (RDWP) including 124 Raman spectra of weathered particles for accurate identification of MPs in natural environments, which is open to all users.<sup>263</sup> Additionally, it is suggested to extend the library with the spectra of expected nonplastic particles and organic materials presented in the marine environment,<sup>258</sup> i.e., quartz, calcite, aragonite, gypsum, soot, cellulose, methylcellulose, cellulose acetate, viscose rayon, keratin, and skin, to improve the exclusion of nonplastic (but MP resembling) particles. Very recently, Cowger et al. introduced a new open-source library (Open Specy) of reference Raman and IR spectra, which allows user to view, process, identify, and share their spectra to a community library.<sup>279</sup>

Alternative to instance-based characteristics used for spectral correlation, model-based supervised machine learning approach, i.e., a random forest classification, can be applied. This approach, first proposed for the time efficient identification of MPs using large FTIR imaging data,<sup>180</sup> was recently adopted for assignment of Raman spectra. A training set of 598 spectra (75 spectra per each synthetic polymer) acquired from eight different polymer types, namely PA, PC, PE, PET, PP, PS, PU, and PVC was used to train RFC model.<sup>213</sup> The identification of nonplastic particles with RFC approach has not been demonstrated yet. Although model-based classification requires the creation of training set and the number of polymer types which can be identified is limited yet, the further development of this approach can help to speed up the evaluation of spectral data and improve the assignment of spectra with low signal-to-noise ratio. Especially for the automated RM analysis, the selection of suitable substrates is essential. They should exhibit no or minimal spectral interference (Raman bands and fluorescence) in the region of interest, be chemically inert, and have a flat, homogeneous, preferably reflective surface.<sup>67,182,185</sup> For the Raman imaging of small MP particles Si wafers<sup>262</sup> and Al slides<sup>246</sup> shown to be applicable. The filter membranes should offer good filtration characteristics and have pore size being not significantly lower as the minimal detectable particle size to avoid clogging. Most applicable substrates that meet these requirements are Si filters<sup>182,183,247</sup> or metal (Au or Al)-coated polycarbonate (PC) filters.<sup>49,50,158,185</sup> To minimize PC filter roughness and to facilitate focusing for better optical images and for Raman measurements, special filter holders can be used.<sup>272</sup>

Additionally, fractionated filtration into different size classes, e.g., using filters of different pore sizes, can be helpful to avoid filter overload and to optimize the recognition of particles in optical images and the laser focusing during Raman measurements.<sup>15</sup> To further improve the laser focusing, automated focusing systems can be applied.<sup>67,183,201</sup>

Furthermore, following parameters/options have been shown to be well suited for the automated analysis: 532 nm laser,<sup>201</sup> dark field exposure, and objectives with longer working distance. Additionally, PTFE filters found to be applicable for the analysis in bright field.<sup>271</sup> It has to be noted that in case of polymer-based

filters (PC, PTFE), MPs of according polymer type have to be excluded from results.

Thus, the entire size range of microplastics (1  $\mu\text{m}$  to 5 mm) and also nanoplastics (<1  $\mu\text{m}$ , down to approximately 300 nm) can be analyzed by  $\mu$ -Raman spectroscopy, providing multi-dimensional information, e.g., (i) type of polymer (and pigments), (ii) particle number, (iii) size/size distribution, (iv) particle shape (spheres, irregular particles and fibers), and (v) plastic/nonplastic ratio. Especially for the analysis of small MPs (<20  $\mu\text{m}$ ),  $\mu$ -Raman spectroscopy becomes the method of choice.

Although  $\mu$ -Raman spectroscopy remains most often applied Raman-based technique for MP analysis, recently, a proof of concept for the real time analysis of MPs in streaming water using Raman spectrometer and custom-based flow cell has been demonstrated by Kniggendorf et al.<sup>280</sup> Individual MP particles (microbeads or fragments) of the sizes near 100  $\mu\text{m}$  added to tap water at concentrations of 0.5 g/L were detected in the presence of other particulate and fluorescent contaminants (glass microbeads, surfactant, and humic acid). MP of five different polymers, namely PA, PE, PMMA, PS, and PP, were analyzed in tap water streaming with 1 L/h through flow cell with inner cross-section of  $3 \times 3 \text{ mm}^2$ .<sup>280</sup> The experiment is promising for the future monitoring of MP in (tap) water and beverages, however, the detection limit has to be improved to enable the analysis of real samples, where expected MP concentrations are significantly lower and strongly depends on the lower size limit of the method. For example, Pivokonsky et al. reported on values ranging from  $338 \pm 76$  to  $628 \pm 28$  MPs/L in treated drinking water using  $\mu$ -Raman for the analysis of particles down to 1  $\mu\text{m}$ ; on the other hand, Kirstein et al. found  $0.022 \pm 0.019$  MPs/L for drinking water analyzed by  $\mu$ -FTIR with size limit of 6.6  $\mu\text{m}$ .<sup>53</sup>

To improve the sensitivity of MP analysis in the (flow) cell, the Raman tweezers, namely optical tweezers combined with  $\mu$ -Raman spectroscopy, has been recently introduced.<sup>243,253,281</sup> This approach has been previously successfully used for the analysis of single cells<sup>282</sup> and cell sorting,<sup>283,284</sup> virology,<sup>285</sup> and analysis of nanomaterials.<sup>253,286</sup> The application of Raman tweezers which have shown high potential for optical trapping and chemical identification of microplastics below 20  $\mu\text{m}$  and nanoplastics down to 50 nm, will be addressed in more details in section 3 "Chemical Analysis of Nanoplastics".

**2.3.1.4. Nonconventional Raman Techniques.** The improved sensitivity of Raman analysis can be achieved by applying nonlinear Raman techniques such as coherent anti-Stokes Raman scattering (CARS) and stimulated Raman scattering (SRS). In CARS and SRS, a strong signal is caused by the molecular vibrational modes of interest only. Thus, the problem of fluorescence can be solved completely if fluorescing contaminants exhibit no emission in the frequency region of interest, enabling rapid analysis of environmental samples without removal of (in)organic and biological matrix.

In CARS, the sample is irradiated with two laser beams. The pump laser beam has a fixed frequency ( $\nu_1$ ), whereas the frequency of the Stokes laser beam ( $\nu_2$ ) can be tuned in the range  $\nu_2 < \nu_1$ . The interacting beams give rise to a beat frequency  $\nu_1 - \nu_2$ , which in turn interacts with the sample. As result, nonlinear four-wave mixing process, radiation of frequency  $\nu_3$  is generated, where  $\nu_3 = 2\nu_1 - \nu_2$ . If the beat frequency  $\nu_1 - \nu_2$  coincides with the frequency of Raman active vibration mode, strong anti-Stokes signal at the frequency  $\nu_3$  will be observed.<sup>287,288</sup> Thus, Raman signals can be obtained by CARS via scanning the beat frequency over the spectral range

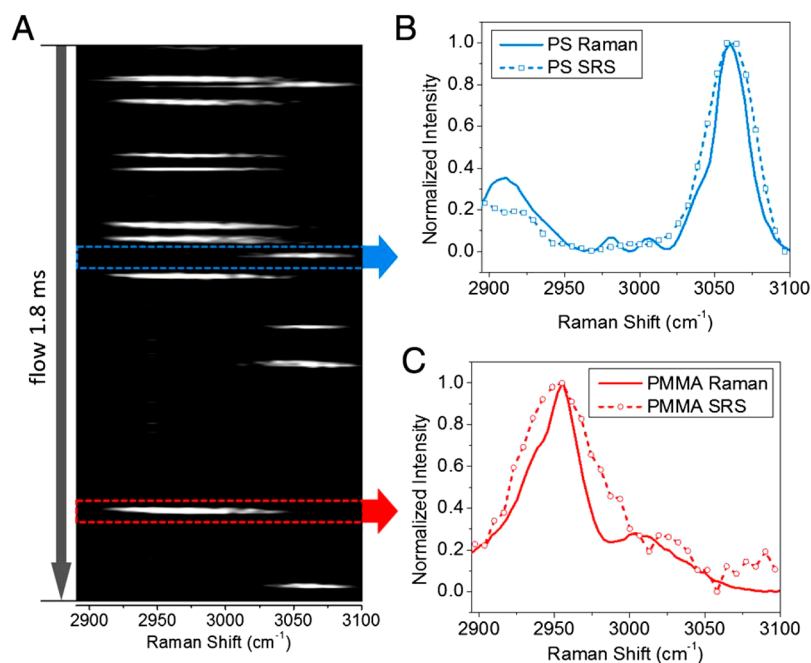


**Figure 9.** Spectral acquisition in SRS-FC for 10  $\mu\text{m}$  MP particles. (A) In a spectrum-time window recorded in 1.8 ms, eight PMMA beads (peak centered at 2955  $\text{cm}^{-1}$ ) and five PS beads (peak centered at 3060  $\text{cm}^{-1}$ ) were detected. (B) SRS (dashed line with open squares) and spontaneous Raman (solid line) spectra of PS beads. (C) SRS (dashed line with open circles) and spontaneous Raman (solid line) spectra of PMMA beads. Reproduced with permission from 295. Copyright 2017 Optical Society of America, under OSA Open Access License.

of interest. The potential of CARS for the detection and imaging of MPs ingested by zooplankton was first shown by Cole et al. in 2013.<sup>289</sup> The authors scanned the region from 2775 to 3100  $\text{cm}^{-1}$  and used Raman bands at 2845 and 3050  $\text{cm}^{-1}$  (aliphatic and aromatic C–H str., respectively) to visualize PS beads (0.4–3.8  $\mu\text{m}$ ) in 2D images. Meanwhile CARS has been applied for the visualization of 8  $\mu\text{m}$  amino-coated and carboxylated PS beads in gills of the shore crab<sup>290</sup> as well as ca. 80 nm and ca. 110 nm nanoparticle-containing acrylic copolymer (ACP) particles in fairy shrimp and zebrafish embryos.<sup>291</sup> Thus, the 2D analysis of small microplastics and even nanoplastics down to 80 nm in biota samples can be realized by CARS. However, CARS application requires complex and expensive instrumental setup and user expertise. Furthermore, the interpretation of results is challenging because CARS can be affected by an electronic, nonchemically specific background, such as those produced from solvents.<sup>288,292</sup>

SRS microscopy is the next promising approach which can provide very fast imaging of MPs. SRS microscopy is based on the coherent interaction of two different laser beams with vibrational levels in the molecules of the sample. The SRS signal is generated when the beams' photon energy difference matches a vibrational state of the molecules in the focal volume. Detection is usually achieved by amplitude modulating one of the beams before the sample and detecting the modulation transfer imposed on the other beam. The obtained SRS signature at different wavenumbers resembles the spontaneous Raman spectrum of the target analyte.<sup>293</sup> Zada et al. have demonstrated the feasibility of this approach for the imaging of MPs of five polymers, namely nylon, PET, PS, PP, and PE. The spectral range from 950 to 1850  $\text{cm}^{-1}$  has been used for the analysis of particles with the spatial resolution limit of 12  $\mu\text{m}$ , 1  $\text{cm}^2$  of the filter has been scanned in less than 5 h.<sup>293</sup> Recently, the applicability of SRS for the determination of natural and synthetic microfibers from environmental samples (i.e., from the

fish gastrointestinal tract, deep-sea, and coastal sediments, surface seawater, and drinking water) has been shown by Laptenok et al.<sup>255</sup> As expected, the majority of the analyzed environmental fibers has a natural origin.

A rapid in situ imaging of MP can be realized by fiber-delivered hand-held SRS microscope as demonstrated by Liao et al.<sup>294</sup> A stimulated Raman signal of PS and PMMA beads (both 5  $\mu\text{m}$  in diameter) has been detected by temporally separating the two ultrafast pulses propagating in the fiber and then overlapping them on a sample through a highly dispersive material (e.g., paper). The reported setup which allows for the imaging in regions 2800–3100  $\text{cm}^{-1}$  (CH str. vibrations) and 1550–1800  $\text{cm}^{-1}$  with spatial resolution down to 1.4  $\mu\text{m}$  seems to be very promising for the chemical analysis of plastic and nonplastic microparticles.

Furthermore, SRS has a potential for high-throughput single-particle analysis, as has been reported by Zhang et al.<sup>295</sup> The developed 32-channel multiplex stimulated Raman scattering flow cytometry (SRS-FC) technique allows for the chemical analysis of single particles (e.g., 10  $\mu\text{m}$  beads of PS and PMMA and polycaprolactone, PCL) at a speed of 5  $\mu\text{s}$  per Raman spectrum. The spectral range from around 2800 to 3100  $\text{cm}^{-1}$  (CH str. vibrations) has been used for the discrimination of different particles in suspension at approximately 0.4 m/s flow speed and a throughput of up to 11 000 particles per second. This is a 4 orders of magnitude improvement in throughput compared to conventional spontaneous Raman flow cytometry. Figure 9 shows an example for the analysis of a mixture of PS and PMMA MPs with a time-dependent spectral graph selected in a 1.8 ms time interval, containing spectra from eight PMMA and five PS beads (Figure 9A) and strong SRS signals at 2956 and 2956  $\text{cm}^{-1}$ , assigned to aliphatic and aromatic C–H str. of PMMA and PS, respectively (Figure 9B,C). By comparing the normalized SRS spectra to spontaneous Raman spectra from the same type of beads, the authors have demonstrated the spectral

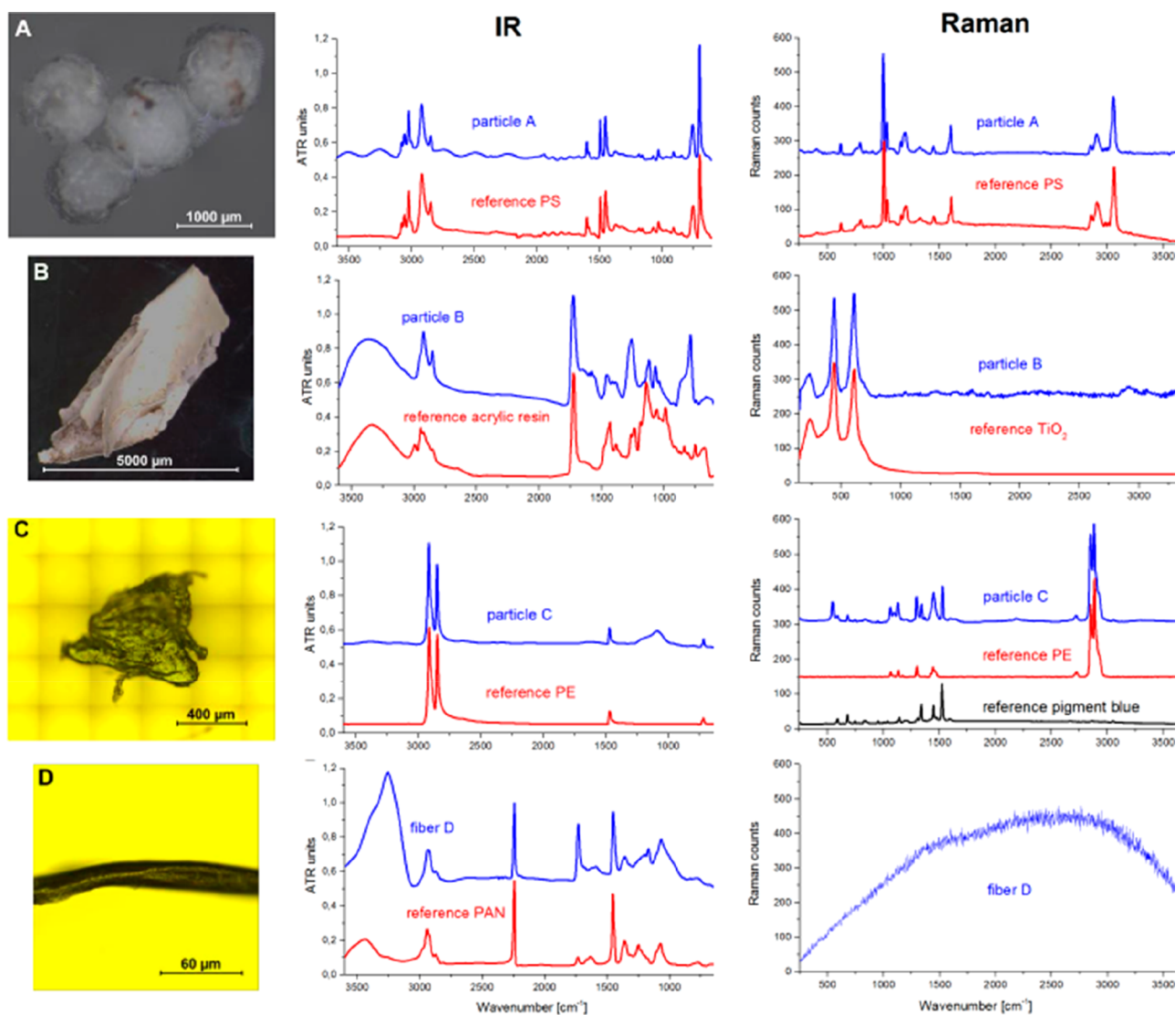


**Figure 10.** Optical microscopic images of four MP particles  $>500 \mu\text{m}$  as well as corresponding ATR-FTIR and Raman spectra. (A) White spherical particles, diameter approximately 1 mm. (B) White fragmented particle, approximately  $5 \text{ mm} \times 2 \text{ mm}$ . (C) Blue particle, approximately  $0.8 \text{ mm} \times 0.8 \text{ mm}$ . (D) Black fiber, diameter approximately  $30 \mu\text{m}$ , length 2–3 mm. Adopted with permission from ref 183. Copyright 2016 Springer.

fidelity of the developed SRS-FC device to spontaneous Raman spectroscopy. The applicability of the setup for the analysis of particles in Raman fingerprint region ( $800\text{--}1800 \text{ cm}^{-1}$ ) has been demonstrated as well.<sup>295</sup>

Thus, SRS-based techniques have a high potential for the fast and sensitive MP analysis, but the complex setup and the need of extended user experience (analogue to CARS) are still the limiting factors for the broad applicability of SRS in MP studies.

**2.3.1.5. Combination of (FT)IR and Raman Analysis.** It is important to underline the complementarity of (FT)IR and Raman analysis. Generally, the molecular vibrations are IR active, if the absorption of IR radiation leads to the change in the dipole moment of the molecule during the process of vibration. The vibrations are Raman active, if the polarizability of the atomic electron shell of the whole molecule changes. Because of different selection rules, IR and Raman spectroscopy result in differing spectra with respect to vibration activities and intensities for different functional groups (polar covalent bonds are more active in IR; nonpolar, aromatic, double and triple bonds, and bonds involving heavy atoms are pronounced

in Raman). Therefore, complementary information can be gained on the polymers and (in)organic additives.<sup>183,208</sup>

The critical comparison and validation of both spectroscopic methods with respect to MPs have been presented by K ppler et al., who investigated environmental samples by both Raman and FTIR spectroscopy. The authors conclude that both methods are in principle suitable for the identification of MP particles from the environment.<sup>183</sup> However, in some cases, especially for colored particles, a combination of both spectroscopic methods was necessary for the complete and reliable characterization of the chemical composition. While FTIR spectroscopy was found to be superior for the identification of acrylic resin (e.g., typical for paint particles) as well as for the characterization of particles which exhibit high fluorescence background (e.g., some fibers),  $\mu$ -Raman spectroscopy have shown to provide detailed information on pigments (e.g.,  $\text{TiO}_2$  in form of anatase and/or rutile and  $\text{Cu(II)}$ -phthalocyanine used as blue dye), which was not achievable by IR analysis (as illustrated in Figure 10). Furthermore, for the particles deposited on Si filter substrate (fraction  $<400 \mu\text{m}$ ), the authors have found significant underestimation (about 35%) of MP by FTIR imaging

(transmission mode) compared to Raman, especially in the size range  $<20\ \mu\text{m}$ . On the other hand, the Raman imaging has illustrated to be considerably more time-consuming. Therefore, for the analysis of particles on the filters (MP  $< 500\ \mu\text{m}$ ), the authors proposed the size division of samples onto two fractions at  $50\ \mu\text{m}$  and the use of rapid FTIR imaging or detailed but more time-consuming Raman imaging for particle fractions  $>50\ \mu\text{m}$  or  $<50\ \mu\text{m}$ , respectively.<sup>183</sup>

The proposed size division at  $50\ \mu\text{m}$  has been recently applied by Kumar et al. for the analysis of MP down to a size of  $3\ \mu\text{m}$  in commercially important mussels.<sup>213</sup> The number of MPs per sample found in the size fraction  $>50\ \mu\text{m}$  using FPA  $\mu$ -FTIR imaging varied from 0.13 to 2.45/gram wet weight (g ww) of the mussel samples with an average number of  $0.63 \pm 0.59$  MP particles/g ww. The most common synthetic polymer types detected were PP ( $39\% \pm 6.3\%$ ), PET ( $32\% \pm 2.8\%$ ), PAN ( $8.2\% \pm 1.4\%$ ), and PE ( $7.2\% \pm 0.6\%$ ). In the fraction  $<50\ \mu\text{m}$ , where 211 MP particles were detected by  $\mu$ -Raman spectroscopy, the most common synthetic polymer types were PA (40.2%), PP (16.5%), PE (14.6%), and PAN (13.2%). The results suggest that the different size fractions of MP particles can be dominated by different polymer types, e.g., PP and PET or PA for the particle fractions  $>50\ \mu\text{m}$  or  $<50\ \mu\text{m}$ , respectively.<sup>213</sup>

Cabernard et al. compared the performance of FPA  $\mu$ -FTIR (reflection mode) and  $\mu$ -Raman combined with automated particle recognition for the quantification of MP particles from the aquatic environment (surface water from North Sea) deposited on Au-coated PC filters.<sup>158</sup> They found that for MPs  $\leq 500\ \mu\text{m}$ ,  $\mu$ -Raman analysis quantified two times higher MP numbers but required a four times longer time compared to FTIR imaging. Furthermore,  $\mu$ -Raman approach enabled identification of 19 different polymer types, compared to 10 polymer types detected by FTIR imaging. On the basis of these results, the authors have concluded that the environmental concentration of MPs  $\leq 500\ \mu\text{m}$  may have been underestimated until now, which may be attributed to the exceptional increase in concentration with decreasing MP size.<sup>158</sup>

This conclusion is in agreement with the results reported by Pivokovski et al.<sup>51</sup> The authors analyzed particle size fractions  $>10\ \mu\text{m}$  and  $1\text{--}10\ \mu\text{m}$  from raw and treated drinking water with FTIR and Raman imaging, respectively, and found that MPs smaller than  $10\ \mu\text{m}$  were the most plentiful in all samples, accounting for up to 95%.

The discussed results indicate clearly that the combination of (FT)IR and Raman analysis can provide complementary results and allow for the reliable size resolved chemical analysis of MPs. The detailed and valid information on MP contamination is of high relevance for the assessment of MP associated risks for the environment and human health. Special attention has to be paid to the identification and quantification of small MP particles, which number is unknown or most probably underestimated yet because this MP fraction is most significant concerning ecotoxicity.<sup>158</sup>

While until now  $\mu$ -Raman spectroscopy has been the sole method applied for the identification and quantification of MP fraction  $<10\ \mu\text{m}$ , due to the diffraction limited size limitation by the (FT)IR applications, the recent development of optical photothermal (O-PT) IR spectroscopy allows performing of the noncontact IR analysis with submicrometer resolution.<sup>10</sup> This technique utilizes a visible laser probe (532 nm) to measure the photothermal response of the targeted particles following IR absorption induced by a tunable pulsed laser for the MIR region.

Furthermore, the configurations are available for the simultaneous IR and Raman analysis at the same spot and with same spatial resolution via additional detection of inelastic light scattering caused by the visible probe laser,<sup>223,224</sup> as discussed in more detail at the end of section 2.3.1.1 "IR Spectroscopy". This opens unique possibilities for the complementary IR and Raman analysis of (plastic) particles with submicrometer resolution in the future.<sup>10,226</sup>

**2.3.2. Additional Techniques for Particle-based Chemical Analysis of MPs.** As already mentioned above by the discussion of ICP-MS technique, its application in the single-particle mode (SP-ICP-MS) has a potential for the detection and quantification of MPs in the size range from approximately  $1\ \mu\text{m}$  to  $5\text{--}10\ \mu\text{m}$ . However, the identification of polymer type(s) has to be performed by other methods, e.g., FTIR spectroscopy.<sup>141,142</sup>

The analysis of MPs in the lower  $\mu$ -range<sup>296–298</sup> and the characterization of weathered plastic surfaces<sup>299</sup> can be performed by time-of-flight secondary ion mass spectrometry (ToF-SIMS). This is a surface analysis technique with a high molecular specificity and imaging capability. It is suitable for the analysis of inorganic elements and organic compounds, and can carry out rapid mass spectrometry scanning and characteristic organic ion imaging. ToF-SIMS has been already widely used for the investigation of different environmental samples.<sup>297</sup> In the field of MP studies, this technique can provide information on the identity and degradation state of particles as well as on their size and distribution in complex samples. Jungnikel et al. reported on the applicability of ToF-SIMS for the analysis and imaging of small PE microparticles formed during sea surf simulation using primary PE pellets. The measurements of MPs smaller than  $10\ \mu\text{m}$  were performed directly in the model system Ottawa sand using nano-Bi primary ion beam source. The lateral and depth resolution in imaging mode was 70 and 9 nm, respectively, and scans with a field of view of  $500 \times 500\ \mu\text{m}^2$  were obtained, applying a  $2048 \times 2048$  pixel measurement raster. To enhance the ion count per pixel, the pixel binning was used to reduce the image array down to a size of  $128 \times 128$  for the environmental samples. The authors found that ion with  $m/z$  113 derived from the PE matter is suitable to detect and visualize microplastic particles directly within Ottawa sand without the removal of matrix. The formation of MPs was observed already after 14 days of sea surf simulation. Within the subsequent period of 14 days to 1 month of exposure, the number of detected smallest-sized particles ( $1\text{--}1.4\ \mu\text{m}^2$ ) increased significantly (50%) while the second smallest fraction ( $1.5\text{--}2.4\ \mu\text{m}^2$ ) increased even further to 350%.<sup>296</sup> Recently, Du et al. have reported on the suitability of ToF-SIMS for the characterization of MPs in soils.<sup>297,298</sup> Four types of MPs, namely PP, PVC, PET, and PA 6 were successfully identified in terms of particle size and abundance by combining the high molecular specificity with ion imaging capability of ToF-SIMS using nano-Bi primary ion beam source for the rastering over  $500 \times 500\ \mu\text{m}^2$  area with  $128 \times 128$  pixels in 2D image mode. The analysis of standard samples revealed positive characteristic ions for PVC ( $\text{C}_4\text{HCl}^+$ ), PET ( $\text{C}_8\text{H}_5\text{O}_3^+$ ) and PA 6 ( $\text{CH}_4\text{N}^+$ ) which were further used as fingerprints for polymer identification. While PE and PP produced almost the same ions, it was found that the ion ratio  $\text{C}_5\text{H}_{11}^+/\text{C}_6\text{H}_{11}^+$  of PP was higher than that of PE, enabling to distinguish PP and PE in the samples. For farmland soil samples, fractions  $<25\ \mu\text{m}$  were analyzed after sieving step and removal of natural organic matter using 30%  $\text{H}_2\text{O}_2$ . Although PVC and PA 6 were detected in this

type of soils, PP was found to be most abundant. The authors explained this finding by an extended use of plastic mulching (made of PP) for agriculture production in analyzed area. In the analyzed fractions ( $<25\ \mu\text{m}$ ), the proportion of MPs  $< 15\ \mu\text{m}$  was over 59%.<sup>297</sup> In the following study, the authors investigated soil fractions  $<35\ \mu\text{m}$  in suburb region and found completely different picture in term of found polymers and size distribution. While four types of MPs (PP, PVC, PET and PA 6) were identified, PET and PA 6 accounted for the largest proportion (up to approximately 30% for each). For the investigated soil fractions ( $<35\ \mu\text{m}$ ), the proportion of MPs  $< 10\ \mu\text{m}$  was more than 26.3%, while that of  $20\text{--}25\ \mu\text{m}$  and  $25\text{--}35\ \mu\text{m}$  were relatively small (17.83% and 9.3%, respectively).<sup>298</sup> The results clearly indicate the high potential of ToF-SIMS for the analysis of different MPs in lower  $\mu\text{m}$ -range, nevertheless further research is needed to clarify the applicability of this technique for the detection of nanoplastics and to ensure the representativity of obtained data.

#### 2.4. Combination of Different Methods for Comprehensive MP Analysis

##### 2.4.1. Identification of Individual MP Particles.

Although different mass-based and particle-based methods can be applied for the MP identification and quantification, MP particles are highly complex and diverse, having high variety physical, chemical, and biological characteristics (e.g., polymer type(s), size, shape, surface properties, additives, etc.). Therefore, no method along can provide data sufficient for the comprehensive characterization of this extremely challenging analyte. The one example on complementary results has been already discussed for the combination of IR and Raman spectroscopy data.

Regarding the identification of MP particles, very valuable complementary information can be achieved by a combination of such fundamentally different approaches as Py-GC/MS and spectroscopic methods. K appler et al. have performed critical comparison of Py-GC/MS and  $\mu\text{-ATR-FTIR}$  methods by analyzing MPs in environmental samples and conclude that both methods are well suited to characterize the chemical nature of environmental MPs and can complement each other. Being nondestructive and more time-efficient (about one min for one spectrum), IR approach allowed for the identification of the polymer type and inorganic additives. On the other hand, destructive and time-consuming (about 30 min for one run) Py-GC/MS provided the additional information on organic additives and heterogeneous/multicomponent polymer systems (e.g., alkyd paints).<sup>81</sup> Hermabessiere et al., who compared Py-GC/MS and Raman analysis of MPs have also report on their complementarity. While the MP particles were identified by both methods, Py-GC/MS led to results with a finer polymer identification, i.e., two particles classified as PP by  $\mu\text{-Raman}$  were identified as PE–PP copolymer. Furthermore, one PA particle was found to contain PE, PP, and PA 6.<sup>80</sup>

**2.4.2. Simultaneous Identification and Quantification of Polymers from Complex Samples.** The comparison between results derived by applying mass-based and particle-based methods is essential for the harmonization in the field of MP analysis. Recently, Kirstein et al. have used  $\mu\text{-FTIR}$  and Py-GC/MS to assess the MP contamination of drinking water.<sup>53</sup> An aliquot of 20–52% for the sample or blank and the rest were analyzed by spectroscopic and thermoanalytical approach, respectively. Both methods successfully determined low MP contents in drinking water with values between zero and  $0.022 \pm$

$0.019\ \text{MPs/L}$  (analyzed down to  $6.6\ \mu\text{m}$ ). However,  $\mu\text{-FTIR}$  and Py-GC/MS identified different polymer types. While eight polymer types were found by  $\mu\text{-FTIR}$ , namely PA, PES, acrylic compounds, PVC, PS and less frequently PE, PU and PP, only five of those were identified with Py-GC/MS (PE, PU, and acrylic compounds were not detected or below LODs). Besides information on number and size of particles, the mass of polymers has been estimated based on  $\mu\text{-FTIR}$  data according to Simon et al.<sup>157</sup> Briefly, the particle volume was calculated by assuming that particles are ellipsoids, the third dimension was defined as 0.67 times the minor dimension. Following, the mass was estimated using the resulting particle volume and the respective density of the polymer. The estimated and determined mass concentrations based on  $\mu\text{-FTIR}$  and Py-GC/MS data, respectively were of the same order of magnitude throughout all drinking water samples, and became more comparable with increasing concentration of a given polymer type. Most detected MPs were smaller than  $150\ \mu\text{m}$ , and 32% were smaller than  $20\ \mu\text{m}$ .<sup>53</sup> Independently and simultaneously, Primpke et al. reported on the  $\mu\text{-FTIR}$  and Py-GC/MS analysis performed on a set of environmental samples (surface water, sediment, and wastewater samples after matrix removal) which differ in the complexity and degree of MP contamination. The measurements were conducted consecutively, and exactly for the same samples. First, the samples deposited on aluminum oxide filters were investigated with  $\mu\text{-FTIR}$ . Subsequently, these were crushed, transferred to glass fiber filters, in pyrolysis cups, and measured via Py-GC/MS. Although the overall trends in MP contamination were very similar, differences were observed in polymer compositions, i.e., FTIR indicated a particularly high presence of the PMMA/PUR group, and Py-GC/MS detected higher shares of PE and PVC. While the PP shares were comparable, the relative PET and PS contents varied between both methods.<sup>85</sup> While the polymer masses empirically calculated from FTIR data according to Simon et al.<sup>157</sup> deviated from the masses derived based on Py-GC/MS data (from 10 time underestimation to 6 time overestimation), the accuracy of the estimation improved with decreasing contamination level. To optimize the FTIR-based mass estimation, a modified mass calculation was performed, which combines various particle shapes and sizes present into a reference particle. For this purpose, the average particle length and minimum width were calculated for each polymer type and used as a reference particle in terms of mass. The area of the individual particles was divided by the reference area calculating the reference particles represented, and multiplied by the reference particle mass. The application of the improved mass calculation approach has reduced the difference compared with the results of Py-GC/MS down to a factor of 3.<sup>85</sup> The presented data clearly demonstrated the complementarity of  $\mu\text{-FTIR}$  and Py-GC/MS for the simultaneous identification and quantification of MP in complex samples. While  $\mu\text{-FTIR}$  detects a broad range and even very low numbers of smaller sized MP particles, Py-GC/MS, when exceeding a detection threshold, enables a condensed overview of polymer types represented by a shared chemical backbone expressed by basic polymer clusters (i.e., “PE” or “PS”). These comprehensive data are essential for the future modeling and source tracking studies.<sup>85</sup>

**2.4.3. Electron Microscopy for Detailed Characterization of MP Particles.** To perform detailed characterization of plastic particles, the established methods for their chemical analysis, like Py-GC/MS, FTIR and  $\mu\text{-Raman}$  spectroscopy are often complemented by scanning electron microscopy/energy

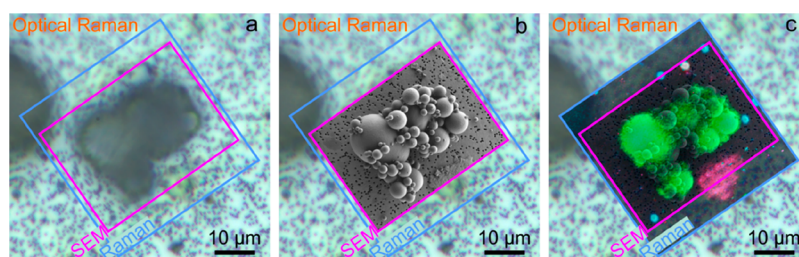


**Figure 11.** Morphological and chemical imaging of clustered MP particles at (a) low optical and (b) high SEM spatial resolution along with the Raman composition overlay indicating mainly (c) PE agglomerated particles. Reproduced with permission from ref 313. Copyright 2020 SAGE.

dispersive X-ray spectroscopy (SEM/EDX).<sup>51,77,131,186,263,266,300</sup> SEM is a powerful technique which provides information on size, shape and surface properties of plastic particles and fibers<sup>300–302</sup> as well as on their weathering,<sup>186</sup> microbial colonization<sup>39</sup> and (bio)-degradation<sup>303,304</sup> with spatial resolution in the nm-range. Furthermore, this technique has also a high potential for the characterization of nanoplastics<sup>252,305–307</sup>. The measurements can be performed in high vacuum ( $<10^{-4}$  Pa), in this case the coating of insulating samples by metal (Au, Al, Pt) or carbon is often required to improve the quality of images. Alternatively, uncoated samples can be analyzed utilizing so-called environmental or variable pressure mode with chamber pressure in the range from 1 to 2000 Pa using nitrogen, atmospheric gas or water vapor (e.g., for analysis of wet samples).<sup>67,308,309</sup> In combination with EDX, SEM can be efficiently applied for the discrimination between organic (plastic and nonplastic) and inorganic MP particles<sup>308</sup> and for the detection of PVC and PTFE particles based on EDX signals of the chlorine and fluorine elements, respectively.<sup>266</sup>

**2.4.3.1. Combined Application of Electron Microscopy with Spectroscopic Techniques.** Because almost all MP types are characterized by carbon-dominant EDX signals, the applicability of SEM/EDX as a sole technique for the quantitative analysis of MP particles is more than questionable,<sup>310</sup> the identification has to be confirmed by e.g., spectroscopic methods. For example, Wagner et al. reported on the successful identification of MP particles (PE, PP and blended PE+PP and PS) in fish gut using  $\mu$ -FTIR and  $\mu$ -Raman after detecting potential MPs by SEM/EDX.<sup>308</sup> To facilitate more time-efficient workflow, several high-precision repositioning technologies have been developed.<sup>67,311</sup> An excellent possibility for the detailed chemical and morphological analysis of (plastic) micro- and nanoparticles offers correlated  $\mu$ -Raman spectroscopy and SEM/EDX.<sup>306,312,313</sup> Sarau et al. recently reported on the analysis of standard MP particles by hyphenated SEM-Raman system.<sup>313</sup> By merging the obtained data in one software, it was possible to navigate on the entire filter surface and correlate at identical locations MP morphology at the spatial resolutions of electron (1.6 nm at 1 kV for the used SEM, and approximately 100 nm minimum MP size) and optical (approximately 1–10  $\mu$ m) microscopies with chemical identification by  $\mu$ -Raman spectroscopy. It was found that low-voltage SEM works without a conductive coating of MPs providing high-resolution surface imaging of single and clustered MP particles and enabling subsequent Raman measurements. An example for the correlative analysis is shown in Figure 11. The optical image of such an object under the Raman objective is blurred (Figure 11a). The SEM image reveals the three-dimensional structural details of the agglomerate which consists of many sticking particles with varying sizes ranging from approximately 100 nm

to 13  $\mu$ m (Figure 11b), while Raman imaging indicates its main PE composition (Figure 11c).<sup>313</sup>

**2.4.3.2. Transmission Electron Microscopy.** Besides SEM, transmission electron microscopy (TEM) has also been applied for the characterization of microplastics and nanoplastics in soil samples.<sup>94,314,315</sup> For example, Watteau et al. applied TEM/EDX together with Py-GC/MS for the MP detection in soil amended with municipal solid waste composts.<sup>94</sup> For the TEM/EDX measurements subsamples for different size fractions were fixed in osmium tetroxide, dehydrated, embedded in epoxy resin and cut in ultrathin sections using ultramicrotome. The authors used ultrastructural specific features of plastics as well as EDX signals of Ti and Ba (which are initially added during the polymer production) to distinguish plastics from soil organic matter. The presence of PS has been confirmed by Py-GC/MS analysis.<sup>94</sup>

It has to be noted that SEM and TEM techniques are very time-consuming and often requires laborious sample preparation steps and, hence, cannot be applied for the analysis of high number of particles required for representative studies. However, they provide very valuable detailed information on particle morphology and elemental composition, and help to perform comprehensive analysis of diverse NMPs.

**2.4.4. Methods for Chemical Characterization of Weathered NMPs.** Because weathered NMPs are expected to have a higher toxicity potential,<sup>36,316–319</sup> the methods for the characterization of the chemical alteration of plastic particles are of importance. The process of weathering contributes to the degradation of NMPs and is driven by biotic (e.g., microbial colonization) and abiotic (e.g., photo-oxidation) factors, resulting in a modified surface topography and changes to the surface chemistry.<sup>316,320</sup> For the chemical analysis of particle surface modified due to weathering, FTIR technique was shown to be very efficient. Usually, the appearance of additional absorption bands corresponding to OH, C=O, and COOH groups can be observed.<sup>186,187</sup> As reported by ter Halle et al., all ketone, carboxylic acid and ester functional groups formed upon UV irradiation contribute to the carbonyl signal (1650–1850  $\text{cm}^{-1}$ ) in ATR-FTIR spectra. Therefore, carbonyl index can be used as the aging index by the characterization of weathered plastic particles.<sup>186</sup> Furthermore, byproducts of oxidative degradation and erosion of NMPs can be analyzed by FTIR spectroscopy after solvent extraction from the environmental samples (e.g., coastal sediments), as shown by Ceccarini et al.<sup>83</sup> The authors found signals typical for oxidized moieties, such as aliphatic carbonyl (C=O str. at 1720–1740  $\text{cm}^{-1}$  with shoulder down to 1660  $\text{cm}^{-1}$  from conjugated ketone C=O str.) and hydroxyl groups (broad O–H str. band at 3430–3400  $\text{cm}^{-1}$  and C–O str. at 1020  $\text{cm}^{-1}$ ). The spectra were generally comparable to those from artificially aged PE, PP, and PS reference samples. It was also reported that GPC followed by Py-GC/MS or <sup>1</sup>H

NMR can be applied for the analysis of polymer extracts, in order to separate and chemically characterize higher and lower molecular weight fractions.<sup>83</sup> Moreover, volatile photodegradation products can be determined using an analytical procedure combining headspace with needle trap microextraction and GC/MS. Such analysis performed by Lomonaco et al. revealed that plastic debris can release harmful VOCs (e.g., acrolein, benzene, propanal, methyl vinyl ketone, and methyl propenyl ketone).<sup>36</sup>

### 3. CHEMICAL ANALYSIS OF NANOPLASTICS

#### 3.1. Challenges and Objectives

Nanoplastics (NPLs, plastic particles 1 nm – 1  $\mu\text{m}$ )<sup>18–21</sup> represent an emerging topic of relevance in environmental and food science<sup>42,44,45,68,321</sup> as well as in human toxicology.<sup>59,60,322,323</sup> For example, when tested on a model of human intestinal epithelium, nano-PET particles showed high propensity to cross the gut barrier, with unpredictable long-term effects on health and potential transport of associated chemicals.<sup>60</sup> It is assumed that because of the large surface-to-volume ratio of NPL particles, they may (ad)sorb larger amounts of external toxic compounds than MPs. The factors influencing the sorption/desorption of chemicals associated with NPLs are still to be known, but may be assimilated to a Trojan horse effect mechanism, in which the plastic debris contribute toward the flux of contaminants.<sup>324</sup> NPLs have been recently recognized as one of the least studied types of marine litter but potentially one of the most hazardous.<sup>1,325</sup> Thus, information on the chemical composition (including polymer type, additives and sorbed contaminants), number concentrations, size/size distribution and mass of NPL particles as well as on their shapes and surface properties are essential for the understanding of NPL impacts on the environment and human health. Furthermore, the knowledge on the formation and (bio)degradation of NPL particles, on their colloidal behavior and heteroaggregation with inorganic colloids and natural organic matter (NOM) in the environment will help to understand the sources, transport and fate of this challenging particulate analyte.<sup>21,68,326–329</sup> It is worth mentioning that the influence of the NOM on NPLs fate, effects and detectability strongly depends on the particle size. The NOM is a minor component compared with the host plastic at the microscale. As the plastic size decreases, the contribution of NOM increases and it becomes analytically challenging to discriminate the plastic component, especially given similar carbon-based structures.<sup>329</sup>

While several studies reported on NPLs in the environment (North Atlantic surface water<sup>97</sup> and coast,<sup>330</sup> Alpine snow<sup>120</sup> and soil<sup>331</sup>) as well as in personal care products,<sup>332</sup> the degree of the contamination remains largely unknown. However, taking into account that with decreasing size, the particle number concentration increases substantially for MPs found in both environmental and food samples,<sup>50,51,156,158</sup> a high abundance of NPLs could be generally assumed for the same samples. Analogue to microplastics, nanoplastic particles can be intentionally produced (primary NPLs, generated e.g., for cleaning products or as calibration standards for nanoparticles) or formed by the degradation and fragmentation of (micro)plastics (secondary NPLs). For example, Gigault described the generation of NPL particles from millimeter scale plastics by UV radiation.<sup>333</sup> Lambert and Wagner found the formation of NPLs during the degradation of PS disposable coffee cup lid,<sup>334</sup> whereas Dawson reported that MP particles (approximately 30

$\mu\text{m}$ ) ingested by a planktonic crustacean (Antarctic krill) were fragmented into pieces less than 1  $\mu\text{m}$  in diameter.<sup>335</sup>

At this point, it has to be mentioned that the analysis of engineered nanoparticles (ENPs) is already well established and the knowledge with respect to the tools and methods developed as well as the experience in handling particulate contaminations can serve as a solid basis for the NPLs studies.<sup>326</sup> However, these tools are not fully fit for the purpose. While ENPs are mostly inorganic, NPLs are mainly carbon-based with low or no crystallinity and the limited elements incorporated. Therefore, new approaches have to be developed for the determination of their chemical composition.

Thus, by the analysis of NPLs we are facing a considerable methodological gap.<sup>68</sup> On the one hand, similar to MPs, the NMP particles are diverse, having a high variety of physicochemical characteristics (e.g., polymer type, size, surface properties, etc.), while even less structural diversity compared to MPs can be expected due to the substantially larger number of fragmentations during NPLs formation.<sup>68</sup> Hence, the experience from the realm of MPs is essential for NPL studies. On the other hand, the methods developed for the analysis of MP particles can only partially be transferred to NPLs due to their small masses and sizes.

Following challenges have to be carefully considered:

- NPL particles in real samples can have relatively low concentrations (mass-fraction) and their number can be comparable or even lower as the number of nonplastic particles in the (colloidal) matrix. Furthermore, the contribution of the NOM in heteroaggregates increases with decreasing of NPL size. Hence, similar to the MP analysis, we are searching for a needle in a haystack, but numbers of (nonplastic) particles are considerably larger. This underlines the importance of appropriate approaches for the preconcentration and enrichment of NPLs from complex matrices;
- Sensitivity of the existing mass-based methods can be insufficient for the NPLs detection and quantification (high LODs and LOQs) making the optimization of already existing and the development of new methods as well as their combination with efficient preconcentration and enrichment for NPLs necessary;
- Particle size detection limit of the most nondestructive particle-based methods is diffraction limited, impeding the analysis of NPLs below approximately 300 nm. Hence, the approaches which combine the techniques providing information on particle number and size/size distribution in nm-range, and enabling the identification of particles are required. In this context, the methods allowing for the representative NPL analysis have to be developed;
- There are only restricted number of reference materials which resemble real NPL particles, hampering the development, optimization and validation of methods for sampling, sample preparation and detection of NPLs.
- Level of contamination within the nm-range is significantly higher compared to the  $\mu$ -range, making the contamination prevention and the analysis of procedural and laboratory blanks inevitable.

#### 3.2. Preconcentration, Enrichment and Fractionation of Nanoplastic Samples

For the reliable and representative analysis of NPLs, methods for the preconcentration (increasing number of particles in the sample) and/or enrichment (increasing plastic to nonplastic

particles ratio) are essential. The methods suitable for the preconcentration can rely on the membrane filtration,<sup>97,100</sup> whereas cascade of the filters with decreasing pore size can prevent/minimize the pore clogging and hence facilitate the process. Moreover, the size fractionation of (NPL) particles can be achieved by the cascade filtration, as reported by Hernandez et al.<sup>332</sup> They obtained the several fractions containing NPLs larger and smaller than 100 nm from personal care product samples and detected PE particles using FTIR and X-ray photoelectron spectroscopy for bulk measurements. Furthermore, ultrafiltration,<sup>98,333</sup> ultracentrifugation<sup>336</sup> and evaporation of solvent<sup>307</sup> can be utilized as summarized in recent review article by Schwaferts et al.<sup>68</sup>

In case when no information on the number and size of particles is desired and only the mass of the polymer(s) has to be determined (e.g., using Py-GC/MS or HPLC), liquid extraction of soluble polymers, or depolymerization of polymers insoluble in common solvents (e.g., PA, PET and PC)<sup>118,147,148</sup> can be applied, as already discussed in section 2.2 “Mass-based Methods for Analysis of Microplastics”.

For the enrichment of NPLs for the subsequent particle-based analysis, the digestion of organic matrix using H<sub>2</sub>O<sub>2</sub>, acid (e.g., 65% HNO<sub>3</sub>) or alkaline treatment can be applied.<sup>68,321,337</sup> Enzymatic treatment was found to be useful for the tissue digestion.<sup>68,337</sup> The density separation (e.g., with ZnCl<sub>2</sub>) tested for the extraction of NPLs e.g., from biosolids and soils was found to be rather inefficient for the removal of inorganic matrix (enrichment <30% for 0.05 and 1.0 μm PS beads).<sup>338</sup> Recently, a new method for the enticement of MPs in environmental waters has been proposed by Zhou et al.<sup>99</sup> The method is based on cloud-point extraction using Triton X-45 and allowed to achieve an enrichment factor of up to 500 for NPL particles made of PS (approximately 65 nm) and PMMA (approximately 85 nm), without disturbing their original morphology and sizes. The concentration of extracted NPLs has been quantified using Py-GC/MS.<sup>99</sup>

Besides preconcentration and enrichment, the size fractionation of polydisperse mixture of (plastic) particles is highly desired. While the cascade filtration using filters with small pore size (e.g., below 100 nm) is characterized by low flow rates and, hence, the restricted sample volume, several other techniques can be applied for this purpose. Field-flow fractionation (FFF) is a separation technique which utilizes a perpendicular force on particles in flow. Depending on their diffusivity, determined by characteristics like size, shape and/or density, particles are retained in the flow channel for different durations, resulting in the fractionation of particles in the sample. FFF works without a stationary phase, precluding interactions between plastic particles, however, their interactions with the membrane of the flow channel can occur making optimization steps necessary.<sup>68</sup> Nowadays, different FFF types exist, using various separating fields, like thermal, electric, gravity (or centrifugal), or cross-flow (e.g., asymmetrical flow FFF, AF4), which cover the whole nm-range and can extend to the low μm-range. Furthermore, the latter technique is also able to preconcentrate to some extent by creating a focusing flow that collects up to 50 mL of the sample at the beginning of the flow channel.<sup>68,339</sup> Among all other FFF-based techniques AF4 is more frequently used for the fractionation of NPLs,<sup>68,98,281,321,323,340,341</sup> whereas even better separation of particles (characterized e.g., by the same size but different density, as was shown for PS and PMMA, both 500 nm in diameter) can be achieved by the applying of centrifugal FFF (CF3).<sup>281</sup>

Further separation techniques can be based on chromatography, where a stationary phase is utilized for the separation of the analytes. For example, hydrodynamic chromatography (HDC), being a solution-phase liquid separation method, combines the advantages of fluid dynamics and exclusion chromatography and allows for particle size determination in the range from 10 to 1000 nm.<sup>69,342</sup> Pirok et al. developed an online two-dimensional separation system which combines HDC with size-exclusion chromatography (SEC) and allows relating the particle-size distribution of the particles to the molecular-weight distribution of constituting polymers.<sup>343</sup> In the first dimension, HDC was used to obtain information on the particle size distribution after that separated particles were dissolved in THF. In the second dimension, SEC was applied to separate the constituting polymer molecules according to their hydrodynamic radius for each of 80 to 100 separated fractions. Using the developed system, the combined two-dimensional distribution of the particle-size and the molecular-size of a mixture of various PS (of approximately 900 nm, 500 and 200 nm) and polyacrylate (PACR of approximately 80 and 60 nm) nanoparticles were obtained.<sup>343</sup> The applicability of HDC for the separation of NPLs originating from fragmentation, which may have rough surfaces, has not been demonstrated yet and it remains unclear whether the separation could suffer from the particle interaction with the stationary phase.

An elegant approach for the characterization of NPLs from complex matrices (tissues of salt-water mussels) based on a microcavity size selection and the subsequent size-exclusion Raman analysis has been recently proposed by Valsesia et al.<sup>344</sup> The approach combines a step of enzymatic digestion/filtering to eliminate the biological matrix with a detection/identification procedure, which uses a micromachined surface, composed of arrays of cavities with well-defined submicrometer depths and diameters. To create arrays of cavities on a standard silicon chips, a SEM instrument equipped with a focal ion beam has been used. Two different patterns have been prepared: holes with 1.25 μm separated by 2 μm and three holes of 300 nm size positioned on the vertexes of an equilateral triangle with side of 1 μm. This sensor surface, exploits capillary forces in a drying droplet of analyte solution to drive the self-assembly of suspended nanoparticles into the cavities, leaving the individual particles isolated from each other over the surface. The resulting array, when analyzed using confocal μ-Raman spectroscopy, permitted the size selective analysis of the individual submicrometer NPLs trapped in the cavities structure. The developed approach has been successfully tested for the detection of NPLs in mussels which were exposed to PS beads.<sup>344</sup>

Although several applicable methods for the preconcentration, enrichment, and fractionation of NPLs have been already developed, low concentrations of NPLs in real samples and the complexity of matrices with a high number of nonplastic particles make the sample preparation really challenging, hampering the reliable analysis of NPLs in environmental and food samples.

### 3.3. Mass-based Methods for Analysis of Nanoplastics

Depending on analytical question, the information on the presence of NPLs and their mass in distinct size fraction (e.g., < 1 μm) may be sufficient, e.g., for the monitoring and modeling. In this case, mass-based methods can be applied. Till now Py-GC/MS remains most often used.<sup>97–99</sup> Ter Halle et al. first reported on the detection of nanoplastics in North Atlantic

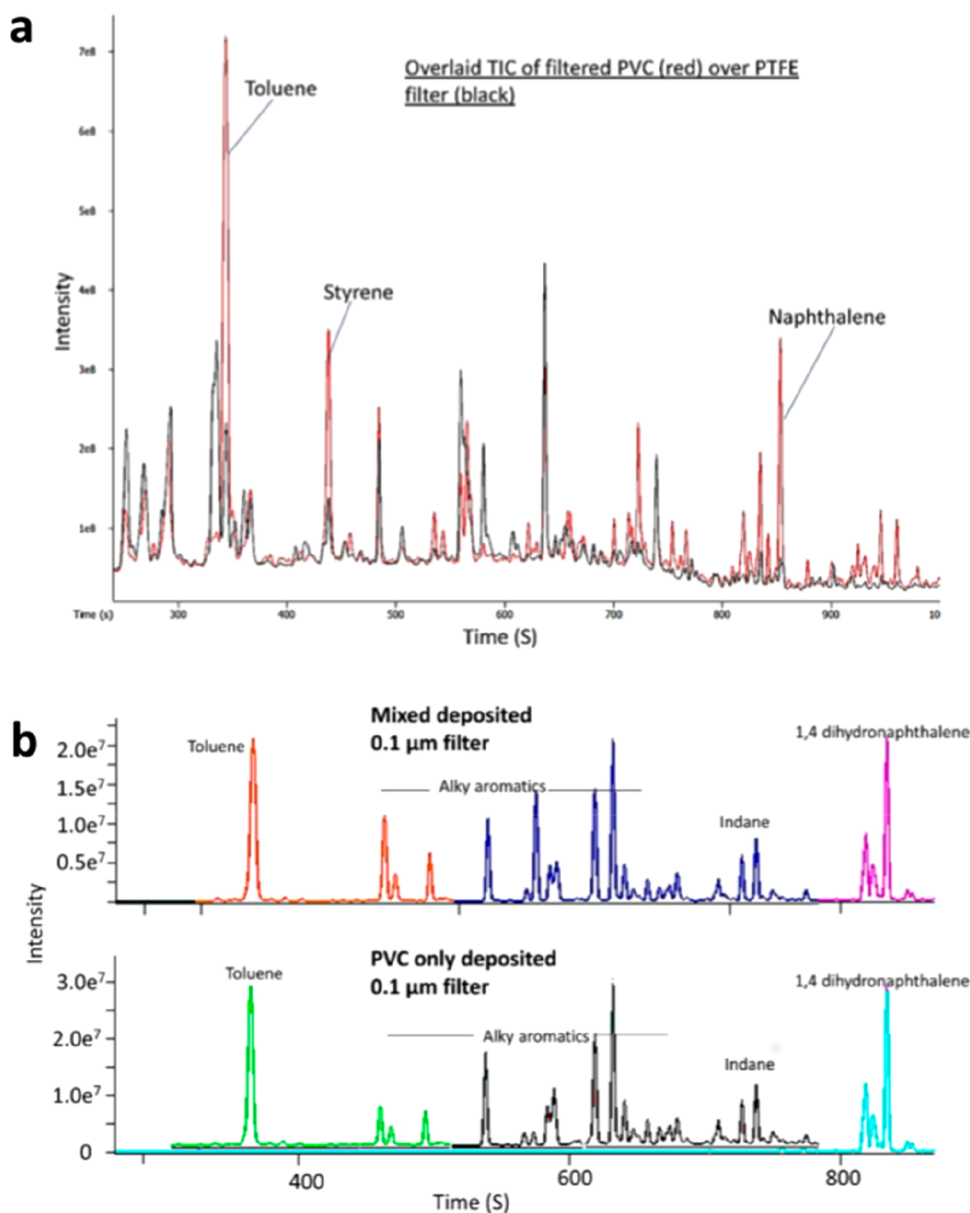


**Figure 12.** (a) Overlaid total ion chromatogram of PCV deposited by filtration compared with PTFE filter blank ( $0.1 \mu\text{m}$  pore size) with clearly identifiable signals from PVC decomposition products, namely toluene, styrene, and naphthalene. (b) Comparison of extracted ions ( $91, 117, 130 m/z$ ) for PVC from sample deposited with only PVC (bottom) particles and a sample deposited with a mix of plastics particles (PP, PS, PVC) (above) deposited on  $0.1 \mu\text{m}$  filter. Adapted with permission from ref 100. Copyright 2020 Elsevier.

Subtropical Gyre (NASG) using Py-GC/MS.<sup>97</sup> For the identification of polymers, a database of commercial polymers was combined with chemometric approach using PCA. The analysis of the colloidal fraction  $<1.2 \mu\text{m}$  after filtration revealed the presence of PVC, PET, PS, and PE with relative proportion of their anthropogenic pyrolytic fingerprints being 70, 17, 9, and 4, respectively. Although these numbers cannot be transformed into the proportion of plastics in the sample because the pyrolytic efficiency is not the same for each type of plastic, they indicate the relatively high abundance of NPLs made of PVC and PET compared to PE, PS, and PP (not detected in NPL fractions), which are found to be predominant for MP fractions.<sup>97</sup> Recently, Py-GC/MS was applied to demonstrate the presence of NPLs (PS and PVC) in sand water extracts from coast exposed to NASG.<sup>330</sup> However, the identification of NPLs in complex environmental matrices remains a challenge due to

low concentrations of NPLs compared to the NOM, as was pointed out by Blanco et al.<sup>345</sup> The authors applied Py-GC/MS for the identification of PP and PS and studied possible interferences with environmental matrices by spiking NPLs in various organic matter suspensions (i.e., algae, soil natural organic matter, and soil humic acid) and analyzing an environmental suspension of NPLs. Two different and complementary strategies were developed depending on the plastics composition and the NOM content. While PP NPLs can be directly identified in complex media, PS NPLs require a preliminary treatment. For this purpose,  $\text{H}_2\text{O}_2$  and UV light were used to selectively degrade NOM without affecting NPLs. The proposed strategies open new possibilities for the detection/identification of NPLs in environmental matrices such as soil, dust, and biota.<sup>345</sup>

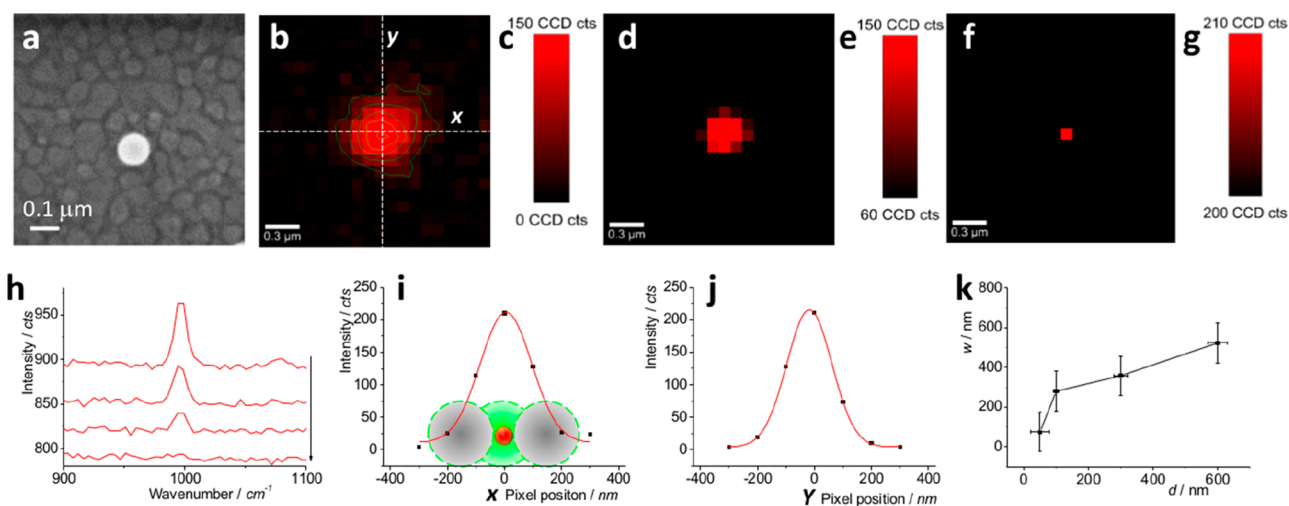


**Figure 13.** SEM (a), Raman images (b–g), spectra (h), intensity distribution (i,j), and the relationship between the Gaussian peak width ( $w$ ) and the diameter of nanoplastics ( $d$ ) (k). NPLs 100 nm in diameter were distributed on a gold wafer surface and mapped with the pixel size of 100 nm  $\times$  100 nm with contour lines (b) and without color interpolation, (d,f) are the offsetting images of (b); (h) shows the spectra (from top to bottom) at each pixel along the  $x$ -axis, from the center to the left boundary in (b). Reproduced with permission from ref 305. Copyright 2020 Elsevier.

Mintinig et al. developed an approach for the analysis of NPLs in aqueous environmental samples, which combines cross-flow ultrafiltration, AF4, and Py-GC/MS.<sup>99</sup> The authors used PS NPLs (50, 100, 200, 500, and 1000 nm in diameter) as model particles to spike different environmental samples (drinking and surface water) and found LODs and LOQs ranging for 50–100 ng and for 100–250 ng, respectively (estimated values were based on the signal of tristyrene, which is specific for PS, NPLs of 200 nm diameter were applied for calibration). Under the given settings and pyrolyzed volumes of 25  $\mu$ L, the LOD and LOQ of 4 mg/L and 4–10 mg/L were assessed. Preconcentrating NPLs by cross-flow ultrafiltration enabled for the identification of PS when its original concentration in an aqueous sample was  $>20$   $\mu$ g/L. Very recently, Wahl et al. demonstrated feasibility of coupling AF4 to Py-GC/MS for the identification of NPLs in NOM-reach environmental sample, namely in a soil amended with plastic debris. The AF4-based size fractionation of water extracts ( $<0.8$   $\mu$ m fractions) prior to chemical analysis makes it possible to circumvent the organic matter impact on NPL detection. Using this approach, PP, PS, and PVC NPLs with a size ranging from 20 to 150 nm were identified in soil for the first time.<sup>331</sup>

Sensitive analysis of different NPL particles with the size limit down to 100 nm can be achieved using Py-GC/ToF spectrometry, as recently reported by Sullivan et al.<sup>100</sup> The preconcentration of samples utilizing PTFE membranes as sample support allowed for the identification and quantification of model NPLs (PP, PS, and PVC) extracted from spiked aqueous samples with LODs  $< 50$   $\mu$ g/L. Figure 12 gives an example on the analysis of PVC particles deposited on the filter with 0.1  $\mu$ m pore size. Decomposition products of PVC (toluene, styrene, and naphthalene) can be clearly distinguished from the filter background (Figure 12a) and identified in the mixture of PVC with PP and PS (Figure 12b). For the verification of the developed method the analysis of a complex sample (river water) was performed, revealing the presence of PS with a semiquantifiable result of 241.8  $\mu$ g/L.<sup>100</sup>

Furthermore, a promising method providing very sensitive identification and (semi)quantification of NMPs, which is based on thermal desorption-proton transfer reaction-mass spectrom-

etry (TD-PTR/MS), was recently proposed by Materic et al. The estimated LOD for PS was below 1 ng, and it was possible to detect PS in complex samples (snow with DOM) down to 10 ng.<sup>100</sup> Alternative approach based on the use of HPLC after polymer extraction and depolymerization has been developed by Castelvetro et al. The approach providing LOD and LOQ of 15.3 and 51.1  $\mu$ g/L, respectively, for PET, is shown to be suitable for the identification and quantification of PET and PANMPs in complex samples (e.g., WWTP sludge),<sup>118</sup> as discussed in more detail in section 2.2 "Mass-based Methods for Analysis of Microplastics". Thus, several methods have been developed and already tested for the identification and (semi)quantification of NPLs in different environmental samples, but further optimization and validation of detection methods as well as application of efficient preconcentration and enrichment for NPLs will improve the analysis reliability.

### 3.4. Nondestructive Spectroscopic Methods for Analysis of Nanoplastics

The spatial resolution of spectroscopic methods established for the analysis of microplastics is governed by the diffraction limit of light and, hence, confined to approximately 10  $\mu$ m and approximately 300 nm for  $\mu$ -(FT)IR and  $\mu$ -Raman, respectively, allowing for the analysis of (almost) entire size range of MPs. Although,  $\mu$ -Raman appears to be partially applicable for the analysis of particles in the nanometer range, the recognition of particles smaller than approximately 500–1000 nm (depending on particle properties, used substrate and illumination mode) is challenging. Therefore, the combination of SEM and  $\mu$ -Raman spectroscopy for high resolution images on the one hand, and the reliable spectroscopic identification of particles on the other hand, has been established and applied for the analysis of small MPs (as discussed in section 2.4.3.1 "Combined Application of Electron Microscopy with Spectroscopic Techniques") and most recently also NPLs.<sup>252,305–307</sup> In this light, Sobhani et al. have demonstrated that Raman imaging can be successfully used to visualize and identify NPLs down to 100 nm by distinguishing the laser spot, the pixel size/image resolution, the NPLs size/position (within a laser spot), the Raman signal intensity, and via the sample preparation.<sup>252</sup> The combined method has been tested for the analysis of paint-polishing dust samples collected

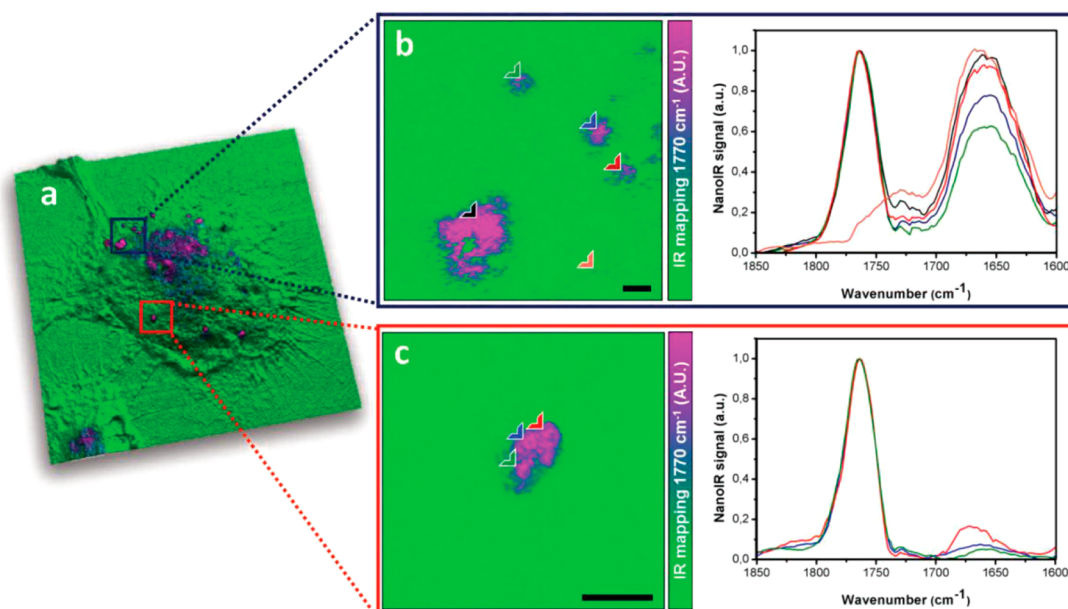


**Figure 14.** Example for the analysis of PLA nanoparticles in the hydrated cell using AFM-IR. (a) 3D display of the IR map at  $1760 \pm 4 \text{ cm}^{-1}$  (the band at  $1760 \pm 4 \text{ cm}^{-1}$  is assigned to the C=O str. vibration of PLA ester groups) of the entire macrophage. (b,c) The two red and blue squares show ROIs containing NLPs, which were further zoomed. For each zoom, an IR map was performed at  $1770 \text{ cm}^{-1}$ , and several IR spectra were acquired in specific locations indicated by arrows. The color of the IR spectra corresponds with that of the related arrows. The scale bar represents 500 nm. Reproduced with permission from ref 360. Copyright 2018 Wiley-VCH.

from a driveway, when a vehicle's clear coating of poly acrylic was polished by hand. The authors estimated that billions–trillions of NMPs with the size down to approximately 200 nm have been generated by hand-polishing an engine hood.<sup>252</sup> In the following study, the authors focused on the visualization and identification of NPLs smaller than the diffraction limit of the laser and examined the lateral intensity distribution of the Raman signal emitted by NPLs in the size range of 30–600 nm within the excitation laser spot as reported by Fang et al.<sup>305</sup> To image and visualize individual nanoplastics, the authors decreased the mapping pixel size and offset the color to intentionally image only the high-intensity portion of the Raman signal (emitted from the center of the laser spot, to determine the exact position of the NPLs as illustrated in Figure 13 for the 100 nm PS particle. The imaging of particles in the range of 30–80 nm was possible but very challenging because the Raman signal becomes very weak and barely distinguishable from the noise. Nevertheless, the high potential of the SEM-Raman combination has been demonstrated. Furthermore, instruments available on the market allow to perform correlative Raman imaging and SEM, opening new possibilities for the optimized and detailed morphological and chemical analysis of NPL particles.

In this context, Zhang et al. applied correlated Raman imaging and SEM for direct observation of the release of NPLs from commercially recycled plastics.<sup>306</sup> Although several difficulties have to be considered when combining SEM and Raman, i.e., carbon deposition on the particles and their damage by electron beam during SEM, challenges in relocating the same particle when switching, and a need for vacuum conditions in the SEM chamber,<sup>67,346</sup> this approach provides detailed morphological and chemical information on NPLs and seems to have a high potential for the analysis of tiny plastic particles.

To tackle the problem of the weak Raman signal for small NPL particles, the applicability of surface-enhanced Raman scattering (SERS) has been recently explored.<sup>347–349</sup> Generally,

Raman signals of analytes can be significantly enhanced if they are located close to or are attached to nanometer-sized metallic structures (Ag or Au), like colloids or rough surfaces. Enhancement factors in the range of  $10^3$ – $10^{11}$  can be achieved due to electromagnetic (“localized surface plasmon resonance, LSPR”) and chemical (“charge transfer, CT”) enhancement effects.<sup>350</sup> Recent paper by Lv et al. has demonstrated that Raman signal of PS beads with 100 and 500 nm in diameter can be significantly enhanced (up to  $5 \times 10^2$  and  $4 \times 10^4$ , respectively) by using Ag colloid (prepared according to Lee and Meisel protocol<sup>351</sup>) as SERS media.<sup>347</sup> In comparison with PS NPLs, the enhancement for PE and PP MPs (both 10  $\mu\text{m}$  in diameter) was not so strong. The authors illustrated the applicability of SERS for sensitive detection of NPLs in pure water and seawater.<sup>347</sup> Independently and almost simultaneously, Zhou et al. reported on SERS enhancement for PS beads with 50 nm in diameter utilizing Ag colloid (prepared according to Leopold and Lendl protocol<sup>352</sup>) and applied the method for the analysis of model NPLs in river water.<sup>348</sup> In this light, Lê et al. developed novel nanostructured Raman substrates for the sensitive detection of NPLs in water.<sup>349</sup> They prepared anisotropic nanostar dimer-embedded nanopore substrates and successfully tested the method for the sensitive detection of PS beads with 400 nm in diameter, whereas no significant enhancement was achieved for PS NMPs with diameters of 800 nm, 2.3  $\mu\text{m}$ , and 4.8  $\mu\text{m}$ .<sup>349</sup> While the SERS enhancement has been demonstrated for PS beads in the size range of 50–500 nm, the applicability of this approach for the detection of other polymer types as well as for fragmented NPLs with irregular shape still has to be proven. Furthermore, interferences of organic residues from the matrix, e.g., humic like substances which are usually present in environmental samples,<sup>353</sup> have to be overruled.

It has to be mentioned that the complementary IR and Raman analysis of NPLs down to approximately 300  $\mu\text{m}$  can be in principle performed by the novel technique, namely optical

photothermal IR spectroscopy,<sup>9,10,223,224</sup> which has been already addressed at the end of section 2.3.1.1 “IR Spectroscopy”. However, the feasibility of this techniques for the characterization of NPL particles has not been demonstrated yet.

**3.4.1. Scanning Probe Microscopy Coupled to Spectroscopy.** While the already discussed vibrational spectroscopic techniques are shown to be powerful for the reliable identification, quantification and characterization of MP and (partially) NPL particles, they cannot solve the restriction on the spatial resolution imposed by the diffraction limit of light.<sup>354</sup> Here, impressive efforts in the development of scanning probe techniques for the chemical analysis at the nanoscale<sup>354–358</sup> suggest a huge potential of these techniques in the field of NPL studies. These nanoscale techniques include atomic force microscopy (AFM) combined with spectroscopy, namely AFM-IR (or photothermal induced resonance), nano-FTIR, and tip-enhanced Raman spectroscopy (TERS). In AFM-IR a pulsed tunable IR laser source is focused on a sample (either from below in total internal reflection or from above) near the AFM tip and tuned to an absorbing band of the sample. The absorbed light leads to the local photothermal expansion of the sample, which is registered by the AFM tip. Because a transient cantilever oscillation is proportional to the IR absorption, measuring the AFM cantilever oscillation amplitude as a function of wavelength (or wavenumber) results in a local absorption spectrum with nanoscale spatial resolution (around 20–50 nm).<sup>355,358</sup> The AFM-IR technique has been already successfully applied for the chemical identification and nanometer-scale chemical imaging of polymer nanostructures by Felts et al. They analyzed PE and PS nanowires deposited on the IR-transparent ZnSe prism in the total internal reflection mode and achieved a spatial resolution better than 100 nm.<sup>359</sup> Furthermore, AFM-IR allows for the localization and chemical characterization of NPLs directly within a cell without labeling as reported by Pancani et al.<sup>360</sup> They analyzed macrophages incubated with PLA NPLs smaller than 200 nm, as such particles are among most employed nanocarriers in drug delivery (e.g., to treat complex pathologies such as cancer and severe infections). As an example, Figure 14 shows a 3D IR map of the dehydrated cell recorded at  $1770\text{ cm}^{-1}$  (the band at  $1760 \pm 4\text{ cm}^{-1}$  is assigned to the C=O str. vibration of PLA ester groups) as well as two regions of interest (ROIs) and corresponding spectra illustrating the detection and identification of PLA particles with mean diameter of approximately 180 nm. The authors concluded that the AFM-IR could become a powerful tool to unravel the fate of individual unlabeled NPL particles inside cells.<sup>360</sup>

The nano-FTIR method is based on scattering type of scanning near field optical microscopy (s-SNOM) and allows measurement of broadband IR absorption spectra of surfaces with spatial resolutions as low as 10–20 nm. In nano-FTIR experiments, the IR-beam (e.g., broadband laser) is focused on the near field probe, typically metal coated tip and a local antenna effect creates a nanoscaled focus with the dimension of the tip. During the scanning of the surface with the tip, periodic changes in near-field interactions between tip and sample occur. The resulting changes in local scattering intensity are detected then using an asymmetric Michelson interferometer. The amplitude and phase of scattered light can be related to the local IR absorption bands of the sample, and the obtained spectra agree well with bulk FTIR data for a wide range of samples.<sup>357</sup> The nano-FTIR has been successfully applied for the analysis of NPLs. For example, already in 2006, Brehm et al.

reported on the detection of PMMA beads with 30–70 nm in diameter.<sup>361</sup> In this light, Huth et al. demonstrated that PMMA samples can be chemically characterized with a spatial resolution of 20 nm.<sup>362</sup> Recently Meyns et al. successfully tested the suitability of library-based search using commercial and open source analysis software (siMPLe) for the identification of different polymers detected by nano-FTIR. It was found that even polymer samples weathered in the environment can be correctly identified by this method without prior cleaning, opening wide fields of applications for the identification and characterization of diverse polymer samples.<sup>363</sup>

Nanoscale Raman spectroscopy (TERS) utilizes AFM (or scanning tunneling microscopy, STM) to scan a plasmonic metal nanostructure over a sample surface in order to locally enhance the field in a manner analogous to SERS. Metallic nanostructures are typically produced by metal coating of nonconductive AFM tips (or electrochemically etching conductive STM wire tips). In TERS experiments, the probe tip is positioned above the sample and a laser excites the particle's localized LSPR, a coherent oscillation of conduction electrons. The LSPR drastically enhances (up to 100–1000-fold) the local electric field in the nanoparticle's vicinity, leading to enhancement factors of up to  $10^8$ .<sup>358</sup> Nowadays, different configurations of TERS systems are available, including bottom-, top-, and side-illumination as well as parabolic mirror-based setup enabling the sensitive chemical analysis with the spatial resolution of approximately 30–50 nm and for some samples (e.g., carbon nanotubes) even down to 1.7 nm (using STM).<sup>354,358,364</sup> Thus, TERS could provide nanoscale resolved chemical information on NPL particles, but currently only one study by Yeo et al. has reported on the TERS analysis of a polymer-blend thin film (made of PS and polyisoprene, PI) with spatial resolution of approximately 20 nm,<sup>365</sup> hence the applicability of this very promising techniques in the field of NPLs still has to be explored.

Obviously, scanning probe techniques enable for the reliable identification and characterization of NPL particles with the spatial resolution below the diffraction limit and thus can foster our understanding of formation, distribution, and modifications of tiny plastic particles in various samples. However, the measurements are laborious and time-consuming, therefore only a small fraction of the sample with restricted number of particles can be analyzed in reasonable time that can hamper the representativeness of the analysis using nanoscale methods.

**3.4.2. Raman-based Analysis of Nanoplastics Enabled by Optical Tweezers.** The Raman analysis of NPLs and small MPs can be performed directly in aqueous media because water is very weak Raman scatterer. Such analysis can be realized by using optical tweezers which hold the particles in the focus of the laser beam, enabling the spectroscopic identification. Gillibert et al. illustrated the applicability of the approach combining optical tweezers and  $\mu$ -Raman spectroscopy for the trapping and chemical identification of NMPs.<sup>253</sup> Plastic particles (PE, PP, PS, PET, PVC, PMMA, and PA 6) in size range from 20  $\mu\text{m}$  and down to 50 nm dispersed in seawater were studied using 633 and 785 nm excitation lasers. The analysis at the single particle level allowed the authors to unambiguously discriminate plastics from organic matter and mineral sediments and to assess the size and shapes of NMPs (beads, fragments, and fibers), with spatial resolution only limited by diffraction. The method was tested on both model particles and naturally aged environmental samples, illustrating its potential for the characterization of real samples.<sup>253</sup>

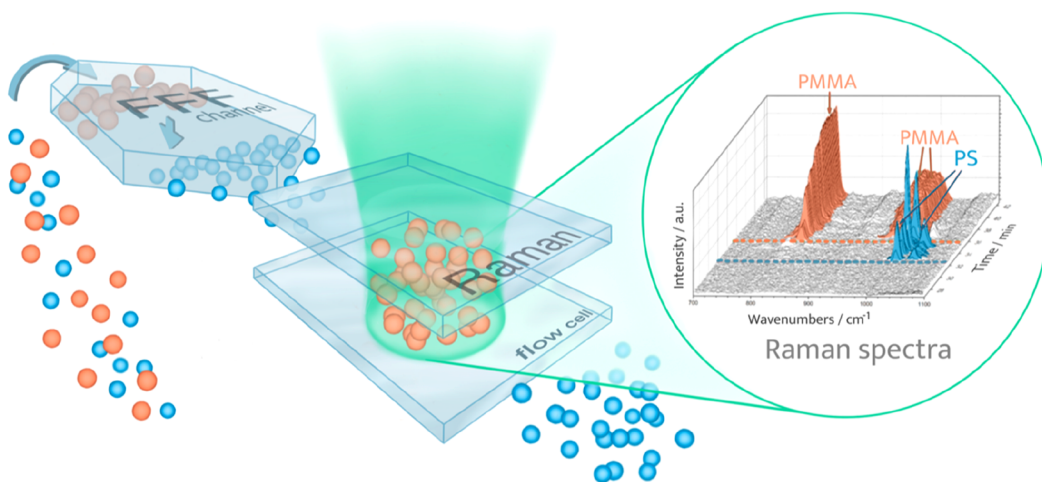


**Figure 15.** Scheme for NPLs analysis by online coupling of FFF and  $\mu$ -Raman spectroscopy enabled by optical tweezers. After the separation by FFF, NPL particles in fractions of 350 and 500 nm were identified by  $\mu$ -Raman as PS and PMMA, respectively. Adopted with permission from ref 281. Copyright 2020 American Chemical Society.

In this context, online coupling of field-flow fractionation and Raman microspectroscopy enabled by optical tweezers for the analysis of NPLs has introduced by Schwaferts et al.<sup>281</sup> The authors realized the hyphenation of particle separation and characterization (using AF4 or CF3 combined with UV- and multiangle light scattering, MALS detectors) with the subsequent chemical identification by online  $\mu$ -Raman spectroscopy in a flow cell, as illustrated in Figure 15. The utilization of 2D optical tweezers for the particle trapping allowed identification of particles of different reference materials (polymers and inorganic, namely PS, PMMA, and SiO<sub>2</sub>) in the size range from 200 nm to 5  $\mu$ m, with concentrations in the order of 1 mg/L (10<sup>9</sup> particles/L). The developed technique showed a high potential for applications in NPL analysis, as well as in many other fields of nanomaterial characterization.<sup>281</sup> However, the efficient preconcentration and enrichment of the NPLs from environmental and food matrices has to be developed in order to enable the reliable and representative analysis of NPL particles in real samples.

It has to be noted that the proper development, optimization, and validation of methods for sampling, sample preparation, and detection of NPLs requires realistic reference materials. Although certified reference materials for NPLs are not available yet, several promising approaches have already been proposed, as discussed in section 4.1. "Reference Materials for Microplastics and Nanoplastics". Furthermore, the issue of contamination during the sampling, sample preparation, and the detection of NPLs has to be carefully considered because the expected numbers of particles within the nanometer range are significantly higher compared to the micrometer range. Therefore, the measures developed for the contamination prevention in the field of MP research have to be extended for the nanometer range (including the filtration of water and chemicals using the filters with small pore size, sample preparation in the laminar flow box or even in clean room, etc.). Altogether, it highlights the importance of procedural and laboratory blanks, as discussed below.

#### 4. VALIDATION OF METHODS, QUALITY ASSURANCE, AND QUALITY CONTROL

The development, optimization, and improvement of chemical analysis by both mass-based and particle-based methods

requires reliable method validation. In this light, the use of blanks to calculate false positives and application of reference plastic particles to estimate the recovery rates (and found false negatives) for the sampling, sample preparation, and detection steps are essential. Furthermore, the comparison of data derived for the same reference materials and especially real samples, analyzed using similar and also different methods, is extremely important and helpful for the proper validation of the methods.

The establishment of a quality program to manage (i.e., quality assurance, QA) and maintain (i.e., quality control, QC) the accuracy and precision for the all steps of the NMP analysis, including sampling, sample preparation, and detection has been recognized as mandatory for reliable NMP studies.<sup>8,13,20,23,178,366–371</sup> Brander et al., who thoroughly addressed this issue, defined QA as "A series of steps or activities put in place in a systematic way to ensure that data that is generated is accurate and reliable" and QC as "The process of verifying or checking all data, results, or reported methods to ensure their validity and correctness and to prevent erroneous conclusions".<sup>369</sup> Several measures are found to be essential to ensure QA/QC: (i) performing of all steps in plastic-free of low-plastic working conditions, i.e., using glass, metal, or ceramic equipment (alternatively items made of seldom or pigmented polymers can be used) and cotton clothes, (ii) using laminar flow box or clean room for the sample preparation, if feasible, (iii) applying an appropriate cleaning procedure for the used equipment, solvents and chemicals, (iv) estimating procedural and laboratory blank values, recovery rates and including replicates, and (v) participating in interlaboratory comparisons and proficiency tests.<sup>8,13,20,23,178,366–370</sup> To perform recovery rate experiments as well as interlaboratory comparisons and proficiency tests, appropriate reference materials for NMPs are required. These reference materials, being homogeneous and stable, have to mimic the diversity of plastic particles, including broad size range as well as different polymer types, shapes, and aging states. Thus, a high variety of reference plastic particles as pure materials or imbedded in simple and complex matrices is required for the reliable harmonization and standardization of methods for the MP analysis.

##### 4.1. Reference Materials for Microplastics and Nanoplastics

Although different reference materials are available and several protocols for the preparation of microplastic and nanoplastic

particles have been proposed,<sup>60,187,372–377</sup> there is no certified products yet. Taking into account the rates of production for different polymers, and the available information on the contamination of environmental and food samples, thermoplastic polymer types, namely PE, PP, PS, PET, PA, and PVC, seems to be more relevant.<sup>20</sup> Furthermore, reference materials for fibers related to textile applications as well as for tire wear particles, which both are supposed to contribute at high extent to MP contamination,<sup>113,378</sup> are required.

The reference plastic particles larger than 30–50  $\mu\text{m}$  can be efficiently produced in “top-down” approach by cryogenic milling using pristine or aged polymers from plastic pellets or plastic products, as was reported by Eitzen et al.<sup>372</sup> and Seghers et al.<sup>373</sup> The resulting particle size distributions are usually very wide (more than 200  $\mu\text{m}$  in mean particle diameter), which corresponds to the environmental occurrence observed.<sup>20,372,373</sup>

For the preparation of reference materials with the particle size smaller than 10–50  $\mu\text{m}$ , the application of cryogenic milling was found to be less efficient because only small fraction of particles in lower micrometer range can be obtained. Furthermore, the handling of very small dried particles is challenging, because they are easily airborne.<sup>20</sup> Therefore, the fragmentation in aqueous medium can be a more suitable alternative for the preparation of NMP particles.<sup>341</sup> In this context, von der Esch et al. proposed a method for simple generation of suspensible secondary microplastic reference particles via ultrasound treatment at alkaline conditions.<sup>187</sup> This approach, tested for PS and PET as well as for biodegradable plastic, namely PLA, is applicable for the preparation of microplastic particles of in the entire size range (1–1000  $\mu\text{m}$ ) and a multitude of shapes (irregular particles, spheres, films, and fibers) as well as nanoplastic particles (<1  $\mu\text{m}$ ). The FTIR analysis revealed modified particle surfaces typical for aged MPs (additional OH, C=O, and COOH groups), explaining the good suspensibility of produced NMPs in water without addition of any surfactants.<sup>187</sup> The “top-down” approach in aqueous medium can be also realized by applying of laser ablation, as demonstrated by Magri et al.<sup>60</sup> The produced PET nanoparticles have an average dimension of approximately 100 nm, with significant size and shape heterogeneity. Furthermore, weak acid groups were detected on the particle surface, similarly to photodegraded PET plastics. Thus, the particles can mimic real environmental nanopollutants. When tested on a model of intestinal epithelium, nano-PET showed a high propensity to cross the human gut barrier.<sup>60</sup>

Particles in the lower micrometer range can be also generated using “bottom-up” approach by a controlled synthesis of polymeric building blocks, as already established for PS particles in the field of nanomaterials.<sup>20</sup> Recently, an alternative method for the production of PE particles with radii between 200 and 800 nm utilizing emulsions of toluene in water with PE dissolved in toluene has been presented by Balakrishnan et al.<sup>374</sup> The yield of PE microparticles was very small in the absence of a surfactant but increased substantially by addition of a surfactant (Tween 60, Tween 80, and a biosurfactant). The authors found that, by using a biosurfactant, the presence of an eco-corona at the surface of the particles could be mimicked, improving the bioavailability of particles in experiments with *Daphnia magna*.<sup>374</sup> For the estimation of recovery rates<sup>379</sup> at different steps of analysis and conductions of exposure experiments with different organisms,<sup>380</sup> micro- and nanoplastics labeled with fluorescence dyes are often applied. However, the use of fluorescence signal alone for the detection of labeled plastic

particles can lead to artifacts in uptake and translocation studies due to the leaching of the fluorescent dye, as has been recently demonstrated by Schür et al.<sup>381</sup> For environmental studies, reference materials labeled with stable isotope (<sup>13</sup>C)<sup>376,382</sup> or radio isotope (<sup>14</sup>C)<sup>377</sup> are found to be very useful. Al-Sid-Cheikh et al. proposed the procedure for the one-step synthesis of <sup>14</sup>C-labeled sulfonate end-capped PS nanoparticles of different sizes (20 and 250 nm), which can be detected and quantified by autoradiography. This radio-labeling approach can be applied for the quantification, mass balance, and recovery of the labeled particles from complex matrices at low predicted environmental concentrations.<sup>377</sup> However, the radiolabeling methodology comes with severe disadvantages, such as stringent and restrictive safety and material handling regulations and the need for instrumentation solely dedicated to analyses of radioactive <sup>14</sup>C-containing samples. These limitations can be circumvented by the application of <sup>13</sup>C-labeled polymers, as reported by Sander et al.<sup>376</sup> This stable isotope labeling approach can be used for the assessment of rates and extents of the environmental transformation of plastic pollutants at and below the nanoscale to low-molecular-weight products and their environmentally harmless microbial transformation products. Understanding the chemical transformation at this scale is critical for assessing potential risks associated with the occurrence of micro- and nanoplastics in the environment.<sup>376</sup> In this light, Taipale et al. used compound-specific isotope analysis to track the fate of fully labeled <sup>13</sup>C-PE MP carbon across the aquatic microbial–animal interface. Isotopic values of respired CO<sub>2</sub> and membrane lipids showed that MP carbon was partly mineralized and partly used for cell growth. Microbial mineralization and assimilation of PE-MP carbon was most active when inoculated microbes were obtained from highly humic waters, which contain recalcitrant substrate sources.<sup>383</sup> An alternative approach utilizing metal-doped materials to investigate the fate, transport, mechanistic behavior, and biological uptake of nanoplastics in complex environmental systems was introduced by Mitrano et al.<sup>375</sup> They reported on a method to synthesize nanoplastic particles doped with a chemically entrapped metal used as a tracer (i.e., Pd), which provides a robust way to detect nanoplastics more easily, accurately, and quantitatively, e.g., using (SP)-ICP-MS. The general structure of the nanoparticles synthesized was a PAN core material that contained the metal tracer, followed by the addition of a cross-linked PS shell.<sup>375</sup> These metal-doped particles are thought to be good proxies for nanoplastics, opening the window to accurately assess the potential environmental hazards that NPLs pose.<sup>325</sup> Recently, the metal-doping method was extended for the production of In-doped PET microfibers, enabling long-term assessment of nanoplastic particles and microplastic fibers (using Pd- and In-labeled materials, respectively) in complex matrices.<sup>384</sup>

## 4.2. Interlaboratory Comparison Studies

Generally, interlaboratory comparison (ILC) tests are conducted for the following purposes: (i) to validate analytical methods, i.e., to evaluate their performance (correctness and precision) and (ii) to check the suitability of laboratories for the analysis of certain samples.<sup>20</sup> To evaluate the performance (correctness and precision) of different methods, applied for the identification and quantification of microplastics and to develop harmonized and standardized methodology for the future studies, ILC tests are essential. In this context, several national and international ILC were already conducted (e.g., in the frame

of projects BMBF-MiWa, BASEMAN, QUASIMEME, and SCCWRP). Becker et al. presented the results of ILC for the identification and mass-based quantification of MP in freshwater suspended organic matter using different thermoanalytical methods. They found that participants utilizing Py-GC/MS, TED-GC/MS, and TGA-FTIR were able to correctly identify all polymers and to report reasonable quantification results in the investigated concentration range (PE, 20.0  $\mu\text{g}/\text{mg}$ ; PP, 5.70  $\mu\text{g}/\text{mg}$ ; PS, 2.20  $\mu\text{g}/\text{mg}$ ; PET, 18.0  $\mu\text{g}/\text{mg}$ ).<sup>125</sup> Isole et al. reported on results for particle-based analysis of MPs in the size range of 0.4–5.7 mm mixed with 1 L of seawater conducted by 12 laboratories. Because large standard deviations for the data obtained without using spectroscopic methods (FTIR and Raman) were found, the authors recommended the spectroscopic identification of small MP particles.<sup>385</sup> The results of ILC for 17 laboratories from eight countries analyzing samples comprised of five different types of MP reference particles (PE, PVC, PET, PMMA, and PS) with diameters ranging from 8 to 140  $\mu\text{m}$  suspended in ultrapure water were presented by Müller et al.<sup>386</sup> While for the identification of polymer type  $\mu$ -Raman and thermoanalytical methods (Py-GC/MS and TED-GC/MS) performed best, the quantification of polymer mass for identified polymer types was questionable for thermoanalytical methods, whereas other methods failed to determine the correct polymer mass. Quantification of particle number per identified polymer type was most successful for  $\mu$ -FTIR. The results indicated clearly the need for the optimization of individual methods and for harmonization and standardization of MP analysis.<sup>386</sup> The another recent comparative test organized by the German Federal Institute of Materials Research and Testing (Bundesanstalt für Materialforschung und -prüfung, BAM) was carried out by 15 laboratories, using MPs made of PE (aged) and PET imbedded in KBr matrix.<sup>387</sup> It was demonstrated that the different analytical methods for the identification and quantification of microplastics within the two approaches, namely thermoanalytical (Py-GC/MA, TED-GC/MS) and spectroscopic ( $\mu$ -FTIR and  $\mu$ -Raman) provide comparable results. All four analytical methods were able to identify the two added polymers (PE and PET). For the thermoanalytical methods, all mass contents fall within the range of the target value. Recovery was better for PE than for PET, probably due to the properties of the marker compound. For the spectroscopic methods, all results are within a  $z$ -value of 2.00, which is generally considered as a solid result and indicates a satisfactory measurement accuracy of the participating laboratories. Briefly, the  $z$ -value was calculated according DIN 38402-45,<sup>388</sup> a German standard for round-robin tests. For this, the difference between the measured value of each individual laboratory (the mean value of the measurement results within a laboratory) and the expected value (mean value over all measured values) was determined and set in relation to the standard deviation over all measured values.<sup>387</sup> The most extended ILC test, where around 100 laboratories from Europe (EU, EFTA, and UK) as well as from Australia, Asia, and the USA took a part, has been recently organized by Joint Research Center (JRC), European Commission, in collaboration with the BAM.<sup>389</sup> The participants obtained two sample kits, each comprising of PET particles (size range approximately 30–200  $\mu\text{m}$  with particle number of  $797 \pm 151$  and particle mass of  $293 \pm 41 \mu\text{g}$  as mean and SD, respectively)<sup>373</sup> imbedded in NaCl carrier containing a surfactant (Triton X-100). The kits were provided together with a bottle with 950 mL of water (Milli-Q), into which the content of the vial should be quantitatively transferred and one vial with

60 mL of 0.1% Triton X-100 solution for the transfer of the NaCl–carrier mixture into the water bottle to generate the actual test item, i.e., the water sample containing MP particles. The final report is still in preparation and should be published soon. The preliminary results were made available for the participants of ILC test and indicated that  $\mu$ -(FT)IR and  $\mu$ -Raman spectroscopy were the most applied techniques for the MP analysis (39% and 16% of all participants, respectively), providing the reliable identification and particle-based quantification of MPs > 30  $\mu\text{m}$ . Also, the methods applying pyrolysis combined with GC/MS were found to be suitable for the identification and mass-based quantification of PET in aqueous matrices. Furthermore, both qNMR and HPLC provided reliable results.<sup>389</sup> Following ILC tests using different polymers in the lower micrometer range in simple (e.g., NaCl) or more complex (e.g., sediment) matrices should help to validate further different mass-based and particle-based methods for the chemical analysis of MP in different complex samples and to contribute to the harmonization and standardization in the field of MP studies. Because the methods for the identification and quantification of nanoplastics are still under development, no comparative tests were carried out yet and will be a subject of future efforts.

## 5. SUMMARY AND PERSPECTIVES

Microplastics and, recently, nanoplastics have been recognized as emerging particulate anthropogenic pollutants, and this triggered a high scientific and public interest and growing concern. The urgent questions, on the occurrence of these tiny particles in the environment, drinking water, food, etc., on their sources and sinks, on fragmentation and degradation of NMPs, on the transport and fate of particles and associated (in)organic contaminants, and, especially, on effects of NMPs on the environment and human health, stimulated an avalanche of studies in this field. These studies become more and more interdisciplinary, including analytical and environmental chemistry, polymer and material science, recycling, water and waste management, agricultural and food science, toxicology, and medicine as well as social science and legislation.

However, to investigate the high complexity and diversity of this (probably one of the most challenging) analyte, the essential necessity to adopt and optimize the existing and to develop and validate new efficient methods is evident. To fulfill all requirements, the methods have to enable reliable and sensitive identification, quantification, and characterization of NMPs in the entire size range and in different media. Therefore, on the one hand, time- and cost-efficient methods suitable for the representative and high throughput analysis are required for monitoring studies. On the other hand, methods providing detailed information on the chemical composition, number, size/size distribution, shape, surface properties, associated additives, and sorbed contaminants, weathering state, etc., are needed for better understanding of the NMP fate in the environment and for thorough assessment of the potential ecotoxicological risks. Furthermore, by taking into account the ubiquity of plastic particles and fibers, suitable measures for the contamination prevention during all steps of the MP analysis have to be considered.

Sensitive methods for the chemical identification and mass-based quantification are desired in order to facilitate the regular and repeated MP analysis, e.g., to monitor the level of MP pollution and to control the feasibility and efficiency of measures taken to prevent plastic contamination. These methods have to

be combined with representative sampling and, in the case of low MP contents (typical for the most real samples), efficient sample preparation (e.g., removal of (in)organic matrices or extraction of soluble polymers). The fractionation using, e.g., cascade filtration, can suffer from imprecise separation of MPs according to size classes (e.g., smaller particles can be collected in larger size fractions due to the filter clogging, while long fibers can reach lower size classes due to their smaller diameter), but it can help to achieve (semi)size-related information on the MP occurrence relatively quickly and efficiently. As discussed above, nowadays, Py-GC/MS and TED-GC/MS are the most applicable mass-based methods. While the former is characterized by the higher absolute sensitivity, the latter allows us to analyze relatively large masses of samples (up to 100 mg, which is about 200 times larger than those for Py-GC/MS). Therefore, MP analysis of highly polluted samples (containing more than 0.5–1 wt % for the each of analyzed polymer types) can be performed without the matrix removal. However, taking into account that the expected entire MP content in most environmental and food samples is significantly below 1 wt %, the efficient sample preparation is required for the both methods.

The high sensitivity of Py-GC/MS has been already verified for the detection of NPLs in model and real samples. Moreover, several very sensitive methods for mass-based analysis of NMPs, namely Py-GC/ToF, TD-PTR/MS, and MALDI-ToF/MS, have been recently introduced. Furthermore, soluble polymers can be efficiently identified and quantified by utilizing Py-GC/MS as well as  $^1\text{H}$  NMR and HPLC. While all mass-based methods are destructive and provide information on MP contents of single polymer types, regardless of any particle appearance, they should be considered rather as complementary than competitive to particle-based methods. Thus, mass-based methods can be applied in combined studies consecutively, i.e., after nondestructive analysis, in order to achieve complementary data (e.g., detailed information on copolymers, organic additives, and weathering products, in addition to the data on polymer masses).

The studies on sources and sinks of plastic particles, on their fate and transport, on mechanisms and time scales of fragmentation as well as on eco-toxicological impacts of MPs, require efficient methods for the chemical identification and particle-based quantification. Here, representative sampling and efficient sample preparation are essential. The latter is applied in order to remove (in)organic matrices which can hamper proper identification and quantification of MPs and to increase plastic/nonplastic ratio, thus facilitating representative analysis for similar time efforts. These methods have to deliver reliable information on the occurrence of MPs and, hence, to provide solid basis for toxicological tests at environmentally relevant concentrations. In the context of MP impact on humans, information on MP contamination of drinking water, food, and especially air (which is assumed to be the main source of the NMP uptake by humans, including plastic particles and fibers) is highly desirable. Generally, the (further) development and optimization of methods for MP studies down to lower  $\mu$ -range and, in particular, nanometer range are of high importance for the understanding of risks associated with NMPs because smaller particles are considered to be more hazardous.

Among all methods, including both mass-based and particle-based, IR spectroscopy, which has been already applied in the first MP study conducted by Thompson et al. in 2004,<sup>16</sup> remains the most applicable. This can be explained by the accessibility of

instruments (e.g., ATR-FTIR are available in most analytical laboratories) and also by the reliability of measurements. To tackle the problem of strong water absorption, the thorough drying of the samples is required before the analysis. Being combined with microscopy ( $\mu$ -FTIR), this method becomes applicable for the identification and particle-based quantification (including information on particle number, size/size distribution, and shape) with spatial resolution down to approximately 10–20  $\mu\text{m}$ . The utilization of FPA-based detection, where several detectors are placed in a grid pattern, allows for the time efficient  $\mu$ -FTIR analysis of large filter areas, providing the so-called hyperspectral imaging (which combines spatial and spectral information in one huge data set). This technique has been automated, already resulting in several detailed monitoring studies of different environmental samples, drinking water, and food. Recently, a promising alternative approach, where quantum cascade laser is applied as the light source, has been introduced for the MP analysis. Furthermore, HIS utilizing near- or mid-IR range has been shown to have a high potential for fast screening of samples even without sample preparation.

Another type of vibrational spectroscopy, namely  $\mu$ -Raman spectroscopy, is an efficient method for the chemical identification and quantification of MPs down to 1  $\mu\text{m}$  (and even NPLs down to approximately 300 nm). While this method is applicable for the analysis of MPs in the entire size range, and can detect more particles in the same size range than  $\mu$ -FTIR spectroscopy, the real power of  $\mu$ -Raman lies in the analysis of particles smaller than 10–20  $\mu\text{m}$ , which cannot be assessed by conventional IR techniques. However, the  $\mu$ -Raman analysis is usually more time-consuming and often suffers from the fluorescence interference (which can be minimized by the proper sample preparation and optimization of measurement parameters). Because FPA detectors are not applicable for the Raman instrumentation, only small images are usually obtained. Therefore, the particle recognition approach, utilizing optical image with the subsequent  $\mu$ -Raman analysis in particle-by-particle mode, is used in this case. Meanwhile, commercial and also open-source programs for the automated Raman analysis, enabling detection, identification, and quantification of thousands of (plastic) particles and fibers on the filter, are available. IR and Raman spectroscopy, being complementary, can be efficiently applied for detailed analysis of MP samples. In this context, a novel technique of optical photothermal IR spectroscopy enables simultaneous measurements of IR absorption and Raman scattering at the same location and with the same spatial resolution, thus opening unique possibilities for the complementary NMP analysis down to approximately 1  $\mu\text{m}$  and even below.

It is important to stress that for the reliable identification of MPs in environmental and food samples by both (FT)IR and Raman spectroscopy, suitable spectral libraries are required. To ensure the correct identification, these libraries have to include spectra not only for pristine but also for pigmented and weathered plastics as well as for nonplastic materials. Alternatively, model-based classification methods can be applied for the data analysis, where multivariate models of the actual data are used for the identification.

Besides classical  $\mu$ -Raman spectroscopy, nonconventional Raman techniques, namely anti-Stokes Raman scattering and stimulated Raman scattering, were shown to have a potential for the MP analysis. While complex setups are needed, these techniques do not suffer from the fluorescence interference and enable the fast and sensitive identification and quantification of

MPs. Furthermore, the applicability of ToF-SIMS for the analysis of MPs down to lower  $\mu$ -range has been recently demonstrated.

To facilitate the representative and high throughput analysis of MPs using particle-based methods, the automation of the measurements and data processing is inevitable. Furthermore, statistical models to calculate the minimum number of particles which have to be analyzed for statistically meaningful results have been developed. However, especially for the MP analysis in the lower size range, additional approaches are needed, in order to accelerate the recognition of potentially MP particles. Here, a combination of fluorescent staining (e.g., using Nile Red dye) with the subsequent automated (FT)IR (down to 10  $\mu\text{m}$ ) or Raman (down to 1  $\mu\text{m}$ ) analysis appears promising.

The comparison, harmonization, and standardization within both mass-based and particle-based methods as well as between these two principally different, but highly complementary approaches are needed in order to validate the methods and to obtain an overall picture of the MP occurrence. For this purpose, several interlaboratory comparison tests have already been conducted. However, the availability of suitable reference materials which mimic real MPs, including different polymer types, broad size range, and different shapes is still limited, hampering the development of harmonized and standardized methods for the MP analysis. Methods for the identification and quantification of NPLs are still under development, and therefore their comparison and harmonization will be a topic of future studies.

Extended studies on MP occurrence in the entire size range (1  $\mu\text{m}$  to 1 mm and 1 mm to 5 mm for MPs and large MPs, respectively) and systematic comparison of achieved results are still to be conducted. These studies will help us to assess the differences in the chemical identity of MP particles in different size classes and to understand the relation between size/size range of MP particles and their number concentrations. This information is not only important for the risk assessment but can also allow us to identify suitable criteria and proxy functions for the prediction of MP concentration in the lower  $\mu$ -range (e.g., data on the MP occurrence down to 50  $\mu\text{m}$  can be utilized to estimate MP concentrations down to 1  $\mu\text{m}$ ). This knowledge, inter alia, can be used for the development of time- and cost-efficient in situ and field methods for the routine analysis of MPs.

The detailed characterization of MPs will require the combination of complementary and development of new methods. They are necessary for understanding the behavior of NMP particles, their fragmentation and (bio)degradation, transport and release of (in)organic additives, weathering products, sorbed chemicals, and (pathogenic and/or antibiotic resistant) microorganisms. For the analysis of particle morphology and surface properties, SEM/EDX is often applied in a combination with spectroscopic methods. Here, the correlative SEM-Raman approach is shown to be efficient for the morphological and chemical characterization of small MPs and also NMPs down to 100 nm. Furthermore, detailed information on metals, associated with NMPs in a form of additives and/or sorbed inorganic contaminants can be achieved by the application of (SP)-ICP-MS. While the present review is focused on the chemical analysis of NMPs as particulate anthropogenic analyte and, hence, research topics on sorbed chemicals and microbial communities are not addressed, these issues must be kept in mind when evaluating eco-toxicological effects caused by NMPs.

Special efforts will be necessary for the (further) development, optimization, and validation of methods suitable for the analysis of nanoplastics. NPLs are expected to have greater ecotoxicological impacts. On the one hand, these tiny particles may penetrate through cell membranes. On the other hand, due to their large surface-to-volume ratio, NPLs may sorb larger amounts of external chemicals as compared to MPs of the same mass and therefore are assumed to have the Trojan horse effect in the transport of contaminants. For the detailed characterization of NPLs, the methods allowing nanoscale resolution are required. Here, SEM/EDX, the combination of SEM and Raman instrumentations as well as near-field spectroscopic methods (namely AFM-IR and nano-FTIR) are found to be very useful.

To obtain reliable and representative information on the occurrence of NPLs in the environment, drinking water, and food, combined approaches are necessary which allow for (i) efficient preconcentration, enrichment, and size fractionation, (ii) determination of numbers as well as sizes (and shape) of particles, and (iii) chemical identification. For the analysis of inorganic NPL constituents, the methods developed in the field of engineered nanoparticles studies, namely SP-ICP-MS and SP-ICP-ToF/MS, will be efficient. For the chemical identification of NPL polymers, the methods already applicable in the field of MPs studies can be adopted. In this context, the combination of FFF methods (including particle characterization by UV- and MALS detectors) with the offline (e.g., using Py-GC/MS) or online (using  $\mu$ -Raman spectroscopy) NPLs identification has demonstrated first promising results. However, the development of more sensitive detectors for the online analysis of NPLs is highly desirable. Here, the combination of FFF with stimulated Raman scattering approach seems to have a high potential. Furthermore, the (further) development of the efficient preconcentration and enrichment of NPLs remains to be a critical prerequisite for the feasible analysis of NPL particles in real samples.

Although the systematic work on the optimization, harmonization, and standardization of methods for the MP analysis as well as (further) development in the field of NPLs are in progress, substantial advances have been already achieved. The knowledge gained so far is essential for:

- Evaluation of the NMP occurrence in environmental and food samples, the clarification of their sources and sinks, transport and fate, and, hence, the development of appropriate mitigation measures.
- Understanding of NMP impacts on the environment and human health, which expected to be diverse for NMPs with different characteristics.
- Development of polymer materials with desired properties and clear life cycle, in order to prevent uncontrolled release of NMP particles and fibers in the environment and their occurrence in drinking water and food (including conventional polymers, foreseen for recycling as well as biodegradable materials for different applications, e.g., in agriculture, food packaging and medicine).

Thus, the unforeseen problem of plastic pollution, which followed huge advances in technology, medicine, and lifestyle due to the development of versatile polymer materials, fosters intense research efforts in the field of NMPs. The gained knowledge will hopefully help in preventing such undesirable side effects for novel materials in the future.

To tackle the challenges associated with the analysis of NMPs as particulate anthropogenic pollutants, many available analytical methods have been adopted and optimized. On the other hand, numerous novel approaches have been developed for the comprehensive analysis of this complex and diverse analyte. These approaches enable the automated recognition, characterization, chemical identification, and quantification of (plastic) microparticles as well as automated data processing, and thus the reliable and representative MP analysis can be achieved. Furthermore, the efficient characterization of NPLs can be realized by combining the size fractionation and (online) chemical identification. The developed methods open new possibilities for applications in fields far beyond the NMP research, where information on the chemical composition of (complex) particles including (in)organic and (micro)biological origin is desired together with robust data on particle number, size/size distribution, and shapes. For example, these methods could be applied for the development and characterization of particles with tailored properties for catalysis and pharmacology, while in microbiology, the representative and detailed analysis of morphological and chemical characteristics of samples can be achieved. Thus, NMP research is likely to play a role of an efficient catalyst, stimulating development of novel analytical methods for multiple interdisciplinary fields.

## AUTHOR INFORMATION

### Corresponding Author

**Natalia P. Ivleva** – *Institute of Hydrochemistry, Chair of Analytical Chemistry and Water Chemistry, Technical University of Munich, 81377 Munich, Germany*; [orcid.org/0000-0002-7685-5166](https://orcid.org/0000-0002-7685-5166); Email: [natalia.ivleva@tum.de](mailto:natalia.ivleva@tum.de)

Complete contact information is available at:  
<https://pubs.acs.org/10.1021/acs.chemrev.1c00178>

### Notes

The author declares no competing financial interest.

### Biography

Natalia P. Ivleva studied chemistry and biology at the Southern Federal University (Rostov-on-Don, Russia). After receiving her Ph.D. in Physical Chemistry in 1997 from the Institute of Chemical Physics (Chernogolovka, Russia), she started her postdoc at the same institute. In 2003, she joined the Institute of Hydrochemistry and Chair of Analytical Chemistry at the Technical University of Munich (TUM), where she is now leading the Raman & SEM Group. In 2019, Dr. Ivleva accomplished her habilitation “Raman Microspectroscopy for Environmental Analysis”. Her research interests focus on the analysis of complex environmental and industrial samples/systems by means of Raman microspectroscopy, surface-enhanced Raman scattering, and stable isotope approach, with special attention on automation and online/high-throughput analytics. She combines Raman-based methods with techniques based on electron microscopy and mass spectrometry and also with different separation/fractionation/sorting approaches for the detection, identification, quantification, and characterization of various analytes/matrices/pollutants, ranging from biofilms and microorganisms through engineered (magnetic) nanoparticles and carbonaceous materials to micro- and nanoplastics.

## ACKNOWLEDGMENTS

I warmly thank Barbara Scholz-Böttcher, Sebastian Primpke, Dieter Fischer, Franziska Fischer, Nicole Zumbülte, Martin Jekel, Ulrike Braun, Florian Meier, Benedikt Hufnagl, Martin

Löder, Oliver Knoop, Jörg E. Drewes, Jürgen Geist, Karl Glas, Hannes Imhof, Aaron Beck, Erik Achterberg, Darena Schymanski, Barbara Oßmann, Nizar Benismail, Elzbieta A. Stefaniak, Reinhard Niessner, Martin Elsner, Elisabeth von der Esch, Christian Schwaferts and Oliver Jacob for very helpful discussions. The providing of the original images for publication by Barbara Scholz-Böttcher, Sebastian Primpke, Andrea Käppler, Josef Brandt, George Sarau and Chen Fang as well as the help of Hannes Imhof and Philipp M. Anger in the preparation of Daphnia samples and the acquisition of Raman spectra is gratefully acknowledged. Special thanks goes to Helena Klein for the creation of graphical abstract and FFF-Raman image. I thank the Federal Ministry of Education and Research (Bundesministerium für Bildung und Forschung (BMBF), projects 02WPL1443A “Sub $\mu$ Track” in the call “Plastics in the Environment” and 03F0851B “HOTMIC” in the JPI JPIOceans call) as well as the Bavarian Research Foundation (Bayerische Forschungstiftung (BFS), AZ-1258-16 (“MiPAq”) for the financial support.

## ABBREVIATIONS

ACP = acrylic copolymer  
AFM = atomic force microscopy  
ATR = attenuated total reflection  
CT = charge transfer  
CPE = cloud point extraction  
CARS = coherent anti-Stokes Raman scattering  
CP = Curie point pyrolyzer  
DSC = differential scanning calorimetry  
DOM = dissolved organic matter  
EM-CCD = electron-multiplying charge coupled device detector  
EDX = energy dispersive X-ray spectroscopy  
EGA = evolved gas analysis  
EC = external cavity  
FFF = asymmetrical FFF or AF4 centrifugal FFF or CF3, field-flow fractionation  
FC = flow cytometry  
FPA = focal plane array detector  
FTIR = Fourier transform infrared spectroscopy  
GPC = gel permeation chromatography  
HPLC = high performance liquid chromatography  
HQI = hit quality index  
HDC = hydrodynamic chromatography  
HIS = hyperspectral imaging  
ICP-MS = inductively coupled plasma mass spectrometry  
ILC = interlaboratory comparison test  
LDIR = laser direct infrared analysis  
LOD = limit of detection  
LOQ = limit of quantification  
LSPR = localized surface plasmon resonance  
MALDI-ToF/MS = matrix-assisted laser desorption/ionization time-of-flight mass spectrometry  
MCT = mercury cadmium telluride detector  
MF = micro furnace pyrolyzer  
MPs = microplastics  
MIR = mid-infrared region  
MALS = multiangle light scattering detector  
NPLs = nanoplastics  
NMPs = nanoplastics and microplastics  
NOM = natural organic matter  
NIR = near-infrared region  
NASG = North Atlantic Subtropical Gyre

OES = optical emission spectroscopy  
 O-PT = optical photothermal IR spectroscopy  
 PLS-DA = partial least-squares discriminant analysis  
 PAN = polyacrylonitrile  
 ABS = poly(acrylonitrile-co-styrene-co-butadiene)  
 PA = polyamide  
 PB = polybutadiene  
 PCL = polycaprolactone  
 PBAT = polybutylene adipate-co-terephthalate  
 PE = polyethylene  
 HDPE = PE of high density  
 LDPE = PE of low density  
 PET = polyethylene terephthalate  
 PES = polyester  
 PI = polyisoprene  
 PLA = polylactide  
 PMMA = poly(methyl methacrylate)  
 PP = polypropylene  
 PS = polystyrene  
 PTFE = polytetrafluoroethylene  
 PUR = polyurethane  
 PVA = poly(vinyl acetate)  
 PVC = polyvinyl chloride  
 PLE = pressured liquid extraction  
 PCA = principal component analysis  
 Py-GC/MS = pyrolysis gas chromatography mass spectrometry  
 QA = quality assurance  
 QC = quality control  
 $q^1\text{H}$  NMR = quantitative protonnuclear magnetic resonance  
 QCL = quantum cascade laser  
 RDS = random decision forest classifiers  
 ROI = region of interest  
 SEM = scanning electron microscopy  
 SNOM = scanning near-field optical microscopy  
 STM = scanning tunneling microscopy  
 SI = single-particle mode ICP-MS  
 SEC = size-exclusion chromatography  
 SIMCA = soft independent modeling of class analogy models  
 SRS = stimulated Raman scattering  
 SBR = styrene-butadiene rubber  
 SVR = support vector machine regression  
 SERS = surface-enhanced Raman scattering  
 THF = tetrahydrofuran  
 TD-PTR/MS = thermal desorption-proton transfer reaction-mass spectrometry  
 TDU = thermal desorption unit  
 TED = thermo-extraction and desorption GC/MS  
 TGA = thermogravimetric analyzer  
 ToF-SIMS = time-of-flight secondary ion mass spectrometry  
 TERS = tip-enhanced Raman spectroscopy  
 TRWPs = tire and road wear particles  
 TWP = tire wear particles  
 TEM = transmission electron microscopy  
 UMAP = uniform manifold approximation and projection  
 WWTPs = wastewater treatment plants

## REFERENCES

(1) Koelmans, A. A.; Pahl, S.; Backhaus, T.; Bessa, F.; van Calster, G.; Contzen, N.; Cronin, R.; Galloway, T. S.; Hart, A.; Henderson, L. et al. *A Scientific Perspective on Microplastics in Nature and Society*; SAPEA, 2019.

(2) *Guidelines for the Monitoring and Assessment of Plastic Litter in the Ocean*; Joint Group of Experts on the Scientific Aspects of Marine Environmental Protection (Gesamp), 2019.

(3) *Ocean Protection Council: Statewide Microplastics Strategy*; Senate Bill No. 1263; State of California, 2018; [https://leginfo.ca.gov/faces/billTextClient.xhtml?bill\\_id=201720180SB1263](https://leginfo.ca.gov/faces/billTextClient.xhtml?bill_id=201720180SB1263).

(4) *California Safe Drinking Water Act: Microplastics*; Senate Bill No. 1422; State of California, 2018; [https://leginfo.ca.gov/faces/billTextClient.xhtml?bill\\_id=201720180SB1422](https://leginfo.ca.gov/faces/billTextClient.xhtml?bill_id=201720180SB1422).

(5) Pico, Y.; Alfarhan, A.; Barcelo, D. Nano- and Microplastic Analysis: Focus on Their Occurrence in Freshwater Ecosystems and Remediation Technologies. *TrAC, Trends Anal. Chem.* **2019**, *113*, 409–425.

(6) Wagner, M.; Scherer, C.; Alvarez-Munoz, D.; Brennholt, N.; Bourrain, X.; Buchinger, S.; Fries, E.; Grosbois, C.; Klasmeyer, J.; Marti, T.; et al. Microplastics in Freshwater Ecosystems: What We Know and What We Need to Know. *Environ. Sci. Eur.* **2014**, *26*, 12.

(7) Nguyen, B.; Claveau-Mallet, D.; Hernandez, L. M.; Xu, E. G.; Farmer, J. M.; Tufenkji, N. Separation and Analysis of Microplastics and Nanoplastics in Complex Environmental Samples. *Acc. Chem. Res.* **2019**, *52*, 858–866.

(8) Prata, J. C.; da Costa, J. P.; Duarte, A. C.; Rocha-Santos, T. Methods for Sampling and Detection of Microplastics in Water and Sediment: A Critical Review. *TrAC, Trends Anal. Chem.* **2019**, *110*, 150–159.

(9) Hale, R. C. Analytical Challenges Associated with the Determination of Microplastics in the Environment. *Anal. Methods* **2017**, *9*, 1326–1327.

(10) Hale, R. C.; Seeley, M. E.; La Guardia, M. J.; Mai, L.; Zeng, E. Y. A Global Perspective on Microplastics. *J. Geophys. Res.: Oceans* **2020**, *125*, No. e2018JC014719.

(11) Dehaut, A.; Hermabessiere, L.; Duflos, G. Current Frontiers and Recommendations for the Study of Microplastics in Seafood. *TrAC, Trends Anal. Chem.* **2019**, *116*, 346–359.

(12) Li, J.; Liu, H.; Paul Chen, J. Microplastics in Freshwater Systems: A Review on Occurrence, Environmental Effects, and Methods for Microplastics Detection. *Water Res.* **2018**, *137*, 362–374.

(13) Silva, A. B.; Bastos, A. S.; Justino, C. I. L.; da Costa, J. P.; Duarte, A. C.; Rocha-Santos, T. A. P. Microplastics in the Environment: Challenges in Analytical Chemistry - a Review. *Anal. Chim. Acta* **2018**, *1017*, 1–19.

(14) Delgado-Gallardo, J.; Sullivan, G. L.; Esteban, P.; Wang, Z.; Arar, O.; Li, Z.; Watson, T. M.; Sarp, S. From Sampling to Analysis: A Critical Review of Techniques Used in the Detection of Micro- and Nanoplastics in Aquatic Environments. *ACS EST Water* **2021**, *1*, 748–764.

(15) Ivelva, N. P.; Wiesheu, A. C.; Niessner, R. Microplastic in Aquatic Ecosystems. *Angew. Chem., Int. Ed.* **2017**, *56*, 1720–1739.

(16) Thompson, R. C.; Olsen, Y.; Mitchell, R. P.; Davis, A.; Rowland, S. J.; John, A. W. G.; McGonigle, D.; Russell, A. E. Lost at Sea: Where Is All the Plastic? *Science* **2004**, *304*, 838–838.

(17) Arthur, C.; Baker, J.; Bamford, H. *Proceedings of the Second Research Workshop on Microplastic Debris, November 5–6, 2010*; NOAA Technical Memorandum NOS-OR&R-39; Marine Debris Division, Office of Response and Restoration, Ocean Service, NOAA, 2011; <https://marinedebris.noaa.gov/proceedings-second-research-workshop-microplastic-marine-debris>.

(18) Hartmann, N. B.; Hüffer, T.; Thompson, R. C.; Hasselov, M.; Verschoor, A.; Daugaard, A. E.; Rist, S.; Karlsson, T.; Brennholt, N.; Cole, M.; et al. Are We Speaking the Same Language? Recommendations for a Definition and Categorization Framework for Plastic Debris. *Environ. Sci. Technol.* **2019**, *53*, 1039–1047.

(19) *ISO/TT 21960 Plastics—Environmental Aspects—State of Knowledge and Methodologies*; ISO: Geneva, 2020.

(20) Braun, U.; Altmann, K.; Bannick, C. G.; Becker, R.; Bitter, H.; Bochow, M.; Dierkes, G.; Enders, K.; Eslahian, K. A.; Fischer, D. et al. *Status Report: Analysis of Microplastics—Sampling, Preparation and Detection Methods within the Scope of the Bmbf Research Focus Plastics in the Environment: Sources, Sinks, Solutions*, 2020.

- (21) Gigault, J.; Halle, A. T.; Baudrimont, M.; Pascal, P.-Y.; Gauffre, F.; Phi, T.-L.; El Hadri, H.; Grassl, B.; Reynaud, S. Current Opinion: What Is a Nanoplastic? *Environ. Pollut.* **2018**, *235*, 1030–1034.
- (22) *Plastics—The Facts 2020*; PlasticsEurope, 2020.
- (23) Koelmans, A. A.; Mohamed Nor, N. H.; Hermesen, E.; Kooi, M.; Mintenig, S. M.; De France, J. Microplastics in Freshwaters and Drinking Water: Critical Review and Assessment of Data Quality. *Water Res.* **2019**, *155*, 410–422.
- (24) Lambourne, R.; Strivens, T. A. *Paint and Surface Coatings—Theory and Practice*; Woodhead Publishing Ltd: Abington, Cambridge, 1999.
- (25) Cole, M.; Lindeque, P.; Halsband, C.; Galloway, T. S. Microplastics as Contaminants in the Marine Environment: A Review. *Mar. Pollut. Bull.* **2011**, *62*, 2588–2597.
- (26) Frias, J. P. G. L.; Nash, R. Microplastics: Finding a Consensus on the Definition. *Mar. Pollut. Bull.* **2019**, *138*, 145–147.
- (27) Ivar do Sul, J. A.; Spengler, A.; Costa, M. F. Here, There and Everywhere. Small Plastic Fragments and Pellets on Beaches of Fernando De Noronha (Equatorial Western Atlantic). *Mar. Pollut. Bull.* **2009**, *58*, 1236–1238.
- (28) Ng, K. L.; Obbard, J. P. Prevalence of Microplastics in Singapore's Coastal Marine Environment. *Mar. Pollut. Bull.* **2006**, *52*, 761–767.
- (29) Peeken, I.; Primpke, S.; Beyer, B.; Gütermann, J.; Katlein, C.; Krumpfen, T.; Bergmann, M.; Hehemann, L.; Gerdt, G. Arctic Sea Ice Is an Important Temporal Sink and Means of Transport for Microplastic. *Nat. Commun.* **2018**, *9*, 1505.
- (30) Cincinelli, A.; Scopetani, C.; Chelazzi, D.; Lombardini, E.; Martellini, T.; Katsoyiannis, A.; Fossi, M. C.; Corsolini, S. Microplastic in the Surface Waters of the Ross Sea (Antarctica): Occurrence, Distribution and Characterization by FTIR. *Chemosphere* **2017**, *175*, 391–400.
- (31) Van Cauwenberghe, L.; Vanreusel, A.; Mees, J.; Janssen, C. R. Microplastic Pollution in Deep-Sea Sediments. *Environ. Pollut.* **2013**, *182*, 495–499.
- (32) Cunningham, E. M.; Ehlers, S. M.; Dick, J. T. A.; Sigwart, J. D.; Linse, K.; Dick, J. J.; Kiriakoulakis, K. High Abundances of Microplastic Pollution in Deep-Sea Sediments: Evidence from Antarctica and the Southern Ocean. *Environ. Sci. Technol.* **2020**, *54*, 13661–13671.
- (33) Napper, I. E.; Davies, B. F. R.; Clifford, H.; Elvin, S.; Koldewey, H. J.; Mayewski, P. A.; Miner, K. R.; Potocki, M.; Elmore, A. C.; Gajurel, A. P.; et al. Reaching New Heights in Plastic Pollution—Preliminary Findings of Microplastics on Mount Everest. *One Earth* **2020**, *3*, 621–630.
- (34) Lithner, D.; Larsson, A.; Dave, G. Environmental and Health Hazard Ranking and Assessment of Plastic Polymers Based on Chemical Composition. *Sci. Total Environ.* **2011**, *409*, 3309–3324.
- (35) Tian, Z.; Zhao, H.; Peter, K. T.; Gonzalez, M.; Wetzel, J.; Wu, C.; Hu, X.; Prat, J.; Mudrock, E.; Hettlinger, R.; et al. A Ubiquitous Tire Rubber-Derived Chemical Induces Acute Mortality in Coho Salmon. *Science* **2021**, *371*, 185–189.
- (36) Lomonaco, T.; Manco, E.; Corti, A.; La Nasa, J.; Ghimenti, S.; Biagini, D.; Di Francesco, F.; Modugno, F.; Ceccarini, A.; Fuoco, R.; et al. Release of Harmful Volatile Organic Compounds (VOCs) from Photo-Degraded Plastic Debris: A Neglected Source of Environmental Pollution. *J. Hazard. Mater.* **2020**, *394*, 122596.
- (37) Bakir, A.; Rowland, S. J.; Thompson, R. C. Enhanced Desorption of Persistent Organic Pollutants from Microplastics under Simulated Physiological Conditions. *Environ. Pollut.* **2014**, *185*, 16–23.
- (38) Brennecke, D.; Duarte, B.; Paiva, F.; Caçador, I.; Canning-Clode, J. Microplastics as Vector for Heavy Metal Contamination from the Marine Environment. *Estuarine, Coastal Shelf Sci.* **2016**, *178*, 189–195.
- (39) Zettler, E. R.; Mincer, T. J.; Amaral-Zettler, L. A. Life in the “Plastisphere”: Microbial Communities on Plastic Marine Debris. *Environ. Sci. Technol.* **2013**, *47*, 7137–7146.
- (40) Bank, M. S.; Ok, Y. S.; Swarzenski, P. W. Microplastic's Role in Antibiotic Resistance. *Science* **2020**, *369*, 1315–1315.
- (41) Lenz, R.; Enders, K.; Nielsen, T. G. Microplastic Exposure Studies Should Be Environmentally Realistic. *Proc. Natl. Acad. Sci. U. S. A.* **2016**, *113*, E4121–E4122.
- (42) Triebskorn, R.; Braunbeck, T.; Grummt, T.; Hanslik, L.; Huppertsberg, S.; Jekel, M.; Knepper, T. P.; Kraus, S.; Mueller, Y. K.; Pittroff, M.; et al. Relevance of Nano- and Microplastics for Freshwater Ecosystems: A Critical Review. *TrAC, Trends Anal. Chem.* **2019**, *110*, 375–392.
- (43) Burton, G. A. Stressor Exposures Determine Risk: So, Why Do Fellow Scientists Continue to Focus on Superficial Microplastics Risk? *Environ. Sci. Technol.* **2017**, *51*, 13515–13516.
- (44) Ferreira, I.; Venâncio, C.; Lopes, I.; Oliveira, M. Nanoplastics and Marine Organisms: What Has Been Studied? *Environ. Toxicol. Pharmacol.* **2019**, *67*, 1–7.
- (45) Mattsson, K.; Johnson, E. V.; Malmendal, A.; Linse, S.; Hansson, L.-A.; Cedervall, T. Brain Damage and Behavioural Disorders in Fish Induced by Plastic Nanoparticles Delivered through the Food Chain. *Sci. Rep.* **2017**, *7*, 11452.
- (46) Vianello, A.; Jensen, R. L.; Liu, L.; Vollertsen, J. Simulating Human Exposure to Indoor Airborne Microplastics Using a Breathing Thermal Manikin. *Sci. Rep.* **2019**, *9*, 8670.
- (47) Catarino, A.; Macchia, V.; Sanderson, W.; Thompson, R.; Henry, T. Low Levels of Microplastics (Mp) in Wild Mussels Indicate That MP Ingestion by Humans Is Minimal Compared to Exposure Via Household Fibres Fallout During a Meal. *Environ. Pollut.* **2018**, *237*, 675–684.
- (48) Paul, M. B.; Stock, V.; Cara-Carmona, J.; Lisicki, E.; Shopova, S.; Fessard, V.; Braeuning, A.; Sieg, H.; Böhmert, L. Micro- and Nanoplastics - Current State of Knowledge with the Focus on Oral Uptake and Toxicity. *Nanoscale Adv.* **2020**, *2*, 4350–4367.
- (49) Schymanski, D.; Goldbeck, C.; Humpf, H.-U.; Fürst, P. Analysis of Microplastics in Water by Micro-Raman Spectroscopy: Release of Plastic Particles from Different Packaging into Mineral Water. *Water Res.* **2018**, *129*, 154–162.
- (50) Obmann, B. E.; Sarau, G.; Holtmannspötter, H.; Pischetsrieder, M.; Christiansen, S. H.; Dicke, W. Small-Sized Microplastics and Pigmented Particles in Bottled Mineral Water. *Water Res.* **2018**, *141*, 307–316.
- (51) Pivokonsky, M.; Cermakova, L.; Novotna, K.; Peer, P.; Cajthaml, T.; Janda, V. Occurrence of Microplastics in Raw and Treated Drinking Water. *Sci. Total Environ.* **2018**, *643*, 1644–1651.
- (52) Mintenig, S. M.; Löder, M. G. J.; Primpke, S.; Gerdt, G. Low Numbers of Microplastics Detected in Drinking Water from Ground Water Sources. *Sci. Total Environ.* **2019**, *648*, 631–635.
- (53) Kirstein, I. V.; Hensel, F.; Gomiero, A.; Iordachescu, L.; Vianello, A.; Wittgren, H. B.; Vollertsen, J. Drinking Plastics? - Quantification and Qualification of Microplastics in Drinking Water Distribution Systems by  $\mu$ -FTIR and Py-GCMS. *Water Res.* **2021**, *188*, 116519.
- (54) Fischer, M.; Goßmann, I.; Scholz-Böttcher, B. M. Fleur De Sel— an Interregional Monitor for Microplastics Mass Load and Composition in European Coastal Waters? *J. Anal. Appl. Pyrolysis* **2019**, *144*, 104711.
- (55) Hernandez, L. M.; Xu, E. G.; Larsson, H. C. E.; Tahara, R.; Maisuria, V. B.; Tufenkji, N. Plastic Teabags Release Billions of Microparticles and Nanoparticles into Tea. *Environ. Sci. Technol.* **2019**, *53*, 12300–12310.
- (56) Van Cauwenberghe, L.; Janssen, C. R. Microplastics in Bivalves Cultured for Human Consumption. *Environ. Pollut.* **2014**, *193*, 65–70.
- (57) Cox, K. D.; Covernton, G. A.; Davies, H. L.; Dower, J. F.; Juanes, F.; Dudas, S. E. Human Consumption of Microplastics. *Environ. Sci. Technol.* **2019**, *53*, 7068–7074.
- (58) Prata, J. C. Airborne Microplastics: Consequences to Human Health? *Environ. Pollut.* **2018**, *234*, 115–126.
- (59) Lehner, R.; Weder, C.; Petri-Fink, A.; Rothen-Rutishauser, B. Emergence of Nanoplastic in the Environment and Possible Impact on Human Health. *Environ. Sci. Technol.* **2019**, *53*, 1748–1765.
- (60) Magri, D.; Sanchez-Moreno, P.; Caputo, G.; Gatto, F.; Veronesi, M.; Bardi, G.; Catelani, T.; Guarnieri, D.; Athanassiou, A.; Pompa, P. P.; et al. Laser Ablation as a Versatile Tool to Mimic Polyethylene

Terephthalate Nanoplastic Pollutants: Characterization and Toxicology Assessment. *ACS Nano* **2018**, *12*, 7690–7700.

(61) Löder, M. G. J.; Gerdt, G. In *Marine Anthropogenic Litter*; Bergmann, M., Gutow, L., Klages, M., Eds.; Springer International Publishing, 2015.

(62) Zarfl, C. Promising Techniques and Open Challenges for Microplastic Identification and Quantification in Environmental Matrices. *Anal. Bioanal. Chem.* **2019**, *411*, 3743–3756.

(63) Hidalgo-Ruz, V.; Gutow, L.; Thompson, R. C.; Thiel, M. Microplastics in the Marine Environment: A Review of the Methods Used for Identification and Quantification. *Environ. Sci. Technol.* **2012**, *46*, 3060–3075.

(64) Shim, W. J.; Song, Y. K.; Hong, S. H.; Jang, M. Identification and Quantification of Microplastics Using Nile Red Staining. *Mar. Pollut. Bull.* **2016**, *113*, 469–476.

(65) Huppertsberg, S.; Knepper, T. P. Instrumental Analysis of Microplastics—Benefits and Challenges. *Anal. Bioanal. Chem.* **2018**, *410*, 6343–6352.

(66) Schymanski, D.; Obmann, B. E.; Benismail, N.; Boukerma, K.; Dallmann, G.; von der Esch, E.; Fischer, D.; Fischer, F.; Gilliland, D.; Glas, K. et al. Analysis of Microplastics in Drinking Water and Other Clean Water Samples with Micro-Raman and Micro-Infrared Spectroscopy: Minimum Requirements and Best Practice Guidelines. *Anal. Bioanal. Chem.* **2021**, DOI: 10.1007/s00216-021-03498-y.

(67) Primpke, S.; Christiansen, S. H.; Cowger, W.; De Frond, H.; Deshpande, A.; Fischer, M.; Holland, E. B.; Meyns, M.; O'Donnell, B. A.; Ossmann, B. E.; et al. Critical Assessment of Analytical Methods for the Harmonized and Cost-Efficient Analysis of Microplastics. *Appl. Spectrosc.* **2020**, *74*, 1012–1047.

(68) Schwaferts, C.; Niessner, R.; Elsner, M.; Ivleva, N. P. Methods for the Analysis of Submicrometer- and Nanoplastic Particles in the Environment. *TrAC, Trends Anal. Chem.* **2019**, *112*, 52–65.

(69) Fu, W.; Min, J.; Jiang, W.; Li, Y.; Zhang, W. Separation, Characterization and Identification of Microplastics and Nanoplastics in the Environment. *Sci. Total Environ.* **2020**, *721*, 137561.

(70) Elert, A. M.; Becker, R.; Duemichen, E.; Eisentraut, P.; Falkenhagen, J.; Sturm, H.; Braun, U. Comparison of Different Methods for Mp Detection: What Can We Learn from Them, and Why Asking the Right Question before Measurements Matters? *Environ. Pollut.* **2017**, *231*, 1256–1264.

(71) Fischer, M.; Scholz-Boettcher, B. M. Simultaneous Trace Identification and Quantification of Common Types of Microplastics in Environmental Samples by Pyrolysis-Gas Chromatography-Mass Spectrometry. *Environ. Sci. Technol.* **2017**, *51*, 5052–5060.

(72) Thompson, R. N.; Nau, C. A.; Lawrence, C. H. Identification of Vehicle Tire Rubber in Roadway Dust. *Am. Ind. Hyg. Assoc. J.* **1966**, *27*, 488–495.

(73) de Leeuw, J. W.; de Leer, E. W. B.; Damste, J. S. S.; Schuyf, P. J. W. Screening of Anthropogenic Compounds in Polluted Sediments and Soils by Flash Evaporation/Pyrolysis Gas Chromatography-Mass Spectrometry. *Anal. Chem.* **1986**, *58*, 1852–1857.

(74) Fabbri, D.; Trombini, C.; Vassura, I. Analysis of Polystyrene in Polluted Sediments by Pyrolysis—Gas Chromatography—Mass Spectrometry. *J. Chromatogr. Sci.* **1998**, *36*, 600–604.

(75) Fabbri, D.; Tartari, D.; Trombini, C. Analysis of Poly(Vinyl Chloride) and Other Polymers in Sediments and Suspended Matter of a Coastal Lagoon by Pyrolysis-Gas Chromatography-Mass Spectrometry. *Anal. Chim. Acta* **2000**, *413*, 3–11.

(76) Fabbri, D. Use of Pyrolysis-Gas Chromatography/Mass Spectrometry to Study Environmental Pollution Caused by Synthetic Polymers: A Case Study: The Ravenna Lagoon. *J. Anal. Appl. Pyrolysis* **2001**, *58–59*, 361–370.

(77) Fries, E.; Dekiff, J. H.; Willmeyer, J.; Nuelle, M.-T.; Ebert, M.; Remy, D. Identification of Polymer Types and Additives in Marine Microplastic Particles Using Pyrolysis-GC/MS and Scanning Electron Microscopy. *Environ. Sci. Processes Impacts* **2013**, *15*, 1949–1956.

(78) Dekiff, J. H.; Remy, D.; Klasmeyer, J.; Fries, E. Occurrence and Spatial Distribution of Microplastics in Sediments from Norderney. *Environ. Pollut.* **2014**, *186*, 248–256.

(79) Nuelle, M.-T.; Dekiff, J. H.; Remy, D.; Fries, E. A New Analytical Approach for Monitoring Microplastics in Marine Sediments. *Environ. Pollut.* **2014**, *184*, 161–169.

(80) Hermabessiere, L.; Himber, C.; Boricaud, B.; Kazour, M.; Amara, R.; Cassone, A.-L.; Laurentie, M.; Paul-Pont, I.; Soudant, P.; Dehaut, A.; et al. Optimization, Performance, and Application of a Pyrolysis-GC/MS Method for the Identification of Microplastics. *Anal. Bioanal. Chem.* **2018**, *410*, 6663–6676.

(81) Käßler, A.; Fischer, M.; Scholz-Böttcher, B. M.; Oberbeckmann, S.; Labrenz, M.; Fischer, D.; Eichhorn, K.-J.; Voit, B. Comparison of  $\mu$ -ATR-FTIR Spectroscopy and Py-GCMS as Identification Tools for Microplastic Particles and Fibers Isolated from River Sediments. *Anal. Bioanal. Chem.* **2018**, *410*, 5313–5327.

(82) Dierkes, G.; Lauschke, T.; Becher, S.; Schumacher, H.; Földi, C.; Ternez, T. Quantification of Microplastics in Environmental Samples Via Pressurized Liquid Extraction and Pyrolysis-Gas Chromatography. *Anal. Bioanal. Chem.* **2019**, *411*, 6959–6968.

(83) Ceccarini, A.; Corti, A.; Erba, F.; Modugno, F.; La Nasa, J.; Bianchi, S.; Castelvetro, V. The Hidden Microplastics: New Insights and Figures from the Thorough Separation and Characterization of Microplastics and of Their Degradation Byproducts in Coastal Sediments. *Environ. Sci. Technol.* **2018**, *52*, 5634–5643.

(84) Doyen, P.; Hermabessiere, L.; Dehaut, A.; Himber, C.; Decodts, M.; Degraeve, T.; Delord, L.; Gaboriaud, M.; Moné, P.; Sacco, J.; et al. Occurrence and Identification of Microplastics in Beach Sediments from the Hauts-De-France Region. *Environ. Sci. Pollut. Res.* **2019**, *26*, 28010–28021.

(85) Primpke, S.; Fischer, M.; Lorenz, C.; Gerdt, G.; Scholz-Böttcher, B. M. Comparison of Pyrolysis Gas Chromatography/Mass Spectrometry and Hyperspectral FTIR Imaging Spectroscopy for the Analysis of Microplastics. *Anal. Bioanal. Chem.* **2020**, *412*, 8283–8298.

(86) McCormick, A. R.; Hoellein, T. J.; London, M. G.; Hittie, J.; Scott, J. W.; Kelly, J. J. Microplastic in Surface Waters of Urban Rivers: Concentration, Sources, and Associated Bacterial Assemblages. *Ecosphere* **2016**, *7*, No. e01556.

(87) Ravit, B.; Cooper, K.; Buckley, B.; Yang, I.; Deshpande, A. Organic Compounds Associated with Microplastic Pollutants in New Jersey, U.S.A. Surface Waters. *AIMS Environ. Sci.* **2019**, *6*, 445.

(88) Dümichen, E.; Eisentraut, P.; Bannick, C. G.; Barthel, A.-K.; Senz, R.; Braun, U. Fast Identification of Microplastics in Complex Environmental Samples by a Thermal Degradation Method. *Chemosphere* **2017**, *174*, 572–584.

(89) Hendrickson, E.; Minor, E. C.; Schreiner, K. Microplastic Abundance and Composition in Western Lake Superior as Determined Via Microscopy, Pyr-GC/MS, and FTIR. *Environ. Sci. Technol.* **2018**, *52*, 1787–1796.

(90) Dehaut, A.; Cassone, A.-L.; Frère, L.; Hermabessiere, L.; Himber, C.; Rinnert, E.; Rivière, G.; Lambert, C.; Soudant, P.; Huvet, A.; et al. Microplastics in Seafood: Benchmark Protocol for Their Extraction and Characterization. *Environ. Pollut.* **2016**, *215*, 223–233.

(91) Dümichen, E.; Barthel, A.-K.; Braun, U.; Bannick, C. G.; Brand, K.; Jekel, M.; Senz, R. Analysis of Polyethylene Microplastics in Environmental Samples, Using a Thermal Decomposition Method. *Water Res.* **2015**, *85*, 451–457.

(92) El Hayany, B.; El Fels, L.; Quéneá, K.; Dignac, M.-F.; Rumpel, C.; Gupta, V. K.; Hafidi, M. Microplastics from Lagooning Sludge to Composts as Revealed by Fluorescent Staining- Image Analysis, Raman Spectroscopy and Pyrolysis-GC/MS. *J. Environ. Manage.* **2020**, *275*, 111249.

(93) O'Brien, S.; Okoffo, E. D.; O'Brien, J. W.; Ribeiro, F.; Wang, X.; Wright, S. L.; Samanipour, S.; Rauer, C.; Toapanta, T. Y. A.; Albarracín, R.; et al. Airborne Emissions of Microplastic Fibres from Domestic Laundry Dryers. *Sci. Total Environ.* **2020**, *747*, 141175.

(94) Watteau, F.; Dignac, M.-F.; Bouchard, A.; Revallier, A.; Houot, S. Microplastic Detection in Soil Amended with Municipal Solid Waste Composts as Revealed by Transmission Electronic Microscopy and Pyrolysis/GC/MS. *Front. Sustain. Food Syst.* **2018**, *2*, 81.

(95) Steinmetz, Z.; Kintzi, A.; Muñoz, K.; Schaumann, G. E. A Simple Method for the Selective Quantification of Polyethylene, Polypropy-

lene, and Polystyrene Plastic Debris in Soil by Pyrolysis-Gas Chromatography/Mass Spectrometry. *J. Anal. Appl. Pyrolysis* **2020**, *147*, 104803.

(96) Fischer, M.; Scholz-Böttcher, B. M. Microplastics Analysis in Environmental Samples - Recent Pyrolysis-Gas Chromatography-Mass Spectrometry Method Improvements to Increase the Reliability of Mass-Related Data. *Anal. Methods* **2019**, *11*, 2489–2497.

(97) ter Halle, A.; Jeanneau, L.; Martignac, M.; Jarde, E.; Pedrono, B.; Brach, L.; Gigault, J. Nanoplastic in the North Atlantic Subtropical Gyre. *Environ. Sci. Technol.* **2017**, *51*, 13689–13697.

(98) Mintenig, S. M.; Baeuerlein, P. S.; Koelmans, A. A.; Dekker, S. C.; van Wezel, A. P. Closing the Gap between Small and Smaller: Towards a Framework to Analyse Nano- and Microplastics in Aqueous Environmental Samples. *Environ. Sci.: Nano* **2018**, *5*, 1640–1649.

(99) Zhou, X.-X.; Hao, L.-T.; Wang, H.-Y.-Z.; Li, Y.-J.; Liu, J.-F. Cloud-Point Extraction Combined with Thermal Degradation for Nanoplastic Analysis Using Pyrolysis Gas Chromatography-Mass Spectrometry. *Anal. Chem.* **2019**, *91*, 1785–1790.

(100) Sullivan, G. L.; Gallardo, J. D.; Jones, E. W.; Holliman, P. J.; Watson, T. M.; Sarp, S. Detection of Trace Sub-Micron (Nano) Plastics in Water Samples Using Pyrolysis-Gas Chromatography Time of Flight Mass Spectrometry (Py-GCToF). *Chemosphere* **2020**, *249*, 126179.

(101) Picó, Y.; Barceló, D. Pyrolysis Gas Chromatography-Mass Spectrometry in Environmental Analysis: Focus on Organic Matter and Microplastics. *TrAC, Trends Anal. Chem.* **2020**, *130*, 115964.

(102) Herrera, M.; Matuschek, G.; Kettrup, A. Fast Identification of Polymer Additives by Pyrolysis-Gas Chromatography/Mass Spectrometry. *J. Anal. Appl. Pyrolysis* **2003**, *70*, 35–42.

(103) Jansson, K. D.; Zawodny, C. P.; Wampler, T. P. Determination of Polymer Additives Using Analytical Pyrolysis. *J. Anal. Appl. Pyrolysis* **2007**, *79*, 353–361.

(104) Reichel, J.; Graßmann, J.; Letzel, T.; Drewes, J. E. Systematic Development of a Simultaneous Determination of Plastic Particle Identity and Adsorbed Organic Compounds by Thermodesorption-Pyrolysis GC/MS (TD-Pyr-GC/MS). *Molecules* **2020**, *25*, 4985.

(105) Okoffo, E. D.; Ribeiro, F.; O'Brien, J. W.; O'Brien, S.; Tschärke, B. J.; Gallen, M.; Samanipour, S.; Mueller, J. F.; Thomas, K. V. Identification and Quantification of Selected Plastics in Biosolids by Pressurized Liquid Extraction Combined with Double-Shot Pyrolysis Gas Chromatography-Mass Spectrometry. *Sci. Total Environ.* **2020**, *715*, 136924.

(106) Funck, M.; Yildirim, A.; Nickel, C.; Schram, J.; Schmidt, T. C.; Tuerk, J. Identification of Microplastics in Wastewater after Cascade Filtration Using Pyrolysis-GC-MS. *MethodsX* **2020**, *7*, 100778.

(107) Fotopoulou, K. N.; Karapanagioti, H. K. *Degradation of Various Plastics in the Environment*; Springer: Berlin, Heidelberg, 2017.

(108) La Nasa, J.; Biale, G.; Fabbri, D.; Modugno, F. A Review on Challenges and Developments of Analytical Pyrolysis and Other Thermoanalytical Techniques for the Quali-Quantitative Determination of Microplastics. *J. Anal. Appl. Pyrolysis* **2020**, *149*, 104841.

(109) Gomiero, A.; Øysæd, K. B.; Agustsson, T.; van Hoytema, N.; van Thiel, T.; Grati, F. First Record of Characterization, Concentration and Distribution of Microplastics in Coastal Sediments of an Urban Fjord in South West Norway Using a Thermal Degradation Method. *Chemosphere* **2019**, *227*, 705–714.

(110) Dibke, C.; Fischer, M.; Scholz-Böttcher, B. M. Microplastic Mass Concentrations and Distribution in German Bight Waters by Pyrolysis-Gas Chromatography-Mass Spectrometry/Thermochemolysis Reveal Potential Impact of Marine Coatings: Do Ships Leave Skid Marks? *Environ. Sci. Technol.* **2021**, *55*, 2285.

(111) Eisentraut, P.; Dümichen, E.; Ruhl, A. S.; Jekel, M.; Albrecht, M.; Gehde, M.; Braun, U. Two Birds with One Stone—Fast and Simultaneous Analysis of Microplastics: Microparticles Derived from Thermoplastics and Tire Wear. *Environ. Sci. Technol. Lett.* **2018**, *5*, 608–613.

(112) Goßmann, I.; Halbach, M.; Scholz-Böttcher, B. M. Car and Truck Tire Wear Particles in Complex Environmental Samples - a Quantitative Comparison with “Traditional” Microplastic Polymer Mass Loads. *Sci. Total Environ.* **2021**, *773*, 145667.

(113) Wagner, S.; Hüffer, T.; Klöckner, P.; Wehrhahn, M.; Hofmann, T.; Reemtsma, T. Tire Wear Particles in the Aquatic Environment - a Review on Generation, Analysis, Occurrence, Fate and Effects. *Water Res.* **2018**, *139*, 83–100.

(114) Dümichen, E.; Eisentraut, P.; Celina, M.; Braun, U. Automated Thermal Extraction-Desorption Gas Chromatography Mass Spectrometry: A Multifunctional Tool for Comprehensive Characterization of Polymers and Their Degradation Products. *J. Chromatogr. A* **2019**, *1592*, 133–142.

(115) Klöckner, P.; Reemtsma, T.; Eisentraut, P.; Braun, U.; Ruhl, A. S.; Wagner, S. Tire and Road Wear Particles in Road Environment - Quantification and Assessment of Particle Dynamics by Zn Determination after Density Separation. *Chemosphere* **2019**, *222*, 714–721.

(116) Klöckner, P.; Seiwert, B.; Eisentraut, P.; Braun, U.; Reemtsma, T.; Wagner, S. Characterization of Tire and Road Wear Particles from Road Runoff Indicates Highly Dynamic Particle Properties. *Water Res.* **2020**, *185*, 116262.

(117) Braun, U.; Altmann, K.; Herper, D.; Knefel, M.; Bednarz, M.; Bannick, C. G. Smart Filters for the Analysis of Microplastic in Beverages Filled in Plastic Bottles. *Food Addit. Contam., Part A* **2021**, *38*, 691–700.

(118) Castelvetro, V.; Corti, A.; Ceccarini, A.; Petri, A.; Vinciguerra, V. Nylon 6 and Nylon 6,6 Micro- and Nanoplastics: A First Example of Their Accurate Quantification, Along with Polyester (Pet), in Wastewater Treatment Plant Sludges. *J. Hazard. Mater.* **2021**, *407*, 124364.

(119) Braun, U.; Eisentraut, P.; Altmann, K.; Kittner, M.; Dümichen, E.; Thaxton, K.; Kleine-Benne, E.; Anumol, T. Accelerated Determination of Microplastics in Environmental Samples Using Thermal Extraction Desorption-Gas Chromatography/Mass Spectrometry (TED-GC/MS), 2020.

(120) Materic, D.; Kasper-Giebl, A.; Kau, D.; Anten, M.; Greiling, M.; Ludewig, E.; van Sebille, E.; Roeckmann, T.; Holzinger, R. Micro- and Nanoplastics in Alpine Snow: A New Method for Chemical Identification and (Semi)Quantification in the Nanogram Range. *Environ. Sci. Technol.* **2020**, *54*, 2353–2359.

(121) Peacock, M.; Materić, D.; Kothawala, D. N.; Holzinger, R.; Futter, M. N. Understanding Dissolved Organic Matter Reactivity and Composition in Lakes and Streams Using Proton-Transfer-Reaction Mass Spectrometry (PTR-MS). *Environ. Sci. Technol. Lett.* **2018**, *5*, 739–744.

(122) Velimirovic, M.; Tirez, K.; Voorspoels, S.; Vanhaecke, F. Recent Developments in Mass Spectrometry for the Characterization of Micro- and Nanoscale Plastic Debris in the Environment. *Anal. Bioanal. Chem.* **2021**, *413*, 7–15.

(123) David, J.; Steinmetz, Z.; Kučerik, J.; Schaumann, G. E. Quantitative Analysis of Poly(Ethylene Terephthalate) Microplastics in Soil Via Thermogravimetry-Mass Spectrometry. *Anal. Chem.* **2018**, *90*, 8793–8799.

(124) Dittmann, D.; Braun, U.; Jekel, M.; Ruhl, A. S. Quantification and Characterisation of Activated Carbon in Activated Sludge by Thermogravimetric and Evolved Gas Analyses. *J. Environ. Chem. Eng.* **2018**, *6*, 2222–2231.

(125) Becker, R.; Altmann, K.; Sommerfeld, T.; Braun, U. Quantification of Microplastics in a Freshwater Suspended Organic Matter Using Different Thermoanalytical Methods - Outcome of an Interlaboratory Comparison. *J. Anal. Appl. Pyrolysis* **2020**, *148*, 104829.

(126) Castañeda, R. A.; Avlijas, S.; Simard, M. A.; Ricciardi, A. Microplastic Pollution in St. Lawrence River Sediments. *Can. J. Fish. Aquat. Sci.* **2014**, *71*, 1767–1771.

(127) Majewsky, M.; Bitter, H.; Eiche, E.; Horn, H. Determination of Microplastic Polyethylene (PE) and Polypropylene (PP) in Environmental Samples Using Thermal Analysis (TGA-DSC). *Sci. Total Environ.* **2016**, *568*, 507–511.

(128) Rodríguez Chialanza, M.; Sierra, I.; Pérez Parada, A.; Fornaro, L. Identification and Quantitation of Semi-Crystalline Microplastics Using Image Analysis and Differential Scanning Calorimetry. *Environ. Sci. Pollut. Res.* **2018**, *25*, 16767–16775.

- (129) Shabaka, S. H.; Ghobashy, M.; Marey, R. S. Identification of Marine Microplastics in Eastern Harbor, Mediterranean Coast of Egypt, Using Differential Scanning Calorimetry. *Mar. Pollut. Bull.* **2019**, *142*, 494–503.
- (130) Bitter, H.; Lackner, S. First Quantification of Semi-Crystalline Microplastics in Industrial Wastewaters. *Chemosphere* **2020**, *258*, 127388.
- (131) Kühn, S.; van Oyen, A.; Booth, A. M.; Meijboom, A.; van Franeker, J. A. Marine Microplastic: Preparation of Relevant Test Materials for Laboratory Assessment of Ecosystem Impacts. *Chemosphere* **2018**, *213*, 103–113.
- (132) Ren, H.; Hu, H.; Yu, B.; Du, Y.; Wu, T. Identification of Polymer Building Blocks by Py-GC/MS and MALDI-ToF MS. *Int. J. Polym. Anal. Charact.* **2018**, *23*, 9–17.
- (133) Lin, Y.; Huang, X.; Liu, Q.; Lin, Z.; Jiang, G. Thermal Fragmentation Enhanced Identification and Quantification of Polystyrene Micro/Nanoplastics in Complex Media. *Talanta* **2020**, *208*, 120478.
- (134) Imhof, H. K.; Laforsch, C.; Wiesheu, A. C.; Schmid, J.; Anger, P. M.; Niessner, R.; Ivleva, N. P. Pigments and Plastic in Limnetic Ecosystems: A Qualitative and Quantitative Study on Microparticles of Different Size Classes. *Water Res.* **2016**, *98*, 64–74.
- (135) Wang, J.; Peng, J.; Tan, Z.; Gao, Y.; Zhan, Z.; Chen, Q.; Cai, L. Microplastics in the Surface Sediments from the Beijiang River Littoral Zone: Composition, Abundance, Surface Textures and Interaction with Heavy Metals. *Chemosphere* **2017**, *171*, 248–258.
- (136) Klöckner, P.; Reemtsma, T.; Wagner, S. The Diverse Metal Composition of Plastic Items and Its Implications. *Sci. Total Environ.* **2021**, *764*, 142870.
- (137) Acosta-Coley, I.; Mendez-Cuadro, D.; Rodriguez-Cavallo, E.; de la Rosa, J.; Olivero-Verbel, J. Trace Elements in Microplastics in Cartagena: A Hotspot for Plastic Pollution at the Caribbean. *Mar. Pollut. Bull.* **2019**, *139*, 402–411.
- (138) Hahladakis, J. N.; Velis, C. A.; Weber, R.; Iacovidou, E.; Purnell, P. An Overview of Chemical Additives Present in Plastics: Migration, Release, Fate and Environmental Impact During Their Use, Disposal and Recycling. *J. Hazard. Mater.* **2018**, *344*, 179–199.
- (139) Wäger, P. A.; Schlupe, M.; Müller, E.; Gloor, R. Rohs Regulated Substances in Mixed Plastics from Waste Electrical and Electronic Equipment. *Environ. Sci. Technol.* **2012**, *46*, 628–635.
- (140) Wijesekara, H.; Bolan, N. S.; Bradney, L.; Obadamudalige, N.; Seshadri, B.; Kunhikrishnan, A.; Dharmarajan, R.; Ok, Y. S.; Rinklebe, J.; Kirkham, M. B.; et al. Trace Element Dynamics of Biosolids-Derived Microbeads. *Chemosphere* **2018**, *199*, 331–339.
- (141) Bolea-Fernandez, E.; Rua-Ibarz, A.; Velimirovic, M.; Tirez, K.; Vanhaecke, F. Detection of Microplastics Using Inductively Coupled Plasma-Mass Spectrometry (ICP-MS) Operated in Single-Event Mode. *J. Anal. At. Spectrom.* **2020**, *35*, 455–460.
- (142) Laborda, F.; Trujillo, C.; Lobinski, R. Analysis of Microplastics in Consumer Products by Single Particle-Inductively Coupled Plasma Mass Spectrometry Using the Carbon-13 Isotope. *Talanta* **2021**, *221*, 121486.
- (143) Peez, N.; Janiska, M.-C.; Imhof, W. The First Application of Quantitative  $^1\text{H}$  NMR Spectroscopy as a Simple and Fast Method of Identification and Quantification of Microplastic Particles (PE, PET, and PS). *Anal. Bioanal. Chem.* **2019**, *411*, 823–833.
- (144) Peez, N.; Becker, J.; Ehlers, S. M.; Fritz, M.; Fischer, C. B.; Koop, J. H. E.; Winkelmann, C.; Imhof, W. Quantitative Analysis of Pet Microplastics in Environmental Model Samples Using Quantitative  $^1\text{H}$ -NMR Spectroscopy: Validation of an Optimized and Consistent Sample Clean-up Method. *Anal. Bioanal. Chem.* **2019**, *411*, 7409–7418.
- (145) Peez, N.; Imhof, W. Quantitative  $^1\text{H}$ -NMR Spectroscopy as an Efficient Method for Identification and Quantification of PVC, ABS and PA Microparticles. *Analyst* **2020**, *145*, 5363–5371.
- (146) Nelson, T. F.; Remke, S. C.; Kohler, H.-P. E.; McNeill, K.; Sander, M. Quantification of Synthetic Polyesters from Biodegradable Mulch Films in Soils. *Environ. Sci. Technol.* **2019**, *54*, 266–275.
- (147) Castelvetro, V.; Corti, A.; Bianchi, S.; Ceccarini, A.; Manariti, A.; Vinciguerra, V. Quantification of Poly(Ethylene Terephthalate) Micro- and Nanoparticle Contaminants in Marine Sediments and Other Environmental Matrices. *J. Hazard. Mater.* **2020**, *385*, 121517.
- (148) Wang, L.; Zhang, J.; Hou, S.; Sun, H. A Simple Method for Quantifying Polycarbonate and Polyethylene Terephthalate Microplastics in Environmental Samples by Liquid Chromatography-Tandem Mass Spectrometry. *Environ. Sci. Technol. Lett.* **2017**, *4*, 530–534.
- (149) Johnson, A. C.; Ball, H.; Cross, R.; Horton, A. A.; Jürgens, M. D.; Read, D. S.; Vollertsen, J.; Svendsen, C. Identification and Quantification of Microplastics in Potable Water and Their Sources within Water Treatment Works in England and Wales. *Environ. Sci. Technol.* **2020**, *54*, 12326–12334.
- (150) Horton, A. A.; Cross, R. K.; Read, D. S.; Jürgens, M. D.; Ball, H. L.; Svendsen, C.; Vollertsen, J.; Johnson, A. C. Semi-Automated Analysis of Microplastics in Complex Wastewater Samples. *Environ. Pollut.* **2021**, *268*, 115841.
- (151) Waddell, E. N.; Lascelles, N.; Conkle, J. L. Microplastic Contamination in Corpus Christi Bay Blue Crabs, *Callinectes Sapidus*. *Limnol. Oceanogr. Lett.* **2020**, *5*, 92–102.
- (152) Renner, G.; Schmidt, T. C.; Schram, J. Analytical Methodologies for Monitoring Micro(Nano)Plastics: Which Are Fit for Purpose? *Curr. Opin. Environ. Sci. Health* **2018**, *1*, 55–61.
- (153) Lorenz, C.; Roscher, L.; Meyer, M. S.; Hildebrandt, L.; Prume, J.; Löder, M. G. J.; Primpke, S.; Gerdtts, G. Spatial Distribution of Microplastics in Sediments and Surface Waters of the Southern North Sea. *Environ. Pollut.* **2019**, *252*, 1719–1729.
- (154) Corami, F.; Rosso, B.; Picone, M.; Gambaro, A.; Barbante, C. Evidence of Small Microplastics (<100  $\mu\text{m}$ ) Ingestion by Pacific Oysters (*Crassostrea Gigas*): A Novel Method of Extraction, Purification, and Analysis Using Micro-FTIR. *Mar. Pollut. Bull.* **2020**, *160*, 111606.
- (155) Mani, T.; Primpke, S.; Lorenz, C.; Gerdtts, G.; Burkhardt-Holm, P. Microplastic Pollution in Benthic Midstream Sediments of the Rhine River. *Environ. Sci. Technol.* **2019**, *53*, 6053–6062.
- (156) Bergmann, M.; Wirzberger, V.; Krumpfen, T.; Lorenz, C.; Primpke, S.; Tekman, M. B.; Gerdtts, G. High Quantities of Microplastic in Arctic Deep-Sea Sediments from the Hausgarten Observatory. *Environ. Sci. Technol.* **2017**, *51*, 11000–11010.
- (157) Simon, M.; van Alst, N.; Vollertsen, J. Quantification of Microplastic Mass and Removal Rates at Wastewater Treatment Plants Applying Focal Plane Array (FPA)-Based Fourier Transform Infrared (FT-IR) Imaging. *Water Res.* **2018**, *142*, 1–9.
- (158) Cabernard, L.; Roscher, L.; Lorenz, C.; Gerdtts, G.; Primpke, S. Comparison of Raman and Fourier Transform Infrared Spectroscopy for the Quantification of Microplastics in the Aquatic Environment. *Environ. Sci. Technol.* **2018**, *52*, 13279–13288.
- (159) Mintenig, S. M.; Int-Veen, I.; Löder, M. G. J.; Primpke, S.; Gerdtts, G. Identification of Microplastic in Effluents of Waste Water Treatment Plants Using Focal Plane Array-Based Micro-Fourier-Transform Infrared Imaging. *Water Res.* **2017**, *108*, 365–372.
- (160) Abel, S. M.; Primpke, S.; Int-Veen, I.; Brandt, A.; Gerdtts, G. Systematic Identification of Microplastics in Abyssal and Hadal Sediments of the Kuril Kamchatka Trench. *Environ. Pollut.* **2021**, *269*, 116095.
- (161) Klein, S.; Worch, E.; Knepper, T. P. Occurrence and Spatial Distribution of Microplastics in River Shore Sediments of the Rhine-Main Area in Germany. *Environ. Sci. Technol.* **2015**, *49*, 6070–6076.
- (162) Comnea-Stancu, I. R.; Wieland, K.; Ramer, G.; Schwaighofer, A.; Lendl, B. On the Identification of Rayon/Viscose as a Major Fraction of Microplastics in the Marine Environment: Discrimination between Natural and Manmade Cellulosic Fibers Using Fourier Transform Infrared Spectroscopy. *Appl. Spectrosc.* **2017**, *71*, 939–950.
- (163) O'Connor, J. D.; Murphy, S.; Lally, H. T.; O'Connor, I.; Nash, R.; O'Sullivan, J.; Bruen, M.; Heerey, L.; Koelmans, A. A.; Cullagh, A.; et al. Microplastics in Brown Trout (*Salmo Trutta* Linnaeus, 1758) from an Irish Riverine System. *Environ. Pollut.* **2020**, *267*, 115572.
- (164) Luo, W.; Su, L.; Craig, N. J.; Du, F.; Wu, C.; Shi, H. Comparison of Microplastic Pollution in Different Water Bodies from Urban Creeks to Coastal Waters. *Environ. Pollut.* **2019**, *246*, 174–182.

- (165) Besseling, E.; Foekema, E. M.; Van Franeker, J. A.; Leopold, M. F.; Kühn, S.; Bravo Rebolledo, E. L.; Heße, E.; Mielke, L.; Ijzer, J.; Kamminga, P.; et al. Microplastic in a Macro Filter Feeder: Humpback Whale Megaptera Novaeangliae. *Mar. Pollut. Bull.* **2015**, *95*, 248–252.
- (166) Wu, P.; Tang, Y.; Dang, M.; Wang, S.; Jin, H.; Liu, Y.; Jing, H.; Zheng, C.; Yi, S.; Cai, Z. Spatial-Temporal Distribution of Microplastics in Surface Water and Sediments of Maozhou River within Guangdong-Hong Kong-Macao Greater Bay Area. *Sci. Total Environ.* **2020**, *717*, 135187.
- (167) Woodall, L. C.; Sanchez-Vidal, A.; Canals, M.; Paterson, G. L. J.; Coppock, R.; Sleight, V.; Calafat, A.; Rogers, A. D.; Narayanaswamy, B. E.; Thompson, R. C. The Deep Sea Is a Major Sink for Microplastic Debris. *R. Soc. Open Sci.* **2014**, *1*, 140317–140317.
- (168) Enders, K.; Käppler, A.; Biniash, O.; Feldens, P.; Stollberg, N.; Lange, X.; Fischer, D.; Eichhorn, K.-J.; Pollehne, F.; Oberbeckmann, S.; et al. Tracing Microplastics in Aquatic Environments Based on Sediment Analogies. *Sci. Rep.* **2019**, *9*, 15207.
- (169) Piehl, S.; Leibner, A.; Löder, M. G. J.; Dris, R.; Bogner, C.; Laforsch, C. Identification and Quantification of Macro- and Microplastics on an Agricultural Farmland. *Sci. Rep.* **2018**, *8*, 17950.
- (170) Ziajahromi, S.; Neale, P. A.; Rintoul, L.; Leusch, F. D. L. Wastewater Treatment Plants as a Pathway for Microplastics: Development of a New Approach to Sample Wastewater-Based Microplastics. *Water Res.* **2017**, *112*, 93–99.
- (171) Tagg, A. S.; Sapp, M.; Harrison, J. P.; Ojeda, J. J. Identification and Quantification of Microplastics in Wastewater Using Focal Plane Array-Based Reflectance Micro-FT-IR Imaging. *Anal. Chem.* **2015**, *87*, 6032–6040.
- (172) Trainic, M.; Flores, J. M.; Pinkas, I.; Pedrotti, M. L.; Lombard, F.; Bourdin, G.; Gorsky, G.; Boss, E.; Rudich, Y.; Vardi, A.; et al. Airborne Microplastic Particles Detected in the Remote Marine Atmosphere. *Commun. Earth. Environ.* **2020**, *1*, 64.
- (173) Cai, L.; Wang, J.; Peng, J.; Tan, Z.; Zhan, Z.; Tan, X.; Chen, Q. Characteristic of Microplastics in the Atmospheric Fallout from Dongguan City, China: Preliminary Research and First Evidence. *Environ. Sci. Pollut. Res.* **2017**, *24*, 24928–24935.
- (174) Weisser, J.; Beer, I.; Hufnagl, B.; Hofmann, T.; Lohninger, H.; Ivleva, N. P.; Glas, K. From the Well to the Bottle: Identifying Sources of Microplastics in Mineral Water. *Water* **2021**, *13*, 841.
- (175) Yang, D.; Shi, H.; Li, L.; Li, J.; Jabeen, K.; Kolandhasamy, P. Microplastic Pollution in Table Salts from China. *Environ. Sci. Technol.* **2015**, *49*, 13622–13627.
- (176) Primpke, S.; Wirth, M.; Lorenz, C.; Gerdt, G. Reference Database Design for the Automated Analysis of Microplastic Samples Based on Fourier Transform Infrared (FTIR) Spectroscopy. *Anal. Bioanal. Chem.* **2018**, *410*, 5131–5141.
- (177) Renner, G.; Nellessen, A.; Schwieters, A.; Wenzel, M.; Schmidt, T. C.; Schram, J. Data Preprocessing & Evaluation Used in the Microplastics Identification Process: A Critical Review & Practical Guide. *TrAC, Trends Anal. Chem.* **2019**, *111*, 229–238.
- (178) Cowger, W.; Gray, A.; Christiansen, S. H.; DeFron, H.; Deshpande, A. D.; Hemabessiere, L.; Lee, E.; Mill, L.; Munno, K.; Ossmann, B. E.; et al. Critical Review of Processing and Classification Techniques for Images and Spectra in Microplastic Research. *Appl. Spectrosc.* **2020**, *74*, 989–1010.
- (179) Renner, G.; Schmidt, T. C.; Schram, J. A New Chemometric Approach for Automatic Identification of Microplastics from Environmental Compartments Based on FT-IR Spectroscopy. *Anal. Chem.* **2017**, *89*, 12045–12053.
- (180) Hufnagl, B.; Steiner, D.; Renner, E.; Löder, M. G. J.; Laforsch, C.; Lohninger, H. A Methodology for the Fast Identification and Monitoring of Microplastics in Environmental Samples Using Random Decision Forest Classifiers. *Anal. Methods* **2019**, *11*, 2277–2285.
- (181) Löder, M. G. J.; Kuczera, M.; Mintenig, S.; Lorenz, C.; Gerdt, G. Focal Plane Array Detector-Based Micro-Fourier-Transform Infrared Imaging for the Analysis of Microplastics in Environmental Samples. *Environ. Chem.* **2015**, *12*, 563–581.
- (182) Käppler, A.; Windrich, F.; Löder, M. G. J.; Malanin, M.; Fischer, D.; Labrenz, M.; Eichhorn, K.-J.; Voit, B. Identification of Microplastics by FTIR and Raman Microscopy: A Novel Silicon Filter Substrate Opens the Important Spectral Range Below 1300 cm<sup>-1</sup> for FTIR Transmission Measurements. *Anal. Bioanal. Chem.* **2015**, *407*, 6791–6801.
- (183) Käppler, A.; Fischer, D.; Oberbeckmann, S.; Schernewski, G.; Labrenz, M.; Eichhorn, K.-J.; Voit, B. Analysis of Environmental Microplastics by Vibrational Microspectroscopy: FTIR, Raman or Both? *Anal. Bioanal. Chem.* **2016**, *408*, 8377–8391.
- (184) Tagg, A. S.; Sapp, M.; Harrison, J. P.; Sinclair, C. J.; Bradley, E.; Ju-Nam, Y.; Ojeda, J. J. Microplastic Monitoring at Different Stages in a Wastewater Treatment Plant Using Reflectance Micro-FTIR Imaging. *Front. Environ. Sci.* **2020**, *8*, 145.
- (185) Oßmann, B. E.; Sarau, G.; Schmitt, S. W.; Holtmannspötter, H.; Christiansen, S. H.; Dicke, W. Development of an Optimal Filter Substrate for the Identification of Small Microplastic Particles in Food by Micro-Raman Spectroscopy. *Anal. Bioanal. Chem.* **2017**, *409*, 4099–4109.
- (186) ter Halle, A.; Ladirat, L.; Martignac, M.; Mingotaud, A. F.; Boyron, O.; Perez, E. To What Extent Are Microplastics from the Open Ocean Weathered? *Environ. Pollut.* **2017**, *227*, 167–174.
- (187) von der Esch, E.; Lanzinger, M.; Kohles, A. J.; Schwaferts, C.; Weisser, J.; Hofmann, T.; Glas, K.; Elsner, M.; Ivleva, N. P. Simple Generation of Suspensible Secondary Microplastic Reference Particles Via Ultrasound Treatment. *Front. Chem. (Lausanne, Switz.)* **2020**, *8*, 169.
- (188) Dris, R.; Gasperi, J.; Saad, M.; Mirande, C.; Tassin, B. Synthetic Fibers in Atmospheric Fallout: A Source of Microplastics in the Environment? *Mar. Pollut. Bull.* **2016**, *104*, 290–293.
- (189) Dris, R.; Gasperi, J.; Rocher, V.; Tassin, B. Synthetic and Non-Synthetic Anthropogenic Fibers in a River under the Impact of Paris Megacity: Sampling Methodological Aspects and Flux Estimations. *Sci. Total Environ.* **2018**, *618*, 157–164.
- (190) Vianello, A.; Boldrin, A.; Guerriero, P.; Moschino, V.; Rella, R.; Sturaro, A.; Da Ros, L. Microplastic Particles in Sediments of Lagoon of Venice, Italy: First Observations on Occurrence, Spatial Patterns and Identification. *Estuarine, Coastal Shelf Sci.* **2013**, *130*, 54–61.
- (191) Salzer, R.; Siesler, H. W. *Infrared and Raman Spectroscopic Imaging*; Wiley-VCH Verlag GmbH & Co. KGaA: Weinheim, 2009.
- (192) Primpke, S. A.; Dias, P. A.; Gerdt, G. Automated Identification and Quantification of Microfibres and Microplastics. *Anal. Methods* **2019**, *11*, 2138–2147.
- (193) Imhof, H. K.; Schmid, J.; Niessner, R.; Ivleva, N. P.; Laforsch, C. A Novel, Highly Efficient Method for the Separation and Quantification of Plastic Particles in Sediments of Aquatic Environments. *Limnol. Oceanogr.: Methods* **2012**, *10*, 524–537.
- (194) Coppock, R. L.; Cole, M.; Lindeque, P. K.; Queirós, A. M.; Galloway, T. S. A Small-Scale, Portable Method for Extracting Microplastics from Marine Sediments. *Environ. Pollut.* **2017**, *230*, 829–837.
- (195) Al-Azzawi, M. S. M.; Kefer, S.; Weißer, J.; Reichel, J.; Schwaller, C.; Glas, K.; Knoop, O.; Drewes, J. E. Validation of Sample Preparation Methods for Microplastic Analysis in Wastewater Matrices—Reproducibility and Standardization. *Water* **2020**, *12*, 2445.
- (196) Tagg, A. S.; Harrison, J. P.; Ju-Nam, Y.; Sapp, M.; Bradley, E. L.; Sinclair, C. J.; Ojeda, J. J. Fenton's Reagent for the Rapid and Efficient Isolation of Microplastics from Wastewater. *Chem. Commun.* **2017**, *53*, 372–375.
- (197) Loeder, M. G. J.; Imhof, H. K.; Ladehoff, M.; Loeschel, L. A.; Lorenz, C.; Mintenig, S.; Piehl, S.; Primpke, S.; Schrank, I.; Laforsch, C.; et al. Enzymatic Purification of Microplastics in Environmental Samples. *Environ. Sci. Technol.* **2017**, *51*, 14283–14292.
- (198) Lusher, A. L.; Munno, K.; Hermabessiere, L.; Carr, S. Isolation and Extraction of Microplastics from Environmental Samples: An Evaluation of Practical Approaches and Recommendations for Further Harmonization. *Appl. Spectrosc.* **2020**, *74*, 1049–1065.
- (199) Liu, F.; Vianello, A.; Vollertsen, J. Retention of Microplastics in Sediments of Urban and Highway Stormwater Retention Ponds. *Environ. Pollut.* **2019**, *255*, 113335.

- (200) Poulain, M.; Mercier, M. J.; Brach, L.; Martignac, M.; Routaboul, C.; Perez, E.; Desjean, M. C.; ter Halle, A. Small Microplastics as a Main Contributor to Plastic Mass Balance in the North Atlantic Subtropical Gyre. *Environ. Sci. Technol.* **2019**, *53*, 1157–1164.
- (201) Brandt, J.; Bittrich, L.; Fischer, F.; Kanaki, E.; Tagg, A.; Lenz, R.; Labrenz, M.; Brandes, E.; Fischer, D.; Eichhorn, K.-J. High-Throughput Analyses of Microplastic Samples Using Fourier Transform Infrared and Raman Spectrometry. *Appl. Spectrosc.* **2020**, *74*, 1185–1197.
- (202) Kang, H.; Park, S.; Lee, B.; Ahn, J.; Kim, S. Modification of a Nile Red Staining Method for Microplastics Analysis: A Nile Red Plate Method. *Water* **2020**, *12*, 3251.
- (203) Maes, T.; Jessop, R.; Wellner, N.; Haupt, K.; Mayes, A. G. A Rapid-Screening Approach to Detect and Quantify Microplastics Based on Fluorescent Tagging with Nile Red. *Sci. Rep.* **2017**, *7*, 44501.
- (204) Mason, S. A.; Welch, V. G.; Neratko, J. Synthetic Polymer Contamination in Bottled Water. *Front. Chem.* **2018**, *6*, 407.
- (205) Harrison, J. P.; Ojeda, J. J.; Romero-Gonzalez, M. E. The Applicability of Reflectance Micro-Fourier-Transform Infrared Spectroscopy for the Detection of Synthetic Microplastics in Marine Sediments. *Sci. Total Environ.* **2012**, *416*, 455–463.
- (206) Bergmann, M.; Mützel, S.; Primpke, S.; Tekman, M. B.; Trachsel, J.; Gerdt, G. White and Wonderful? Microplastics Preval in Snow from the Alps to the Arctic. *Sci. Adv.* **2019**, *5*, No. eaax1157.
- (207) Kedzierski, M.; Falcou-Préfol, M.; Kerros, M. E.; Henry, M.; Pedrotti, M. L.; Bruzard, S. A Machine Learning Algorithm for High Throughput Identification of FTIR Spectra: Application on Microplastics Collected in the Mediterranean Sea. *Chemosphere* **2019**, *234*, 242–251.
- (208) Xu, J.-L.; Thomas, K. V.; Luo, Z.; Gowen, A. A. FTIR and Raman Imaging for Microplastics Analysis: State of the Art, Challenges and Prospects. *TrAC, Trends Anal. Chem.* **2019**, *119*, 115629.
- (209) Andrade, J. M.; Ferreiro, B.; López-Mahía, P.; Muniategui-Lorenzo, S. Standardization of the Minimum Information for Publication of Infrared-Related Data When Microplastics Are Characterized. *Mar. Pollut. Bull.* **2020**, *154*, 111035.
- (210) Primpke, S.; Cross, R. K.; Mintenig, S. M.; Simon, M.; Vianello, A.; Gerdt, G.; Vollertsen, J. Toward the Systematic Identification of Microplastics in the Environment: Evaluation of a New Independent Software Tool (SiMPle) for Spectroscopic Analysis. *Appl. Spectrosc.* **2020**, *74*, 1127–1138.
- (211) Liu, F.; Olesen, K. B.; Borregaard, A. R.; Vollertsen, J. Microplastics in Urban and Highway Stormwater Retention Ponds. *Sci. Total Environ.* **2019**, *671*, 992–1000.
- (212) Primpke, S.; Lorenz, C.; Rascher-Friesenhausen, R.; Gerdt, G. An Automated Approach for Microplastics Analysis Using Focal Plane Array (FPA) FTIR Microscopy and Image Analysis. *Anal. Methods* **2017**, *9*, 1499–1511.
- (213) VinayKumar, B. N.; Löschel, L. A.; Imhof, H. K.; Löder, M. G. J.; Laforsch, C. Analysis of Microplastics of a Broad Size Range in Commercially Important Mussels by Combining FT-IR and Raman Spectroscopy Approaches. *Environ. Pollut.* **2021**, *269*, 116147.
- (214) Hahn, A.; Gerdt, G.; Völker, C.; Niebühr, V. Using FTIRS as Pre-Screening Method for Detection of Microplastic in Bulk Sediment Samples. *Sci. Total Environ.* **2019**, *689*, 341–346.
- (215) da Silva, V. H.; Murphy, F.; Amigo, J. M.; Stedmon, C.; Strand, J. Classification and Quantification of Microplastics (<100  $\mu\text{m}$ ) Using a Focal Plane Array-Fourier Transform Infrared Imaging System and Machine Learning. *Anal. Chem.* **2020**, *92*, 13724–13733.
- (216) Wander, L.; Vianello, A.; Vollertsen, J.; Westad, F.; Braun, U.; Paul, A. Exploratory Analysis of Hyperspectral FTIR Data Obtained from Environmental Microplastics Samples. *Anal. Methods* **2020**, *12*, 781–791.
- (217) Scircle, A.; Cizdziel, J. V.; Tisinger, L.; Anumol, T.; Robey, D. Occurrence of Microplastic Pollution at Oyster Reefs and Other Coastal Sites in the Mississippi Sound, USA: Impacts of Freshwater Inflows from Flooding. *Toxics* **2020**, *8*, 35.
- (218) Mughini-Gras, L.; van der Plaats, R. Q. J.; van der Wielen, P. W. J. J.; Bauerlein, P. S.; de Roda Husman, A. M. Riverine Microplastic and Microbial Community Compositions: A Field Study in the Netherlands. *Water Res.* **2021**, *192*, 116852.
- (219) Hildebrandt, L.; El Gareb, F.; Zimmermann, T.; Klein, O.; Emeis, K.-C.; Proefrock, D.; Kerstan, A. Fast, Automated Microplastics Analysis Using Laser Direct Chemical Imaging. *Application Note: Environmental Water Analysis*; Agilent, 2020.
- (220) Ng, E. L.; Lin, S. Y.; Dungan, A. M.; Colwell, J. M.; Ede, S.; Huerta Lwanga, E.; Meng, K.; Geissen, V.; Blackall, L. L.; Chen, D. Microplastic Pollution Alters Forest Soil Microbiome. *J. Hazard. Mater.* **2021**, *409*, 124606.
- (221) Li, Q.; Zeng, A.; Jiang, X.; Gu, X. Are Microplastics Correlated to Phthalates in Facility Agriculture Soil? *J. Hazard. Mater.* **2021**, *412*, 125164.
- (222) Primpke, S.; Godejohann, M.; Gerdt, G. Rapid Identification and Quantification of Microplastics in the Environment by Quantum Cascade Laser-Based Hyperspectral Infrared Chemical Imaging. *Environ. Sci. Technol.* **2020**, *54*, 15893.
- (223) Marcott, C.; Kansiz, M.; Dillon, E.; Cook, D.; Mang, M. N.; Noda, I. Two-Dimensional Correlation Analysis of Highly Spatially Resolved Simultaneous IR and Raman Spectral Imaging of Bioplastics Composite Using Optical Photothermal Infrared and Raman Spectroscopy. *J. Mol. Struct.* **2020**, *1210*, 128045.
- (224) Li, X.; Zhang, D.; Bai, Y.; Wang, W.; Liang, J.; Cheng, J.-X. Fingerprinting a Living Cell by Raman Integrated Mid-Infrared Photothermal Microscopy. *Anal. Chem.* **2019**, *91*, 10750–10756.
- (225) Beltran, V.; Marchetti, A.; Nuyts, G.; Leeuwestein, M.; Sandt, C.; Borondics, F.; De Wael, K. Nanoscale Analysis of Historical Paintings by Means of O-Ptir Spectroscopy: The Identification of the Organic Particles in L'arlesienne (Portrait of Madame Ginoux) by Van Gogh. *Angew. Chem., Int. Ed.* **2021**, DOI: 10.1002/anie.202106058.
- (226) Marcott, C.; Kansiz, M.; Dillon, E.; Kjoller, K.; Weston, F.; Anderson, J. Application of Submicron Simultaneous Raman and Optical Photothermal Infrared Spectroscopy to Chemically Identify Microplastic Particles, Cultural Artifacts, and Forensic Samples. *Eastern Analytical Symposium, Princeton, NJ, USA, November 19, 2020*, 2020.
- (227) van den Broek, W. H. A. M.; Wienke, D.; Melssen, W. J.; Buydens, L. M. C. Plastic Material Identification with Spectroscopic near Infrared Imaging and Artificial Neural Networks. *Anal. Chim. Acta* **1998**, *361*, 161–176.
- (228) Moroni, M.; Mei, A.; Leonardi, A.; Lupo, E.; Marca, F. L. Pet and Pvc Separation with Hyperspectral Imagery. *Sensors* **2015**, *15*, 2205–2227.
- (229) Karlsson, T. M.; Grahm, H.; van Bavel, B.; Geladi, P. Hyperspectral Imaging and Data Analysis for Detecting and Determining Plastic Contamination in Seawater Filtrates. *J. Near Infrared Spectrosc.* **2016**, *24*, 141–149.
- (230) Shan, J.; Zhao, J.; Zhang, Y.; Liu, L.; Wu, F.; Wang, X. Simple and Rapid Detection of Microplastics in Seawater Using Hyperspectral Imaging Technology. *Anal. Chim. Acta* **2019**, *1050*, 161–168.
- (231) Schmidt, L. K.; Bochow, M.; Imhof, H. K.; Oswald, S. E. Multi-Temporal Surveys for Microplastic Particles Enabled by a Novel and Fast Application of Swir Imaging Spectroscopy - Study of an Urban Watercourse Traversing the City of Berlin, Germany. *Environ. Pollut.* **2018**, *239*, 579–589.
- (232) Zhang, Y.; Wang, X.; Shan, J.; Zhao, J.; Zhang, W.; Liu, L.; Wu, F. Hyperspectral Imaging Based Method for Rapid Detection of Microplastics in the Intestinal Tracts of Fish. *Environ. Sci. Technol.* **2019**, *53*, 5151–5158.
- (233) Shan, J.; Zhao, J.; Liu, L.; Zhang, Y.; Wang, X.; Wu, F. A Novel Way to Rapidly Monitor Microplastics in Soil by Hyperspectral Imaging Technology and Chemometrics. *Environ. Pollut.* **2018**, *238*, 121–129.
- (234) Paul, A.; Wander, L.; Becker, R.; Goedecke, C.; Braun, U. High-Throughput NIR Spectroscopic (NIRS) Detection of Microplastics in Soil. *Environ. Sci. Pollut. Res.* **2019**, *26*, 7364–7374.
- (235) Croombe, R. A. Portable Spectroscopy. *Appl. Spectrosc.* **2018**, *72*, 1701–1751.
- (236) Enders, K.; Lenz, R.; Stedmon, C. A.; Nielsen, T. G. Abundance, Size and Polymer Composition of Marine Microplastics  $\geq 10 \mu\text{m}$  in the

Atlantic Ocean and Their Modelled Vertical Distribution. *Mar. Pollut. Bull.* **2015**, *100*, 70–81.

(237) Zhang, K.; Su, J.; Xiong, X.; Wu, X.; Wu, C.; Liu, J. Microplastic Pollution of Lakeshore Sediments from Remote Lakes in Tibet Plateau, China. *Environ. Pollut.* **2016**, *219*, 450–455.

(238) Wang, W.; Yuan, W.; Chen, Y.; Wang, J. Microplastics in Surface Waters of Dongting Lake and Hong Lake, China. *Sci. Total Environ.* **2018**, *633*, 539–545.

(239) Zhao, S.; Danley, M.; Ward, J. E.; Li, D.; Mincer, T. J. An Approach for Extraction, Characterization and Quantitation of Microplastic in Natural Marine Snow Using Raman Microscopy. *Anal. Methods* **2017**, *9*, 1470–1478.

(240) Imhof, H. K.; Ivleva, N. P.; Schmid, J.; Niessner, R.; Laforsch, C. Contamination of Beach Sediments of a Subalpine Lake with Microplastic Particles. *Curr. Biol.* **2013**, *23*, R867–R868.

(241) Missawi, O.; Bousserhine, N.; Belbekhouche, S.; Zitouni, N.; Alphonse, V.; Boughattas, I.; Banni, M. Abundance and Distribution of Small Microplastics ( $\leq 3 \mu\text{m}$ ) in Sediments and Seaworms from the Southern Mediterranean Coasts and Characterisation of Their Potential Harmful Effects. *Environ. Pollut.* **2020**, *263*, 114634.

(242) Collard, F.; Gilbert, B.; Eppe, G.; Parmentier, E.; Das, K. Detection of Anthropogenic Particles in Fish Stomachs: An Isolation Method Adapted to Identification by Raman Spectroscopy. *Arch. Environ. Contam. Toxicol.* **2015**, *69*, 331–339.

(243) Zhang, S.; Sun, Y.; Liu, B.; Li, R. Full Size Microplastics in Crab and Fish Collected from the Mangrove Wetland of Beibu Gulf: Evidences from Raman Tweezers (1–20  $\mu\text{m}$ ) and Spectroscopy (20–5000  $\mu\text{m}$ ). *Sci. Total Environ.* **2021**, *759*, 143504.

(244) Domogalla-Urbansky, J.; Anger, P. M.; Ferling, H.; Rager, F.; Wiesheu, A. C.; Niessner, R.; Ivleva, N. P.; Schwaiger, J. Raman Microspectroscopic Identification of Microplastic Particles in Freshwater Bivalves (*Unio pictorum*) Exposed to Sewage Treatment Plant Effluents under Different Exposure Scenarios. *Environ. Sci. Pollut. Res.* **2019**, *26*, 2007–2012.

(245) Remy, F.; Collard, F.; Gilbert, B.; Compère, P.; Eppe, G.; Lepoint, G. When Microplastic Is Not Plastic: The Ingestion of Artificial Cellulose Fibers by Macrofauna Living in Seagrass Macrophytodebris. *Environ. Sci. Technol.* **2015**, *49*, 11158–11166.

(246) Levermore, J. M.; Smith, T. E. L.; Kelly, F. J.; Wright, S. L. Detection of Microplastics in Ambient Particulate Matter Using Raman Spectral Imaging and Chemometric Analysis. *Anal. Chem.* **2020**, *92*, 8732–8740.

(247) Wolff, S.; Kerpen, J.; Prediger, J.; Barkmann, L.; Müller, L. Determination of the Microplastics Emission in the Effluent of a Municipal Waste Water Treatment Plant Using Raman Microspectroscopy. *Water Res. X* **2019**, *2*, 100014.

(248) Weber, F.; Kerpen, J.; Wolff, S.; Langer, R.; Eschweiler, V. Investigation of Microplastics Contamination in Drinking Water of a German City. *Sci. Total Environ.* **2021**, *755*, 143421.

(249) Shruti, V. C.; Pérez-Guevara, F.; Kutralam-Muniasamy, G. Metro Station Free Drinking Water Fountain- a Potential “Microplastics Hotspot” for Human Consumption. *Environ. Pollut.* **2020**, *261*, 114227.

(250) Karami, A.; Golieskardi, A.; Ho, Y. B.; Larat, V.; Salamatinia, B. Microplastics in Eviscerated Flesh and Excised Organs of Dried Fish. *Sci. Rep.* **2017**, *7*, 5473.

(251) Wiesheu, A. C.; Anger, P. M.; Baumann, T.; Niessner, R.; Ivleva, N. P. Raman Microspectroscopic Analysis of Fibers in Beverages. *Anal. Methods* **2016**, *8*, 5722–5725.

(252) Sobhani, Z.; Zhang, X.; Gibson, C.; Naidu, R.; Megharaj, M.; Fang, C. Identification and Visualisation of Microplastics/Nanoplastics by Raman Imaging (I): Down to 100 nm. *Water Res.* **2020**, *174*, 115658.

(253) Gillibert, R.; Balakrishnan, G.; Deshoules, Q.; Tardivel, M.; Magazzù, A.; Donato, M. G.; Maragò, O. M.; Lamy de La Chapelle, M.; Colas, F.; Lagarde, F.; et al. Raman Tweezers for Small Microplastics and Nanoplastics Identification in Seawater. *Environ. Sci. Technol.* **2019**, *53*, 9003–9013.

(254) Raman, C. V.; Krishnan, K. S. The Production of New Radiations by Light Scattering. Part I. *Proc. R. Soc. London, A* **1929**, *122*, 23–35.

(255) Laptенок, S. P.; Martin, C.; Genchi, L.; Duarte, C. M.; Liberale, C. Stimulated Raman Microspectroscopy as a New Method to Classify Microfibers from Environmental Samples. *Environ. Pollut.* **2020**, *267*, 115640.

(256) Anger, P. M.; von der Esch, E.; Baumann, T.; Elsner, M.; Niessner, R.; Ivleva, N. P. Raman Microspectroscopy as a Tool for Microplastic Particle Analysis. *TrAC, Trends Anal. Chem.* **2018**, *109*, 214–226.

(257) Araujo, C. F.; Nolasco, M. M.; Ribeiro, A. M. P.; Ribeiro-Claro, P. J. A. Identification of Microplastics Using Raman Spectroscopy: Latest Developments and Future Prospects. *Water Res.* **2018**, *142*, 426–440.

(258) Lenz, R.; Enders, K.; Stedmon, C. A.; Mackenzie, D. M. A.; Nielsen, T. G. A Critical Assessment of Visual Identification of Marine Microplastic Using Raman Spectroscopy for Analysis Improvement. *Mar. Pollut. Bull.* **2015**, *100*, 82–91.

(259) Enders, K.; Lenz, R.; Ivar do Sul, J. A.; Tagg, A. S.; Labrenz, M. When Every Particle Matters: A Quechers Approach to Extract Microplastics from Environmental Samples. *MethodsX* **2020**, *7*, 100784–100784.

(260) Thomas, D.; Schütze, B.; Heinze, W. M.; Steinmetz, Z. Sample Preparation Techniques for the Analysis of Microplastics in Soil—A Review. *Sustainability* **2020**, *12*, 9074.

(261) Moeller, J. N.; Loeder, M. G. J.; Laforsch, C. Finding Microplastics in Soils: A Review of Analytical Methods. *Environ. Sci. Technol.* **2020**, *54*, 2078–2090.

(262) Li, D.; Shi, Y.; Yang, L.; Xiao, L.; Kehoe, D. K.; Gun'ko, Y. K.; Boland, J. J.; Wang, J. J. Microplastic Release from the Degradation of Polypropylene Feeding Bottles During Infant Formula Preparation. *Nat. Food* **2020**, *1*, 746–754.

(263) Dong, M.; Zhang, Q.; Xing, X.; Chen, W.; She, Z.; Luo, Z. Raman Spectra and Surface Changes of Microplastics Weathered under Natural Environments. *Sci. Total Environ.* **2020**, *739*, 139990.

(264) Sujathan, S.; Kniggendorf, A.-K.; Kumar, A.; Roth, B.; Rosenwinkel, K.-H.; Nogueira, R. Heat and Bleach: A Cost-Efficient Method for Extracting Microplastics from Return Activated Sludge. *Arch. Environ. Contam. Toxicol.* **2017**, *73*, 641–648.

(265) Van Cauwenberghe, L.; Devriese, L.; Galgani, F.; Robbins, J.; Janssen, C. R. Microplastics in Sediments: A Review of Techniques, Occurrence and Effects. *Mar. Environ. Res.* **2015**, *111*, 5–17.

(266) Karami, A.; Golieskardi, A.; Choo, C. K.; Larat, V.; Karbalaee, S.; Salamatinia, B. Microplastic and Mesoplastic Contamination in Canned Sardines and Sprats. *Sci. Total Environ.* **2018**, *612*, 1380–1386.

(267) Yonkos, L. T.; Friedel, E. A.; Perez-Reyes, A. C.; Ghosal, S.; Arthur, C. D. Microplastics in Four Estuarine Rivers in the Chesapeake Bay, U.S.A. *Environ. Sci. Technol.* **2014**, *48*, 14195–14202.

(268) Erni-Cassola, G.; Gibson, M. I.; Thompson, R. C.; Christie-Oleza, J. A. Lost, but Found with Nile Red: A Novel Method for Detecting and Quantifying Small Microplastics (1 mm to 20  $\mu\text{m}$ ) in Environmental Samples. *Environ. Sci. Technol.* **2017**, *51*, 13641–13648.

(269) Valliant, R.; Dever, J. A.; Kreuter, F. In *Practical Tools for Designing and Weighting Survey Samples. Statistics for Social and Behavioral Sciences*; Springer: New York, 2013; Vol. 51.

(270) Frère, L.; Paul-Pont, I.; Moreau, J.; Soudant, P.; Lambert, C.; Huvet, A.; Rinnert, E. A Semi-Automated Raman Micro-Spectroscopy Method for Morphological and Chemical Characterizations of Microplastic Litter. *Mar. Pollut. Bull.* **2016**, *113*, 461–468.

(271) Witzig, C. S.; Földi, C.; Wörle, K.; Habermehl, P.; Pittroff, M.; Müller, Y. K.; Lauschke, T.; Fiener, P.; Dierkes, G.; Freier, K. P.; et al. When Good Intentions Go Bad—False Positive Microplastic Detection Caused by Disposable Gloves. *Environ. Sci. Technol.* **2020**, *54*, 12164–12172.

(272) von der Esch, E.; Kohles, A. J.; Anger, P. M.; Hoppe, R.; Niessner, R.; Elsner, M.; Ivleva, N. P. *TUM-ParticleTyper*: A Detection and Quantification Tool for Automated Analysis of (Microplastic) Particles and Fibers. *PLoS One* **2020**, *15*, No. e0234766.

- (273) Anger, P. M.; Prechtel, L.; Elsner, M.; Niessner, R.; Ivleva, N. P. Implementation of an Open Source Algorithm for Particle Recognition and Morphological Characterisation for Microplastic Analysis by Means of Raman Microspectroscopy. *Anal. Methods* **2019**, *11*, 3483–3489.
- (274) Thaysen, C.; Munno, K.; Hermabessiere, L.; Rochman, C. M. Towards Raman Automation for Microplastics: Developing Strategies for Particle Adhesion and Filter Subsampling. *Appl. Spectrosc.* **2020**, *74*, 976–988.
- (275) Schwaferts, C.; Schwaferts, P.; von der Esch, E.; Elsner, M.; Ivleva, N. P. Which Particles to Select, and If Yes, How Many? Subsampling Methods for Raman Microspectroscopic Analysis of Very Small Microplastic. *Anal. Bioanal. Chem.* **2021**, *413*, 3625–3641.
- (276) Brandt, J.; Fischer, F.; Kanaki, E.; Enders, K.; Labrenz, M.; Fischer, D. Assessment of Subsampling Strategies in Microspectroscopy of Environmental Microplastic Samples. *Front. Environ. Sci.* **2021**, *8*, 679676.
- (277) Choy, C. A.; Robison, B. H.; Gagne, T. O.; Erwin, B.; Firl, E.; Halden, R. U.; Hamilton, J. A.; Katija, K.; Lisin, S. E.; Rolsky, C.; et al. The Vertical Distribution and Biological Transport of Marine Microplastics across the Epipelagic and Mesopelagic Water Column. *Sci. Rep.* **2019**, *9*, 7843.
- (278) Munno, K.; De Frond, H.; O'Donnell, B.; Rochman, C. M. Increasing the Accessibility for Characterizing Microplastics: Introducing New Application-Based and Spectral Libraries of Plastic Particles (SLoPP and SLoPP-E). *Anal. Chem.* **2020**, *92*, 2443–2451.
- (279) Cowger, W.; Steinmetz, Z.; Gray, A.; Munno, K.; Lynch, J.; Hapich, H.; Primpke, S.; De Frond, H.; Rochman, C.; Herodotou, O. Microplastic Spectral Classification Needs an Open Source Community: Open Specy to the Rescue! *Anal. Chem.* **2021**, *93*, 7543.
- (280) Kniggendorf, A.-K.; Wetzel, C.; Roth, B. Microplastics Detection in Streaming Tap Water with Raman Spectroscopy. *Sensors* **2019**, *19*, 1839.
- (281) Schwaferts, C.; Sogne, V.; Welz, R.; Meier, F.; Klein, T.; Niessner, R.; Elsner, M.; Ivleva, N. P. Nanoplastic Analysis by Online Coupling of Raman Microscopy and Field-Flow Fractionation Enabled by Optical Tweezers. *Anal. Chem.* **2020**, *92*, 5813–5820.
- (282) Xie, C.; Mace, J.; Dinno, M. A.; Li, Y. Q.; Tang, W.; Newton, R. J.; Gemperline, P. J. Identification of Single Bacterial Cells in Aqueous Solution Using Confocal Laser Tweezers Raman Spectroscopy. *Anal. Chem.* **2005**, *77*, 4390–4397.
- (283) Huang, W. E.; Ward, A. D.; Whiteley, A. S. Raman Tweezers Sorting of Single Microbial Cells. *Environ. Microbiol. Rep.* **2009**, *1*, 44–49.
- (284) Lee, K. S.; Palatinszky, M.; Pereira, F. C.; Nguyen, J.; Fernandez, V. I.; Mueller, A. J.; Menolascina, F.; Daims, H.; Berry, D.; Wagner, M.; et al. An Automated Raman-Based Platform for the Sorting of Live Cells by Functional Properties. *Nat. Microbiol.* **2019**, *4*, 1035–1048.
- (285) Lambert, P. J.; Whitman, A. G.; Dyson, O. F.; Akula, S. M. Raman Spectroscopy: The Gateway into Tomorrow's Virology. *Virology* **2006**, *3*, 51.
- (286) Wu, M. Y.; Ling, D. X.; Ling, L.; Li, W.; Li, Y. Q. Stable Optical Trapping and Sensitive Characterization of Nanostructures Using Standing-Wave Raman Tweezers. *Sci. Rep.* **2017**, *7*, 42930.
- (287) Begley, R. F.; Harvey, A. B.; Byer, R. L. Coherent Anti-Stokes Raman Spectroscopy. *Appl. Phys. Lett.* **1974**, *25*, 387–390.
- (288) Ribeiro-Claro, P.; Nolasco, M. M.; Araújo, C. In *Comprehensive Analytical Chemistry: Characterization and Analysis of Microplastics*; Rocha-Santos, T. A. P., Duarte, A. C., Eds.; Elsevier: Amsterdam, Oxford, Cambridge, 2017.
- (289) Cole, M.; Lindeque, P.; Fileman, E.; Halsband, C.; Goodhead, R.; Moger, J.; Galloway, T. S. Microplastic Ingestion by Zooplankton. *Environ. Sci. Technol.* **2013**, *47*, 6646–6655.
- (290) Watts, A. J. R.; Urbina, M. A.; Goodhead, R.; Moger, J.; Lewis, C.; Galloway, T. S. Effect of Microplastic on the Gills of the Shore Crab *Carcinus Maenas*. *Environ. Sci. Technol.* **2016**, *50*, 5364–5369.
- (291) Galloway, T. S.; Dogra, Y.; Garrett, N.; Rowe, D.; Tyler, C. R.; Moger, J.; Lammer, E.; Landsiedel, R.; Sauer, U. G.; Scherer, G.; et al. Ecotoxicological Assessment of Nanoparticle-Containing Acrylic Copolymer Dispersions in Fairy Shrimp and Zebrafish Embryos. *Environ. Sci.: Nano* **2017**, *4*, 1981–1997.
- (292) Goodhead, R. M.; Moger, J.; Galloway, T. S.; Tyler, C. R. Tracing Engineered Nanomaterials in Biological Tissues Using Coherent Anti-Stokes Raman Scattering (CARS) Microscopy - a Critical Review. *Nanotoxicology* **2015**, *9*, 928–939.
- (293) Zada, L.; Leslie, H. A.; Vethaak, A. D.; Tinnevelt, G. H.; Jansen, J. J.; de Boer, J. F.; Ariese, F. Fast Microplastics Identification with Stimulated Raman Scattering Microscopy. *J. Raman Spectrosc.* **2018**, *49*, 1136–1144.
- (294) Liao, C.-S.; Wang, P.; Huang, C. Y.; Lin, P.; Eakins, G.; Bentley, R. T.; Liang, R.; Cheng, J.-X. In Vivo and in Situ Spectroscopic Imaging by a Handheld Stimulated Raman Scattering Microscope. *ACS Photonics* **2018**, *5*, 947–954.
- (295) Zhang, C.; Huang, K.-C.; Rajwa, B.; Li, J.; Yang, S.; Lin, H.; Liao, C.-S.; Eakins, G.; Kuang, S.; Patsek, V.; et al. Stimulated Raman Scattering Flow Cytometry for Label-Free Single-Particle Analysis. *Optica* **2017**, *4*, 103–109.
- (296) Jungnickel, H.; Pund, R.; Tentschert, J.; Reichardt, P.; Laux, P.; Harbach, H.; Luch, A. Time-of-Flight Secondary Ion Mass Spectrometry (ToF-SIMS)-Based Analysis and Imaging of Polyethylene Microplastics Formation During Sea Surf Simulation. *Sci. Total Environ.* **2016**, *563–564*, 261–266.
- (297) Du, C.; Wu, J.; Gong, J.; Liang, H.; Li, Z. ToF-SIMS Characterization of Microplastics in Soils. *Surf. Interface Anal.* **2020**, *52*, 293–300.
- (298) Du, C.; Liang, H.; Li, Z.; Gong, J. Pollution Characteristics of Microplastics in Soils in Southeastern Suburbs of Baoding City, China. *Int. J. Environ. Res. Public Health* **2020**, *17*, 845.
- (299) Biesinger, M. C.; Corcoran, P. L.; Walzak, M. J. Developing ToF-SIMS Methods for Investigating the Degradation of Plastic Debris on Beaches. *Surf. Interface Anal.* **2011**, *43*, 443–445.
- (300) ter Halle, A.; Ladirat, L.; Gendre, X.; Goudouneche, D.; Pusineri, C.; Routaboul, C.; Tenailleau, C.; Duployer, B.; Perez, E. Understanding the Fragmentation Pattern of Marine Plastic Debris. *Environ. Sci. Technol.* **2016**, *50*, 5668–5675.
- (301) Napper, I. E.; Thompson, R. C. Release of Synthetic Microplastic Plastic Fibres from Domestic Washing Machines: Effects of Fabric Type and Washing Conditions. *Mar. Pollut. Bull.* **2016**, *112*, 39–45.
- (302) Dehghani, S.; Moore, F.; Akhbarzadeh, R. Microplastic Pollution in Deposited Urban Dust, Tehran Metropolis, Iran. *Environ. Sci. Pollut. Res.* **2017**, *24*, 20360–20371.
- (303) Auta, H. S.; Emenike, C. U.; Fauziah, S. H. Screening of Bacillus Strains Isolated from Mangrove Ecosystems in Peninsular Malaysia for Microplastic Degradation. *Environ. Pollut.* **2017**, *231*, 1552–1559.
- (304) Auta, H. S.; Emenike, C. U.; Jayanthi, B.; Fauziah, S. H. Growth Kinetics and Biodeterioration of Polypropylene Microplastics by *Bacillus Sp.* and *Rhodococcus Sp.* Isolated from Mangrove Sediment. *Mar. Pollut. Bull.* **2018**, *127*, 15–21.
- (305) Fang, C.; Sobhani, Z.; Zhang, X.; Gibson, C. T.; Tang, Y.; Naidu, R. Identification and Visualisation of Microplastics/ Nanoplastics by Raman Imaging (II): Smaller Than the Diffraction Limit of Laser? *Water Res.* **2020**, *183*, 116046.
- (306) Zhang, W.; Dong, Z.; Zhu, L.; Hou, Y.; Qiu, Y. Direct Observation of the Release of Nanoplastics from Commercially Recycled Plastics with Correlative Raman Imaging and Scanning Electron Microscopy. *ACS Nano* **2020**, *14*, 7920–7926.
- (307) Schmidt, R.; Nachtnebel, M.; Dienstleder, M.; Mertschnigg, S.; Schroettner, H.; Zankel, A.; Poteser, M.; Hutter, H.-P.; Eppel, W.; Fitzek, H. Correlative SEM-Raman Microscopy to Reveal Nanoplastics in Complex Environments. *Micron* **2021**, *144*, 103034.
- (308) Wagner, J.; Wang, Z.-M.; Ghosal, S.; Rochman, C.; Gassel, M.; Wall, S. Novel Method for the Extraction and Identification of Microplastics in Ocean Trawl and Fish Gut Matrices. *Anal. Methods* **2017**, *9*, 1479–1490.
- (309) Goldstein, J.; Newbury, D. E.; Joy, D. C.; Lyman, C. E.; Echlin, P.; Lifshin, E.; Sawyer, L.; Michael, J. R. *Scanning Electron Microscopy and X-Ray Microanalysis*; Springer Nature: New York, 2018.

- (310) Oßmann, B.; Schymanski, D.; Ivleva, N. P.; Fischer, D.; Fischer, F.; Dallmann, G.; Welle, F. Comment on "Exposure to Microplastics (<10 µm) Associated to Plastic Bottles Mineral Water Consumption: The First Quantitative Study by Zuccarello et al [Water Research 157 (2019) 365–371]. *Water Res.* **2019**, *162*, 516–517; *Water Res.* **2019**, *162*, 516–517.
- (311) Sarau, G.; Yarbakht, M.; Kling, L.; Oßmann, B.; Ast, J.; Vollnhals, F.; Mueller-Deile, J.; Schiffer, M.; Christiansen, S. H. Context Microscopy and Fingerprinting Spectroscopy of Micro- and Nanoplastics and Their Effects on Human Kidney Cells Using NanoGPG and ParticleFinder. *Microplastics and Nanoplastics: Analysis and Method Development*; Horiba Technical Reports, No. 54; Horiba, 2020; pp 23–32
- (312) Ghosal, S.; Wagner, J. Correlated Raman Micro-Spectroscopy and Scanning Electron Microscopy Analyses of Flame Retardants in Environmental Samples: A Micro-Analytical Tool for Probing Chemical Composition, Origin and Spatial Distribution. *Analyst* **2013**, *138*, 3836–3844.
- (313) Sarau, G.; Kling, L.; Oßmann, B. E.; Unger, A.-K.; Vogler, F.; Christiansen, S. H. Correlative Microscopy and Spectroscopy Workflow for Microplastics. *Appl. Spectrosc.* **2020**, *74*, 1155–1160.
- (314) Awet, T. T.; Kohl, Y.; Meier, F.; Straskraba, S.; Grün, A. L.; Ruf, T.; Jost, C.; Drexel, R.; Tunc, E.; Emmerling, C. Effects of Polystyrene Nanoparticles on the Microbiota and Functional Diversity of Enzymes in Soil. *Environ. Sci. Eur.* **2018**, *30*, 11.
- (315) Rowenczyk, L.; Leflaive, J.; Clergeaud, F.; Minet, A.; Ferriol, J.; Gauthier, L.; Gigault, J.; Mouchet, F.; Ory, D.; Pinelli, E.; et al. Heteroaggregates of Polystyrene Nanospheres and Organic Matter: Preparation, Characterization and Evaluation of Their Toxicity to Algae in Environmentally Relevant Conditions. *Nanomaterials* **2021**, *11*, 482.
- (316) Rummel, C. D.; Jahnke, A.; Gorokhova, E.; Kühnel, D.; Schmitt-Jansen, M. Impacts of Biofilm Formation on the Fate and Potential Effects of Microplastic in the Aquatic Environment. *Environ. Sci. Technol. Lett.* **2017**, *4*, 258–267.
- (317) Ramsperger, A. F. R. M.; Narayana, V. K. B.; Gross, W.; Mohanraj, J.; Thelakkat, M.; Greiner, A.; Schmalz, H.; Kress, H.; Laforsch, C. Environmental Exposure Enhances the Internalization of Microplastic Particles into Cells. *Sci. Adv.* **2020**, *6*, No. eabd1211.
- (318) Jahnke, A.; Arp, H. P. H.; Escher, B. I.; Gewert, B.; Gorokhova, E.; Kühnel, D.; Ogonowski, M.; Potthoff, A.; Rummel, C.; Schmitt-Jansen, M.; et al. Reducing Uncertainty and Confronting Ignorance About the Possible Impacts of Weathering Plastic in the Marine Environment. *Environ. Sci. Technol. Lett.* **2017**, *4*, 85–90.
- (319) Castelvetro, V.; Corti, A.; Biale, G.; Ceccarini, A.; Degano, I.; La Nasa, J.; Lomonaco, T.; Manariti, A.; Manco, E.; Modugno, F. et al. New Methodologies for the Detection, Identification, and Quantification of Microplastics and Their Environmental Degradation by-Products. *Environ. Sci. Pollut. Res.* **2021**, DOI: 10.1007/s11356-021-12466-z.
- (320) Carbery, M.; O'Connor, W.; Palanisami, T. Trophic Transfer of Microplastics and Mixed Contaminants in the Marine Food Web and Implications for Human Health. *Environ. Int.* **2018**, *115*, 400–409.
- (321) Correia, M.; Loeschner, K. Detection of Nanoplastics in Food by Asymmetric Flow Field-Flow Fractionation Coupled to Multi-Angle Light Scattering: Possibilities, Challenges and Analytical Limitations. *Anal. Bioanal. Chem.* **2018**, *410*, 5603–5615.
- (322) Magri, D.; Veronesi, M.; Sánchez-Moreno, P.; Tolardo, V.; Bandiera, T.; Pompa, P. P.; Athanassiou, A.; Fragouli, D. Pet Nanoplastics Interactions with Water Contaminants and Their Impact on Human Cells. *Environ. Pollut.* **2021**, *271*, 116262.
- (323) Hesler, M.; Aengenheister, L.; Ellinger, B.; Drexel, R.; Straskraba, S.; Jost, C.; Wagner, S.; Meier, F.; von Briesen, H.; Büchel, C.; et al. Multi-Endpoint Toxicological Assessment of Polystyrene Nano- and Microparticles in Different Biological Models in Vitro. *Toxicol. In Vitro* **2019**, *61*, 104610.
- (324) Pessoni, L.; Veclin, C.; El Hadri, H.; Cugnet, C.; Davranche, M.; Pierson-Wickmann, A.-C.; Gigault, J.; Grassl, B.; Reynaud, S. Soap- and Metal-Free Polystyrene Latex Particles as a Nanoplastic Model. *Environ. Sci.: Nano* **2019**, *6*, 2253–2258.
- (325) Koelmans, A. A. Proxies for Nanoplastic. *Nat. Nanotechnol.* **2019**, *14*, 307–308.
- (326) Hüffer, T.; Praetorius, A.; Wagner, S.; von der Kammer, F.; Hofmann, T. Microplastic Exposure Assessment in Aquatic Environments: Learning from Similarities and Differences to Engineered Nanoparticles. *Environ. Sci. Technol.* **2017**, *51*, 2499–2507.
- (327) Pradel, A.; Ferreres, S.; Veclin, C.; El Hadri, H.; Gautier, M.; Grassl, B.; Gigault, J. Stabilization of Fragmental Polystyrene Nanoplastic by Natural Organic Matter: Insight into Mechanisms. *ACS ES&T Water* **2021**, *1*, 1198–1208.
- (328) Venel, Z.; Tabuteau, H.; Pradel, A.; Pascal, P.-Y.; Grassl, B.; El Hadri, H.; Baudrimont, M.; Gigault, J. Environmental Fate Modeling of Nanoplastics in a Salinity Gradient Using a Lab-on-a-Chip: Where Does the Nanoscale Fraction of Plastic Debris Accumulate? *Environ. Sci. Technol.* **2021**, *55*, 3001.
- (329) Gigault, J.; El Hadri, H.; Nguyen, B.; Grassl, B.; Rowenczyk, L.; Tufenkji, N.; Feng, S.; Wiesner, M. Nanoplastics Are Neither Microplastics nor Engineered Nanoparticles. *Nat. Nanotechnol.* **2021**, *16*, 501–507.
- (330) Davranche, M.; Lory, C.; Juge, C. L.; Blanche, F.; Dia, A.; Grassl, B.; El Hadri, H.; Pascal, P.-Y.; Gigault, J. Nanoplastics on the Coast Exposed to the North Atlantic Gyre: Evidence and Traceability. *NanoImpact* **2020**, *20*, 100262.
- (331) Wahl, A.; Le Juge, C.; Davranche, M.; El Hadri, H.; Grassl, B.; Reynaud, S.; Gigault, J. Nanoplastic Occurrence in a Soil Amended with Plastic Debris. *Chemosphere* **2021**, *262*, 127784.
- (332) Hernandez, L. M.; Yousefi, N.; Tufenkji, N. Are There Nanoplastics in Your Personal Care Products? *Environ. Sci. Technol. Lett.* **2017**, *4*, 280–285.
- (333) Gigault, J.; Pedrono, B.; Maxit, B.; Ter Halle, A. Marine Plastic Litter: The Unanalyzed Nanofraction. *Environ. Sci.: Nano* **2016**, *3*, 346–350.
- (334) Lambert, S.; Wagner, M. Characterisation of Nanoplastics During the Degradation of Polystyrene. *Chemosphere* **2016**, *145*, 265–268.
- (335) Dawson, A. L.; Kawaguchi, S.; King, C. K.; Townsend, K. A.; King, R.; Huston, W. M.; Bengtson Nash, S. M. Turning Microplastics into Nanoplastics through Digestive Fragmentation by Antarctic Krill. *Nat. Commun.* **2018**, *9*, 1001.
- (336) Laborda, F.; Bolea, E.; Cepriá, G.; Gómez, M. T.; Jiménez, M. S.; Pérez-Arategui, J.; Castillo, J. R. Detection, Characterization and Quantification of Inorganic Engineered Nanomaterials: A Review of Techniques and Methodological Approaches for the Analysis of Complex Samples. *Anal. Chim. Acta* **2016**, *904*, 10–32.
- (337) Rist, S.; Baun, A.; Hartmann, N. B. Ingestion of Micro- and Nanoplastics in *Daphnia Magna* - Quantification of Body Burdens and Assessment of Feeding Rates and Reproduction. *Environ. Pollut.* **2017**, *228*, 398–407.
- (338) Wang, Z.; Taylor, S. E.; Sharma, P.; Flury, M. Poor Extraction Efficiencies of Polystyrene Nano- and Microparticles from Biosolids and Soil. *PLoS One* **2018**, *13*, No. e0208009.
- (339) Prestel, H.; Niessner, R.; Panne, U. Increasing the Sensitivity of Asymmetrical Flow Field-Flow Fractionation: Slot Outlet Technique. *Anal. Chem.* **2006**, *78*, 6664–6669.
- (340) Gigault, J.; El Hadri, H.; Reynaud, S.; Deniau, E.; Grassl, B. Asymmetrical Flow Field Flow Fractionation Methods to Characterize Submicron Particles: Application to Carbon-Based Aggregates and Nanoplastics. *Anal. Bioanal. Chem.* **2017**, *409*, 6761–6769.
- (341) Davranche, M.; Veclin, C.; Pierson-Wickmann, A.-C.; El Hadri, H.; Grassl, B.; Rowenczyk, L.; Dia, A.; Ter Halle, A.; Blanche, F.; Reynaud, S.; et al. Are Nanoplastics Able to Bind Significant Amount of Metals? The Lead Example. *Environ. Pollut.* **2019**, *249*, 940–948.
- (342) Lespes, G.; Gigault, J. Hyphenated Analytical Techniques for Multidimensional Characterisation of Submicron Particles: A Review. *Anal. Chim. Acta* **2011**, *692*, 26–41.
- (343) Pirok, B. W. J.; Abdhussain, N.; Aalbers, T.; Wouters, B.; Peters, R. A. H.; Schoenmakers, P. J. Nanoparticle Analysis by Online Comprehensive Two-Dimensional Liquid Chromatography Combining Hydrodynamic Chromatography and Size-Exclusion Chromatog-

raphy with Intermediate Sample Transformation. *Anal. Chem.* **2017**, *89*, 9167–9174.

(344) Valsesia, A.; Quarato, M.; Ponti, J.; Fumagalli, F.; Gilliland, D.; Colpo, P. Combining Microcavity Size Selection with Raman Microscopy for the Characterization of Nanoplastics in Complex Matrices. *Sci. Rep.* **2021**, *11*, 362.

(345) Blanco, F.; Davranche, M.; Hadri, H. E.; Grassl, B.; Gigault, J. Nanoplastics Identification in Complex Environmental Matrices: Strategies for Polystyrene and Polypropylene. *Environ. Sci. Technol.* **2021**, *55*, 8753–8759.

(346) Cardell, C.; Guerra, I. An Overview of Emerging Hyphenated SEM-EDX and Raman Spectroscopy Systems: Applications in Life, Environmental and Materials Sciences. *TrAC, Trends Anal. Chem.* **2016**, *77*, 156–166.

(347) Lv, L.; He, L.; Jiang, S.; Chen, J.; Zhou, C.; Qu, J.; Lu, Y.; Hong, P.; Sun, S.; Li, C. In Situ Surface-Enhanced Raman Spectroscopy for Detecting Microplastics and Nanoplastics in Aquatic Environments. *Sci. Total Environ.* **2020**, *728*, 138449.

(348) Zhou, X.-X.; Liu, R.; Hao, L.-T.; Liu, J.-F. Identification of Polystyrene Nanoplastics Using Surface Enhanced Raman Spectroscopy. *Talanta* **2021**, *221*, 121552.

(349) Lê, Q. T.; Ly, N. H.; Kim, M.-K.; Lim, S. H.; Son, S. J.; Zoh, K.-D.; Joo, S.-W. Nanostructured Raman Substrates for the Sensitive Detection of Submicrometer-Sized Plastic Pollutants in Water. *J. Hazard. Mater.* **2021**, *402*, 123499.

(350) Schlücker, S. Surface-Enhanced Raman Spectroscopy: Concepts and Chemical Applications. *Angew. Chem., Int. Ed.* **2014**, *53*, 4756–4795.

(351) Lee, P. C.; Meisel, D. Adsorption and Surface-Enhanced Raman of Dyes on Silver and Gold Sols. *J. Phys. Chem.* **1982**, *86*, 3391–3395.

(352) Leopold, N.; Lendl, B. A New Method for Fast Preparation of Highly Surface-Enhanced Raman Scattering (SERS) Active Silver Colloids at Room Temperature by Reduction of Silver Nitrate with Hydroxylamine Hydrochloride. *J. Phys. Chem. B* **2003**, *107*, 5723–5727.

(353) Kühn, M.; Ivleva, N. P.; Klitzke, S.; Niessner, R.; Baumann, T. Investigation of Coatings of Natural Organic Matter on Silver Nanoparticles under Environmentally Relevant Conditions by Surface-Enhanced Raman Scattering. *Sci. Total Environ.* **2015**, *535*, 122–130.

(354) Verma, P. Tip-Enhanced Raman Spectroscopy: Technique and Recent Advances. *Chem. Rev.* **2017**, *117*, 6447–6466.

(355) Dazzi, A.; Prater, C. B. AFM-IR: Technology and Applications in Nanoscale Infrared Spectroscopy and Chemical Imaging. *Chem. Rev.* **2017**, *117*, 5146–5173.

(356) Xiao, L.; Schultz, Z. D. Spectroscopic Imaging at the Nanoscale: Technologies and Recent Applications. *Anal. Chem.* **2018**, *90*, 440–458.

(357) Hermann, R. J.; Gordon, M. J. Nanoscale Optical Microscopy and Spectroscopy Using near-Field Probes. *Annu. Rev. Chem. Biomol. Eng.* **2018**, *9*, 365–387.

(358) Kuroski, D.; Dazzi, A.; Zenobi, R.; Centrone, A. Infrared and Raman Chemical Imaging and Spectroscopy at the Nanoscale. *Chem. Soc. Rev.* **2020**, *49*, 3315–3347.

(359) Felts, J. R.; Kjoller, K.; Lo, M.; Prater, C. B.; King, W. P. Nanometer-Scale Infrared Spectroscopy of Heterogeneous Polymer Nanostructures Fabricated by Tip-Based Nanofabrication. *ACS Nano* **2012**, *6*, 8015–8021.

(360) Pancani, E.; Mathurin, J.; Bilent, S.; Bernet-Camard, M.-F.; Dazzi, A.; Deniset-Besseau, A.; Gref, R. High-Resolution Label-Free Detection of Biocompatible Polymeric Nanoparticles in Cells. *Part. Part. Syst. Char.* **2018**, *35*, 1700457.

(361) Brehm, M.; Taubner, T.; Hillenbrand, R.; Keilmann, F. Infrared Spectroscopic Mapping of Single Nanoparticles and Viruses at Nanoscale Resolution. *Nano Lett.* **2006**, *6*, 1307–1310.

(362) Huth, F.; Goyadinov, A.; Amarie, S.; Nuansing, W.; Keilmann, F.; Hillenbrand, R. Nano-FTIR Absorption Spectroscopy of Molecular Fingerprints at 20 nm Spatial Resolution. *Nano Lett.* **2012**, *12*, 3973–3978.

(363) Meyns, M.; Primpke, S.; Gerdt, G. Library Based Identification and Characterisation of Polymers with Nano-FTIR and IR-sSNOM Imaging. *Anal. Methods* **2019**, *11*, 5195–5202.

(364) Chen, C.; Hayazawa, N.; Kawata, S. A 1.7nm Resolution Chemical Analysis of Carbon Nanotubes by Tip-Enhanced Raman Imaging in the Ambient. *Nat. Commun.* **2014**, *5*, 3312.

(365) Yeo, B.-S.; Amstad, E.; Schmid, T.; Stadler, J.; Zenobi, R. Nanoscale Probing of a Polymer-Blend Thin Film with Tip-Enhanced Raman Spectroscopy. *Small* **2009**, *5*, 952–960.

(366) Elkhatib, D.; Oyanedel-Craver, V. A Critical Review of Extraction and Identification Methods of Microplastics in Wastewater and Drinking Water. *Environ. Sci. Technol.* **2020**, *54*, 7037–7049.

(367) Mai, L.; Bao, L.-J.; Shi, L.; Wong, C. S.; Zeng, E. Y. A Review of Methods for Measuring Microplastics in Aquatic Environments. *Environ. Sci. Pollut. Res.* **2018**, *25*, 11319–11332.

(368) Miller, E.; Sedlak, M.; Lin, D.; Box, C.; Holleman, C.; Rochman, C. M.; Sutton, R. Recommended Best Practices for Collecting, Analyzing, and Reporting Microplastics in Environmental Media: Lessons Learned from Comprehensive Monitoring of San Francisco Bay. *J. Hazard. Mater.* **2021**, *409*, 124770.

(369) Brander, S. M.; Renick, V. C.; Foley, M. M.; Steele, C.; Woo, M.; Lusher, A.; Carr, S.; Helm, P.; Box, C.; Cherniak, S.; et al. Sampling and Quality Assurance and Quality Control: A Guide for Scientists Investigating the Occurrence of Microplastics across Matrices. *Appl. Spectrosc.* **2020**, *74*, 1099–1125.

(370) Schymanski, D.; Oßmann, B. E.; Benismail, N.; Boukerma, K.; Dallmann, G.; von der Esch, E.; Fischer, D.; Fischer, F.; Gilliland, D.; Glas, K. et al. Analysis of Microplastics in Drinking Water and Other Clean Water Samples with Micro-Raman and Micro-Infrared Spectroscopy: Minimum Requirements and Best Practice Guidelines. *Anal. Bioanal. Chem.* **2021**, DOI: 10.1007/s00216-021-03498-y

(371) Hanvey, J. S.; Lewis, P. J.; Lavers, J. L.; Crosbie, N. D.; Pozo, K.; Clarke, B. O. A Review of Analytical Techniques for Quantifying Microplastics in Sediments. *Anal. Methods* **2017**, *9*, 1369–1383.

(372) Eitzen, L.; Paul, S.; Braun, U.; Altmann, K.; Jekel, M.; Ruhl, A. S. The Challenge in Preparing Particle Suspensions for Aquatic Microplastic Research. *Environ. Res.* **2019**, *168*, 490–495.

(373) Seghers, J.; Stefaniak, E. A.; La Spina, R.; Cella, C.; Mehn, D.; Gilliland, D.; Held, A.; Jacobsson, U.; Emteborg, H. Preparation of a Reference Material for Microplastics in Water—Evaluation of Homogeneity. *Anal. Bioanal. Chem.* **2021**, DOI: 10.1007/s00216-021-03198-7

(374) Balakrishnan, G.; Déniel, M.; Nicolai, T.; Chassenieux, C.; Lagarde, F. Towards More Realistic Reference Microplastics and Nanoplastics: Preparation of Polyethylene Micro/Nanoparticles with a Biosurfactant. *Environ. Sci.: Nano* **2019**, *6*, 315–324.

(375) Mitrano, D. M.; Beltzung, A.; Frehland, S.; Schmiedgruber, M.; Cingolani, A.; Schmidt, F. Synthesis of Metal-Doped Nanoplastics and Their Utility to Investigate Fate and Behaviour in Complex Environmental Systems. *Nat. Nanotechnol.* **2019**, *14*, 362–368.

(376) Sander, M.; Kohler, H.-P. E.; McNeill, K. Assessing the Environmental Transformation of Nanoplastic through <sup>13</sup>C-Labelled Polymers. *Nat. Nanotechnol.* **2019**, *14*, 301–303.

(377) Al-Sid-Cheikh, M.; Rowland, S. J.; Kaegi, R.; Henry, T. B.; Cormier, M.-A.; Thompson, R. C. Synthesis of <sup>14</sup>C-Labelled Polystyrene Nanoplastics for Environmental Studies. *Commun. Mater.* **2020**, *1*, 97.

(378) Dris, R.; Gasperi, J.; Mirande, C.; Mandin, C.; Guerrouache, M.; Langlois, V.; Tassin, B. A First Overview of Textile Fibers, Including Microplastics, in Indoor and Outdoor Environments. *Environ. Pollut.* **2017**, *221*, 453–458.

(379) Wolff, S.; Weber, F.; Kerpen, J.; Winkhofer, M.; Engelhart, M.; Barkmann, L. Elimination of Microplastics by Downstream Sand Filters in Wastewater Treatment. *Water* **2021**, *13*, 33.

(380) Imhof, H. K.; Rusek, J.; Thiel, M.; Wolinska, J.; Laforsch, C. Do Microplastic Particles Affect *Daphnia Magna* at the Morphological, Life History and Molecular Level? *PLoS One* **2017**, *12*, No. e0187590.

(381) Schür, C.; Rist, S.; Baun, A.; Mayer, P.; Hartmann, N. B.; Wagner, M. When Fluorescence Is Not a Particle: The Tissue

Translocation of Microplastics in *Daphnia Magna* Seems an Artifact. *Environ. Toxicol. Chem.* **2019**, *38*, 1495–1503.

(382) Zumstein, M. T.; Schintlmeister, A.; Nelson, T. F.; Baumgartner, R.; Woebken, D.; Wagner, M.; Kohler, H.-P. E.; McNeill, K.; Sander, M. Biodegradation of Synthetic Polymers in Soils: Tracking Carbon into CO<sub>2</sub> and Microbial Biomass. *Sci. Adv.* **2018**, *4*, No. eaas9024.

(383) Taipale, S. J.; Peltomaa, E.; Kukkonen, J. V. K.; Kainz, M. J.; Kautonen, P.; Tirola, M. Tracing the Fate of Microplastic Carbon in the Aquatic Food Web by Compound-Specific Isotope Analysis. *Sci. Rep.* **2019**, *9*, 19894.

(384) Frehland, S.; Kaegi, R.; Hufenus, R.; Mitrano, D. M. Long-Term Assessment of Nanoplastic Particle and Microplastic Fiber Flux through a Pilot Wastewater Treatment Plant Using Metal-Doped Plastics. *Water Res.* **2020**, *182*, 115860.

(385) Isobe, A.; Buenaventura, N. T.; Chastain, S.; Chavanich, S.; Cózar, A.; DeLorenzo, M.; Hagmann, P.; Hinata, H.; Kozlovskii, N.; Lusher, A. L.; et al. An Interlaboratory Comparison Exercise for the Determination of Microplastics in Standard Sample Bottles. *Mar. Pollut. Bull.* **2019**, *146*, 831–837.

(386) Müller, Y. K.; Wernicke, T.; Pittroff, M.; Witzig, C. S.; Storck, F. R.; Klinger, J.; Zumbülte, N. Microplastic Analysis—Are We Measuring the Same? Results on the First Global Comparative Study for Microplastic Analysis in a Water Sample. *Anal. Bioanal. Chem.* **2020**, *412*, 555–560.

(387) Altmann, K.; Braun, U.; Fischer, D.; Fischer, F.; Ivleva, N. P.; Sturn, H.; Witzig, C.; Zumbülte, N. Comparative Test: Results within the Scope of the BMBF Research Focus Plastics in the Environment: Sources, Sinks, Solutions. *Ecologic Institute 2021*, 2020; <https://www.youtube.com/watch?v=HIPZ8AMq448>.

(388) Normenausschuss Wasserwesen (NAW) Im DIN. *Deutsche Einheitsverfahren Zur Wasser-, Abwasser- Und Schlammuntersuchung—Allgemeine Angaben (Gruppe a)*; Teil. 45: Ringversuche Zur Eignungsprüfung Von Laboratorien (a 45); Beuth Verlag, 2014.

(389) JRC/BAM Inter-Laboratory Comparison on Microplastics in Water. *Draft Study Report*; JRC/BAM, 2021.